

Doctoral Dissertation

**SPATIAL ANALYSIS OF COASTLINE CHANGE AND
VULNERABILITY ASSESSMENT TO ENHANCED
SEA LEVEL RISE**

海岸線変化の空間分析と海面上昇に対する脆弱性評価に関する研究

March 2024

AMANDANGI WAHYUNING HASTUTI

**Graduate School of Sciences and Technology for Innovation
Yamaguchi University**

Acknowledgments

This doctoral degree would not be complete without the support and assistance from many people and institutions. I praise Allah SWT and Prophet Muhammad SAW for allowing me to reach a higher level of knowledge—our prayers of thanks.

I would like to express my sincere and most profound gratitude to my supervisor, Prof. Masahiko Nagai, for his attention, guidance, knowledge, and support throughout my scientific journey. I have learned so many things while studying under his supervision. I am also thankful to my graduate committee, Prof. Takahiro Osawa, Prof. Tsuyoshi Imai, Prof. Koji Asai, and Prof. Toshikazu Samura, for their insightful comments and suggestions, which have significantly contributed to the refinement of this research.

I am indebted to the Japan International Cooperation Agency (JICA) - Agriculture Studies Networks for Food Security (Agri-Net) program, whose financial support made this study possible. Furthermore, I thank The Institute for Information Management of Marine and Fisheries Resources (InFoMarFish), on behalf of the Ministry of Marine Affairs and Fisheries - Republic of Indonesia, for supporting my study.

Other great thanks go to Dr. I Nyoman Radiarta, M.Sc. - Chairman of the Agency for Marine and Fisheries Research and Human Resources, for fruitful discussion and motivation from the very start of my study. Dr. Adi Wijaya and Komang Iwan Suniada M.Si., for helping me conduct the fieldwork in Bali.

Thanks to all my laboratory members, Space Utilization Engineering Laboratory, for the knowledge exchange, help, and cooperation throughout my study period, especially to Dr. Vaibhav Katiyar for the valuable input, comments, and necessary technical suggestions during my study.

To my family, who is constantly showering me with their best prayers and unconditional love, for giving me the privilege of free thinking, the opportunity to explore the world, and the freedom to make mistakes and learn from them.

I also place on record my gratitude to all who, directly or indirectly, have lent a helping hand in this venture. Without the support and contributions of these individuals and organizations, this dissertation would not have been possible.

Preface

This dissertation is being submitted to Yamaguchi University - Graduate School of Science and Technology for Innovation in partial fulfillment of the Doctor of Engineering degree requirements. The dissertation is the author's original contribution, and relevant references are provided in the dissertation itself, wherever the author has used the results or data from previous studies.

The publications that have been published in the course of the research and which have contributed significantly to the chapters of this dissertation are as follows:

[1] Peer-reviewed Journal Paper

a. Coastal Vulnerability Assessment of Bali Province, Indonesia, Using Remote Sensing and GIS Approaches

Amandangi Wahyuning Hastuti, Masahiko Nagai, and Komang Iwan Suniada

Journal: Remote Sensing (MDPI)

Publication: *Remote Sens.* **2022**, *14*(17), 4490; <https://doi.org/10.3390/rs14174409>

b. Coastline Change Detection Based on Sentinel-2 Imagery Data in Jembrana Regency, Bali Province

Amandangi Wahyuning Hastuti, Masahiko Nagai, and Komang Iwan Suniada

Journal: Journal of Evolving Space Activities

Publication: Vol. 1, Article No. 23, 2023 DOI: 10.57350/jesa.23

c. Sea Level Rise-Induced Coastal Flooding and Its Potential Impacts in Bali Province, Indonesia

Amandangi Wahyuning Hastuti, Neira Purwanty Ismail, and Masahiko Nagai

Journal: Journal of Evolving Space Activities

Publication: *Accepted with major revision*

d. Spatiotemporal Analysis of Shoreline Change Trends and Adaptation in Bali Province, Indonesia

Amandangi Wahyuning Hastuti, Masahiko Nagai, Neira Purwanty Ismail, Bayu Priyono, Komang Iwan Suniada, and Adi Wijaya

Journal: Regional Studies in Marine Science

Publication: *submitted*

[2] Peer-reviewed Conference Paper

a. Detection of Coastline Changes using Multi-Temporal Satellite Images: A Case Study of Gianyar and Klungkung Regency, Bali

Amandangi Wahyuning Hastuti, Komang Iwan Suniada, and Masahiko Nagai

Proceeding: International Conference on Sustainable Coastal Management: The 2nd Sustainability and Resilience of Coastal Management (SRCM 2021) November 30, 2021. Surabaya, Indonesia.

Publication: *IOP Conf. Ser.: Earth Environ Sci.* **1095** (2022) 102003 DOI: 10.1088/1755-1315/1095/1/012003

b. Coastline Change Detection Using High-Resolution Satellite Images: A Case Study in Amurang Coasts—South Minahasa, North Sulawesi

Amandangi Wahyuning Hastuti, Neira Purwanty Ismail, and Masahiko Nagai

Proceeding: The International Seminar on Ocean Sciences and Sustainability (ISOSS-2022) August 4–5, 2022. Bogor, Indonesia.

Publication: *IOP Conf. Ser.: Earth Environ Sci.* **1251** (2023) 012011 DOI: 10.1088/1755-1315/1251/1/012011

c. Analysis of Coastline Extraction Indices Using Sentinel-2 and Google Earth Engine in Bali, Indonesia

Amandangi Wahyuning Hastuti, Neira Purwanty Ismail, and Masahiko Nagai

Proceeding: The 5th International Conference on Marine Science 2023 (ICMS-2023) October 25–26, 2023. Bogor, Indonesia.

Publication: *submitted*

d. Monitoring Land Use and Land Cover (LULC) Changes of Jembrana Coastal Areas Using PlanetScope Imageries Data

Amandangi Wahyuning Hastuti, Adi Wijaya, and Masahiko Nagai

Proceeding: 2023 Asian Conference on Remote Sensing (ACRS-2023) October 30–November 3, 2023. Taipei, Taiwan.

Publication: *submitted*

Summary

Climate change, with its associated rising sea level and possible increases in the frequency and/or intensity of storms and changes in wave climate, can be expected to significantly increase the risk of coastal erosion and flooding in most coastal locations, especially in low-lying areas. Bali Province is a well-known tourist destination dependent on sun-and-beach recreation activities. However, about 86 km or 20% of the length of the existing beaches has been eroded, and environmental degradation has occurred due to natural factors and human activities. As a natural coastal defense system, beaches are important in reducing coastal erosion risks. Thus, their retreat and eventual disappearance increase their vulnerability to hazardous events. In addition, beach narrowing threatens beach environmental services critical to tourist destinations' economy since recreational activities depend on the beach backshore. Considering the threat of sea-level rise in coastal areas and on small islands, it is necessary to conduct a study to determine the degree of vulnerability experienced by a coast since measuring vulnerability is a fundamental phase towards effective risk reduction.

Therefore, the main finding of this study is to investigate and assess the vulnerability of the Bali Province coast to the effect of rising sea levels through remote sensing and Geographic Information System (GIS) technology, considering the geological and physical characteristics of coastal processes. Remote sensing is the science and art of obtaining information about an object on the Earth's surface through analyzing data acquired without directly contacting the object. Considering its low cost and extensive coverage, this advanced technology is frequently used in environmental and natural resources monitoring. The combination of remote sensing and GIS technology will provide valuable spatial information to evaluate environmental changes and has proved its effectiveness in providing accurate information for monitoring coastal areas.

Assessing coastal vulnerability is one of the methods generally used to measure the degree of coastal vulnerability. This study considered six parameters in creating the Coastal Vulnerability Index (CVI): geomorphology, shoreline change rate, coastal elevation, sea-level change rate, tidal range, and significant wave height. The study revealed that about 138 km (22%) of the mapped shoreline is classified as very high vulnerability, and 164 km (26%) of the shoreline is highly vulnerable. Of the remaining shoreline, 168 km (26%) and 169 km (26%) are moderately vulnerable categories and low vulnerable categories, respectively. The data analysis found that the geological variables, which are geomorphology, shoreline change, elevation, and significant wave height, are the major factors that determine the risk level of coastal vulnerability since the physical variables (sea-level change rate and tidal range) were given the same risk level along the coast. Moreover, it is verified that the method applied agrees well with the Kappa coefficient value of 0.80.

Additionally, the rise in sea level-induced intensification of coastal floods is a serious threat to Bali's coastal areas near the ocean. Although severe flood events are rare, they can entail enormous damage costs, especially when built-up areas and/or agricultural fields are inundated. To address the gap and analyze the regional impacts of climate change and sea level rise on the coastal areas of Bali Province, we simulated coastal inundation due to rising sea

levels in multiple scenarios of projected sea level height in 2025, 2030, 2070, and 2100. This assessment aims to identify the area submergence in different sea level scenarios based on the derived annual SLR rates and estimate the potential impacts of coastal inundation on land use. At the current rising rate, 7077.42 ha of Bali Province will be below the water level in 2100.

As one of the main parameters to determine coastal vulnerability, shoreline change must be monitored continuously to understand how the sediment moves in a coastal compartment. This study also presents an application of satellite remote sensing techniques to detect and analyze the dynamic changes in shoreline position. This study uses high-resolution PlanetScope imagery data. Multitemporal shorelines were extracted using the Normalized Difference Water Index (NDWI) to delineate seawater from distinct land-cover types. The end point rate (EPR) model was then used to statistically quantify the shoreline change rates. The results revealed variations in the positions of the shorelines over the duration of the study, with rapid erosion emerging as a major concern in Bali Province, primarily driven by human activities and/or coastal hydrodynamics. During the study period, the shoreline in Bali Province decreased from 668.64 km to 662.59 km at an average rate of -1.21 m/yr due to continuous erosion, with the most significant retreat occurring at Klungkung Regency. The method applied has been verified with an overall accuracy of 78.38%.

Addressing the issues provided by shoreline changes is essential to protecting the coastal ecosystem, supporting economic growth, and preserving the cultural significance of the region for future generations. Moreover, a comprehensive analysis of studies on sea level rise, including a detailed assessment of the cost and benefit associated with potential adaptations and mitigation, should be undertaken to evaluate the possible actions for coastal protection strategies.

概要

気候変動は、それに伴う海面上昇、暴風雨の頻度や強度の増加、波候の変化の可能性を伴い、多くの沿岸地域において、海岸浸食や洪水リスクを著しく増大させることが予想されている。インドネシアのバリ州は、経済のほとんどを観光業に依存している世界的リゾート地である。一方で、バリ州全体の海岸線の20%にあたる約86kmで沿岸浸食が発生し、自然要因や人間活動によって環境の悪化が起きている。自然の海岸防御システムにおいて、砂浜は海岸浸食のリスクを軽減する上で重要な役割を果たしているが、海岸線の後退と消滅は、災害等のリスクに対する脆弱性を増大させる。さらに、リゾート地としての浜辺の役割は大きく、浜辺の狭小化は、観光地の経済にとって大きな問題となる。沿岸地域や小島における海面上昇の脅威に対する脆弱性の評価は、効果的なリスク軽減に向けた基本的な政策策定の段階であるため、沿岸域の脆弱性の程度を決定するための研究を実施することは大きな意義がある。

本研究の目的は、リモートセンシングと地理情報システム（GIS）技術を用い、沿岸プロセスの地質学的・物理学的特性を考慮し、海面上昇の影響に対するバリ州沿岸の脆弱性を調査・評価することである。リモートセンシングとは、地球表面の対象物に直接接触することなく、取得したデータを分析することによって、その対象物に関する情報を得ることができる技術である。低コストで広範囲をカバーできることから、この先端技術は環境や天然資源のモニタリングに頻繁に利用されている。リモートセンシングとGIS技術の組み合わせは、生態系の変化を評価するための重要な空間情報を提供し、沿岸地域のモニタリングに正確な情報を提供する上で有効である。

沿岸の脆弱性の評価は、沿岸の脆弱性の程度を測定するために一般的に用いられている方法の一つである。本研究では、「沿岸脆弱性指数（CVI）」を作成するにあたり、地形、海岸線の変化率、沿岸の標高、海面水位の変化率、潮差、有義波高の6つのパラメータを考慮した。調査の結果、バリ州の海岸線のうち約138km

(22%)が非常に高い脆弱性に分類され、164km(26%)が高い脆弱性に分類された。残りの海岸線のうち、168km(26%)と169km(26%)は、それぞれ中程度と低い脆弱性のカテゴリーである。データ分析の結果、物理的変数（海面水位の変化率と潮差）が海岸に沿って同じリスクレベルを与えられていることから、地形、海岸線の変化、標高、有義波高である地質学的変数が、海岸の脆弱性のリスクレベルを決定する主要な要因であることがわかった。さらに、カップ係数が0.80であり、適用した手法がよく一致することが確認された。

海面上昇による沿岸洪水の激化は、海に近接するバリ州の沿岸地域にとって深刻な脅威である。深刻な洪水が発生することはまれであるが、特に市街地や農地が浸水した場合、莫大な損害が発生する可能性がある。気候変動と海面上昇がバリ州の沿岸地域に及ぼす地域的影響を分析するために、2025年、2030年、2070年、2100

年の海面高さの予測に関する複数のシナリオで、海面上昇による沿岸浸水のシミュレーションを行った。この評価の目的は、導き出された年間海面上昇率に基づき、異なる海面シナリオにおける浸水面積を特定し、沿岸浸水が土地利用に及ぼす潜在的な影響を推定することである。現在の上昇率がそのまま推移すると、2100年にはバリ州の7077.42haが水面下に沈むことになる。

さらに本研究では、衛星画像から海岸線の位置の動的な変化を分析した。高解像度のPlanetScope画像データを使用し、正規化水指数（NDWI）から多時期の海岸線を抽出し、異なる土地被覆タイプから海域を分類した。次に、エンドポイントレート（EPR）モデルを用いて、海岸線の変化率を統計的に定量化した。その結果、調査期間中の海岸線の位置の変動が明らかになり、バリ州では、主に人間活動や沿岸流体力学に起因する急速な浸食が主要な懸念事項として浮上した。調査期間中、バリ州の海岸線は668.64kmから662.59kmに減少し、継続的な浸食により平均-1.21m/年の速度で、最も顕著な後退はクルンクン県で発生した。適用された方法は、78.38%の全体的な精度で検証された。

海岸線の変化によってもたらされる問題に対処することは、沿岸生態系を保護し、経済成長を支え、地域の文化的意義を将来の世代に残すために不可欠である。さらに、可能性のある適応策と緩和策に関連する費用と便益の詳細な評価を含む、海面上昇に関する包括的な分析を行い、沿岸保護戦略のために必要な行動に着手するべきである。

Table of Contents

Acknowledgments	i
Preface	ii
Summary	iv
概要	vi
Table of Contents	viii
List of Figures	xi
Abbreviations	xiv
CHAPTER 1. INTRODUCTION	1
1.1. Background – Sea Level Rise and Its Impacts	1
1.2. Research Problems	4
1.3. Research Objectives	7
1.4. Dissertation Structure	7
CHAPTER 2. LITERATURE REVIEW AND METHODOLOGY	8
2.1. Literature Review	8
2.1.1. Definitions of Hazard, Vulnerability, and Risk	8
2.1.2. Coastal Zone	9
2.1.3. Coastal Vulnerability	10
2.1.4. Coastal Flooding	10
2.1.5. Shoreline Change	11
2.2. Methodology	12
2.2.1. Remote Sensing and GIS Techniques for Disaster Management and Coastal Zone Monitoring	12
2.2.2. Sentinel-2 Image	13
2.2.3. PlanetScope Image	13
2.2.4. Digital Elevation Model (DEM)	14
2.2.5. Overview of The Study Area	16
2.2.6. Accuracy Assessment	17
CHAPTER 3. SHORELINE CHANGE DETECTION	19
3.1. Overview	19
3.2. Materials and Methods	20

3.2.1. Data Sources	20
3.2.2. Extraction and Classification of Shoreline	22
3.2.3. Analysis of Shoreline Change	23
3.2.4. Analysis of Land Area Change	24
3.3. Result and Discussion	24
3.3.1. Shore-type Changes	24
3.3.2. Shoreline and Coastal Area Change Rates	27
3.3.3. Significant Wave Height Analysis	30
3.3.4. Ocean Current Analysis	32
3.3.5. Shoreline Changes Associated with Human Activities	34
3.3.6. Shoreline Change Associated with Global Climate Change	36
3.3.7. Existing Coastal Protection Strategy	37
3.3.8. Accuracy Assessment of The Proposed Method	39
3.4. Conclusion.....	40
CHAPTER 4. COASTAL FLOOD IMPACT DETECTION	41
4.1. Overview	41
4.2. Data Collection and Methods.....	42
4.3. Result.....	45
4.3.1. Sea Levels.....	45
4.3.2. Sea Levels Prediction	47
4.3.3. Flood Risk Map	48
4.3.4. Flood Loss Estimation	51
4.4. Discussion	53
4.5. Conclusion.....	54
CHAPTER 5. COASTAL VULNERABILITY IN BALI PROVINCE FROM PHYSICAL PARAMETERS	56
5.1. Overview	56
5.2. Data Collection and Methods.....	56
5.3. Coastal Vulnerability Index (CVI) Analysis	59
5.4. Field Survey	59
5.5. Result and Discussion	60
5.5.1. Geomorphology	60
5.5.2. Coastline Change	61
5.5.3. Elevation.....	63

5.5.4. Sea Level	64
5.5.5. Tidal Range.....	65
5.5.6. Significant Wave Height	65
5.5.7. Coastal Vulnerability Index of Bali Province.....	66
5.6. Conclusion.....	69
CHAPTER 6. ACCURACY ASSESSMENT OF COASTLINE EXTRACTION	71
6.1. Overview	71
6.2. Data Collection and Method	72
6.3. Result and Discussion	76
6.3.1. Normalized Difference Vegetation Index (NDVI).....	77
6.3.2. Normalized Difference Water Index (NDWI).....	77
6.3.3. Modified Normalized Difference Water Index (MNDWI)	78
6.3.4. Water Ratio Index (WRI)	79
6.3.5. Automated Water Extraction Index (AWEI).....	80
6.3.6. Coastline Change Analysis of Jembrana Regency	82
6.3.7. Coastline Change Analysis of Gianyar and Klungkung Regency	88
6.4. Conclusion.....	91
CHAPTER 7. CONCLUDING REMARKS AND OUTLOOK	92
7.1. Conclusion and Main Findings	92
7.2. Contribution of This Research	93
7.3. Recommendations	93
REFERENCES.....	94

List of Figures

Figure 1-1. The global mean sea-level change rate (Source: “NASA Goddard Space Flight Center”, 2020).	1
Figure 1-2. Region vulnerable to flooding caused by sea level.	2
Figure 1-3. Asian cities at risk from sea level rise.	3
Figure 1-4. Coastal erosion in Bali Province.....	5
Figure 1-5. Coastal flooding events in Bali Province.....	5
Figure 2-1. Risk dimension, categories, and components retrieved from Bangladesh INFORM Sub-National Risk Index 2022 (UNDRR, 2022).	9
Figure 2-2. GIS for disaster management. (Source: Scanpoint Gematics Ltd., 2022)	12
Figure 2-3. The interface of the BIG website provides the DEM tiles.	15
Figure 2-4. The gray-level DEM imagery data of Bali Province has been merged from 19 tile images.	15
Figure 3-1. Location map of the study area.....	21
Figure 3-2. The interpretation of PlanetScope images shows the diverse shoreline types of Bali: (a) Bedrock shoreline, (b) Mangrove shoreline, (c) Sandy shoreline, (d) Silty shoreline, (e) Farm shoreline, (f) Embankment, (g) Man-made infrastructure.	23
Figure 3-3. Bali Province shoreline lengths were defined by type between 2016 and 2021. (Note: The black boxes mark the significant changes in the two periods).	26
Figure 3-4. Shoreline change rate in Bali Province from 2016 to 2021. The color bar represents the regency.	27
Figure 3-5. Examples of shoreline change between 2016 and 2021 were captured in remote sensing images.	28
Figure 3-6. Land area changes in the coastal area of Bali Province between 2016 and 2021.....	29
Figure 3-7. Yearly average distribution of simulated significant wave height in Bali Province between 2016 and 2021. (Data source: E.U. Copernicus Marine Service Information; Global Ocean Waves Analysis and Forecast).	31
Figure 3-8. Monthly average of simulated significant wave height in Bali Province from 2016 to 2021. (Data source: E.U. Copernicus Marine Service Information; Global Ocean Waves Analysis and Forecast).....	32
Figure 3-9. Yearly averaged of simulated current speed distribution in Bali Province from 2016 to 2021. (Data source: Copernicus Marine Service; Global Ocean Physics Reanalysis).....	33
Figure 3-10. Monthly average of simulated surface current in Bali Province from 2016 to 2021. (Data source: Copernicus Marine Service; Global Ocean Physics Reanalysis).	34
Figure 3-11. Destroyed coastal infrastructure in Bali Province due to erosion in sandy shores in Jembrana and Badung Regencies. (Source: field survey, 10—19 March 2023).....	37
Figure 3-12. Various coastal protection structures in the study area: (a) Seawall with stone-filled gabions combined with revetment; (b) Sandbag at Kuta Beach, Badung Regency; (c) Seawall at Perancak Beach, Jembrana Regency; (d) Seawall at Pererenan Beach, Badung Regency; (e) Groins and (f) Offshore breakwater at Samuh Beach, Badung Regency; (g-h) Groins at Candidasa Beach, Karangasem Regency; (i) Offshore breakwaters at Jerman Beach, Badung Regency; (j-k) Groins at Sanur Beach, Denpasar City (Source: field survey, 10—19 March 2023).	38
Figure 4-1. Flow chart showing the methodology.....	43
Figure 4-2. Land use and land cover in Bali Province.....	44

Figure 4-3. Sea level data from altimetry and tide gauge.	46
Figure 4-4. Sea level data from altimetry and tide gauge.	47
Figure 4-5. Sea level rise prediction based on HHWL.	48
Figure 4-6. Land projected to be below annual flood level in 2025.	49
Figure 4-7. Land projected to be below annual flood level in 2030.	49
Figure 4-8. Land projected to be below annual flood level in 2070.	50
Figure 4-9. Land projected to be below annual flood level in 2100.	50
Figure 4-10. Land use projected to be below water level.	52
Figure 4-11. The extent of land damage due to inundation.	53
Figure 5-1. The study area with grid cells along the shoreline.	57
Figure 5-2. Flow chart outlining the process to obtain a CVI map.	58
Figure 5-3. Sampling locations for model validation.	60
Figure 5-4. The vulnerability rank of geomorphology.	61
Figure 5-5. The vulnerability rank of shoreline changes rate.	62
Figure 5-6. The vulnerability rank of coastal elevation.	63
Figure 5-7. The vulnerability rank of sea level change rate.	64
Figure 5-8. The vulnerability rank of tidal range.	65
Figure 5-9. The vulnerability rank of significant wave height.	66
Figure 5-10. The shoreline length of vulnerability categories as determined by CVI.	67
Figure 5-11. The coastal vulnerability index (CVI) map of Bali Province.	67
Figure 6-1. The location of the study area in Southeast of Bali Island, Indonesia.	72
Figure 6-2. Flowchart of coastline extraction indices comparison.	74
Figure 6-3. Study area in Jembrana Regency.	75
Figure 6-4. Study area in Gianyar and Klungkung Regency.	75
Figure 6-5. Section division for coastal slope values in Bali Province.	76
Figure 6-6. Result of coastline extraction using Normalized Difference Vegetation Index (NDVI) ...	77
Figure 6-7. Result of coastline extraction using Normalized Difference Water Index (NDWI).	78
Figure 6-8. Result of coastline extraction using Modified Normalized Difference Water Index (MNDWI).	79
Figure 6-9. Result of coastline extraction using Water Ratio Index (WRI).	79
Figure 6-10. Result of coastline extraction using Automated Water Extraction Index (AWEI).	80
Figure 6-11. Comparison of all coastline extraction indices.	81
Figure 6-12. Coastline change at Melaya Sub-District.	83
Figure 6-13. Coastline change at Negara Sub-District.	84
Figure 6-14. Coastline change at Jembrana Sub-District.	85
Figure 6-15. Coastline change at Mendoyo Sub-District.	86
Figure 6-16. Coastline change at Pekutatan Sub-District.	87
Figure 6-17. Coastline changes of Gianyar Regency.	89
Figure 6-18. Coastline changes of Klungkung Regency.	90

List of tables

Table 2-1. Spectral bands range and spatial resolution of Sentinel-2A and -2B.....	13
Table 2-2. PlanetScope band order and sensor frequencies.....	14
Table 3-1. Astronomical Tide Level Information	21
Table 3-2. Shoreline categories.....	22
Table 3-3. Length ratio and change rate of different coastline types from 2016 to 2021	25
Table 4-1. Population characteristics of Bali Province.	42
Table 4-2. Description of LULC classification taxonomy.....	45
Table 4-3. Tidal constituents.....	46
Table 4-4. The prediction of inundation area.	51
Table 5-1. Sources and period of the different usage parameters in the compiling of CVI	57
Table 5-2. The risk rating for different parameters.	58
Table 6-1. Comparison of all applied indices to PlanetScope baseline (references).....	81
Table 6-2. Information of coastal area changes (m ²) in Jembrana Regency.	82
Table 6-3. Information of coastal changes in Gianyar and Klungkung Regency.	88
Table 6-4. Tidal correction.....	90

Abbreviations

Bappenas	Badan Perencanaan dan Pembangunan Nasional (National Development Planning Agency)
BIG	Badan Informasi Geospasial (Geospatial Information Agency)
BNPB	Badan Nasional Penanggulangan Bencana (National Agency for Disaster Management)
BPS	Badan Pusat Statistik (Center Bureau of Statistics)
BPS-Bali	BPS Bali Province (Statistic of Bali Province)
BWS Bali-Penida	Balai Wilayah Sungai Bali Penida
CVI	Coastal Vulnerability Index
DEM	Digital Elevation Model
GIS	Geographic Information System
HHWL	Highest High-Water Level
KKP	Kementerian Kelautan dan Perikanan (Ministry of Marine Affairs and Fisheries, MMAF)
MRC	Marine Research Center
MSL	Mean Sea Level
SLR	Sea Level Rise
SWH	Significant Wave Height
Kabupaten	Regency/District
Kecamatan	Sub-district
Desa	Village

CHAPTER 1. INTRODUCTION

1.1. Background – Sea Level Rise and Its Impacts

There is evidence of an increase in the number and intensity of natural disasters across the globe that has imposed ecological and socioeconomic losses in recent decades (Govind and Verchick, 2015; van Aalst, 2006; WorldRiskReport 2022, 2022). Statistically, droughts, floods, storms, and hurricanes are among the most frequent and costly disasters in the last thirty years. In 2022, these disasters caused material losses of 3 to 100 billion dollars, forcing hundreds and thousands of people homeless (Rosane, 2023; Thomas, 2017). This phenomenon is strongly associated with anthropogenic activities, which led to increased greenhouse gasses (GHG) in the atmosphere – also known as global climate change (IPCC, 2018). The International Panel on Climate Change (IPCC), the scientific authority on climate change and its associated impacts, projects that if the present rate of warming continues, it will exponentially increase the intensity of storms, floods, droughts, and rising sea levels with adverse impacts in the future (McGranahan et al., 2007).

It is reported that the global sea level has risen more than 20 cm since the data was first recorded in the 1800s. Although the paleo sea levels have been recorded as exceeding 5 m above the current levels, the present rising rate has been much faster than ever in the last decades (Cazenave et al., 2014a; Cazenave and Cozannet, 2014; Church et al., 2008). Recent studies recorded an increase in the rising rate of sea level from 2 mm year⁻¹ to 3.4 mm year⁻¹ (Dasgupta et al., 2009). Figure 1-1 shows the global mean sea level change rate recorded from multi-mission satellites from 1993 until now.

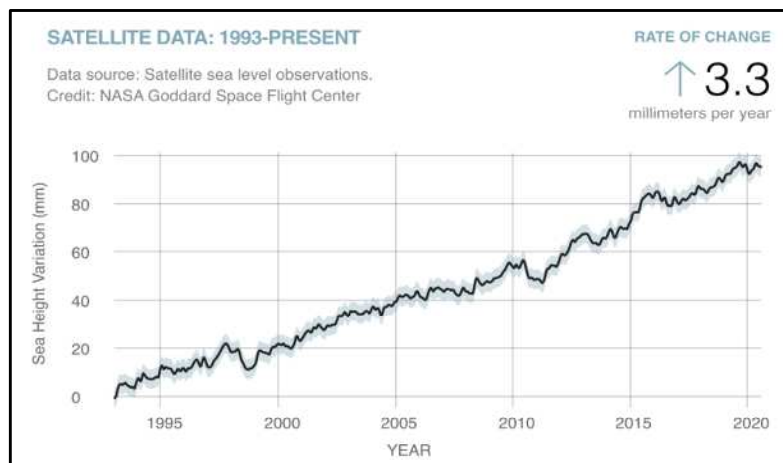


Figure 1-1. The global mean sea-level change rate (Source: “NASA Goddard Space Flight Center”, 2020).

However, the rising rate of sea levels varies around the globe (Cazenave and Cozannet, 2014). Regional processes and climate variability determine the spatial pattern of the sea level rise rate. For example, the rising rate in the western Pacific is higher than in the eastern Pacific due to El Nino-La Nina conditions (Cazenave et al., 2014a; Cazenave and Cozannet, 2014). Consequently, the impact of sea level rise on a global scale cannot be fully implemented on a

regional and local scale. Understanding the impact of sea level rise at the regional and local levels requires further details relative to the local conditions.

Local conditions continuously accelerate the impacts of sea level rise. Four major impacts are possible: 1. inundate and displace wetlands and lowlands; 2. erode shorelines; 3. exacerbate storm flooding and damage; and 4. increase the salinity of estuaries and threaten freshwater aquifers (IPCC, 2001) are already taken as global issues. Some of the impacts also trigger the coastal area vulnerability, which is also pressured by economic activities. Regarding its situation, sea-level rise will be a dramatic problem in future years.

Climate change, with its associated rising sea level and possible increases in the frequency and/or intensity of storms and changes in wave climate, can be expected to significantly increase the risk of coastal erosion and flooding in most coastal locations. The direct impact of the sea-level rise is on the coastal areas, which, aside from being highly resourceful and densely populated, are low-lying and thus would be subjected to erosion and shoreline retreat due to increased wave strength as water depth increases near the shore (Pirazzoli, 1996; Pye and Blott, 2006). The varying topography and acute weather occurrence will affect coastal communities and their capability to withstand such destructive consequences. Since nearly 40% of the global population lives within 100 km of the coastal areas, global climate change poses a significant threat to coastal communities (Cazenave and Cozannet, 2014). Moreover, rising sea levels will devastate the livelihood of the densely populated coastal communities (Church and White, 2011). In addition, more than 200 million people worldwide are vulnerable to flooding by extreme sea levels (Nicholls, 2010). Figure 1-2 shows the vulnerable region that will be flooding caused by sea-level rise (Nicholls and Cazenave, 2010). The above suggests that projecting the impact of sea level rise and their potential exposure to coastal populations is critical for coastal planning and global climate change mitigation.

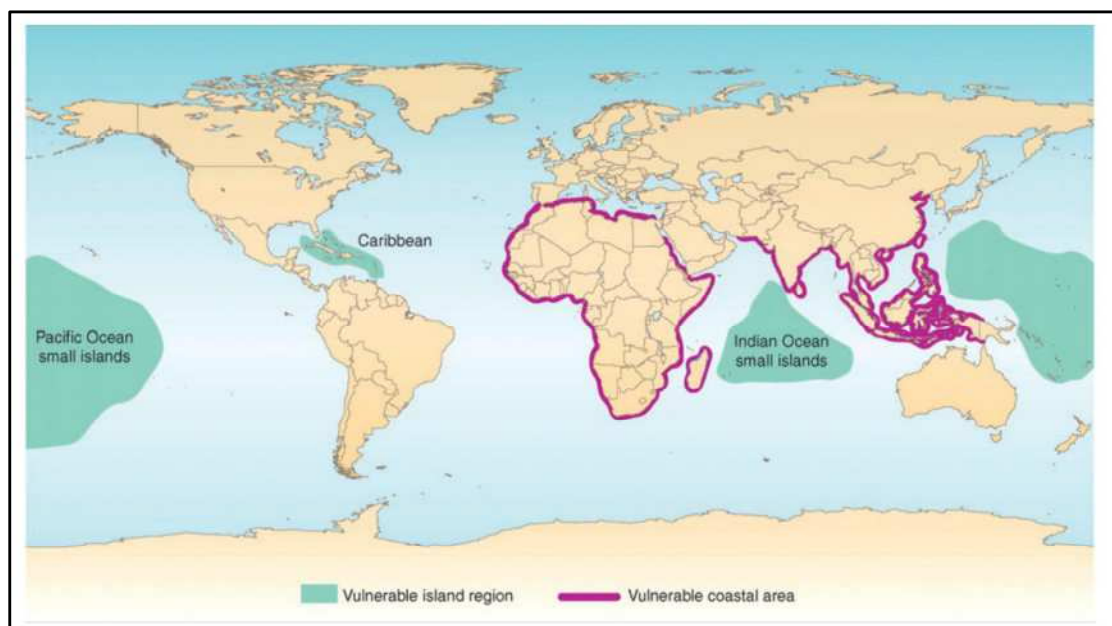


Figure 1-2. Region vulnerable to flooding caused by sea level.

It is now widely accepted that coastal areas, especially low-lying areas, are the most susceptible to the impact of global climate change (Devoy, 2015; Rizzo and Anfuso, 2020), especially its large river deltas (Fuchs, 2010), including Indonesia, are most vulnerable to climate change, potentially affecting the coastal population and natural environment (Brown, 2001). Seventeen percent of the total urban population in Asia lives in the low-elevation coastal zone. In contrast, in South-Eastern Asia, more than one-third of the urban population lives in this extremely vulnerable zone. Figure 1-3 shows the population at risk from sea level rise in Asian cities.

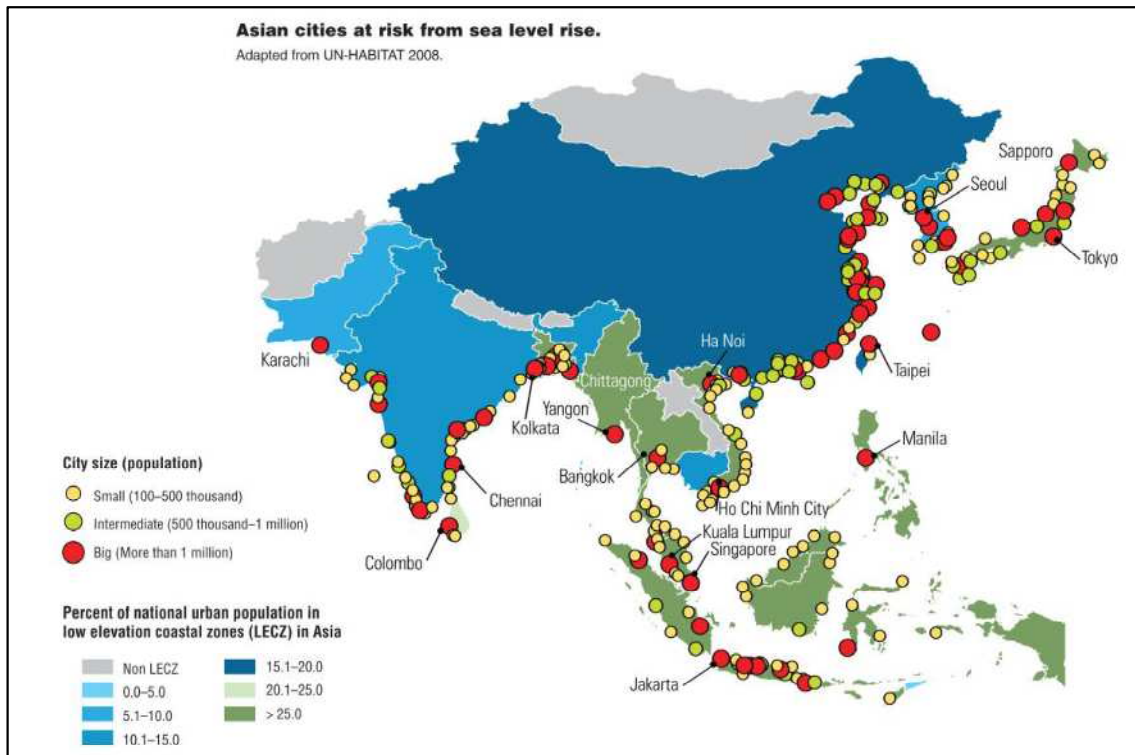


Figure 1-3. Asian cities at risk from sea level rise.

The Indonesian archipelago, situated between the Indian and Pacific oceans, along with other East Asia Pacific countries, is among the most vulnerable to the impacts of climate change (Dasgupta et al., 2009). With approximately 17,508 islands and a coastline length of more than 95,000 km, changes in sea levels will significantly affect the territory of the Indonesian archipelago. Most of the population depends on coastal marine resources and occupies large cities in low-lying coastal areas

Based on observations, from the 1990s to 2019, the sea levels in Indonesian waters show an increasing trend (Han et al., 2022; Zikra et al., 2015). In addition, there are spatial variations in the sea level height in Indonesian waters. The sea levels in Indonesia bordering the Pacific Ocean are generally higher than the Indian Ocean. In addition, seasonal variations and extreme natural phenomena strongly influence the sea level heights in Indonesian waters (Triana and Wahyudi, 2020a). Although several researches have been devoted to investigating the impacts of sea level rise in Indonesia, mainly focusing on Java, the main island (Handiani et al., 2022; Marfai and King, 2008; Putri et al., 2021; Ward et al., 2011) not enough research has been made to investigate the impacts of sea level rise on the rest of the archipelago. . Therefore,

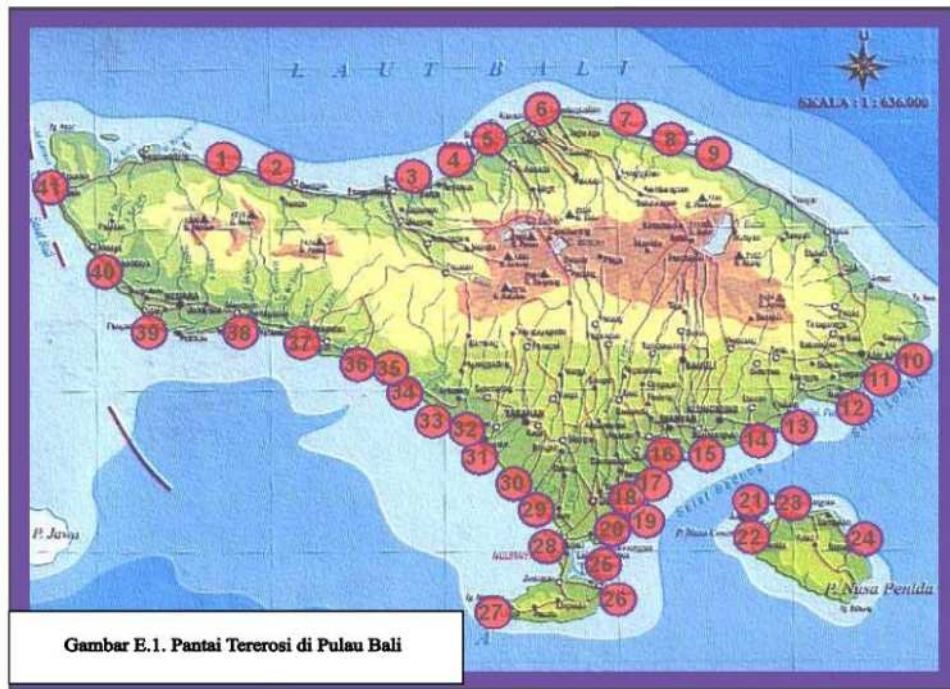
coastal planning and climate change mitigation require serious attention in Indonesia (Setiyowati et al., 2016). The land subsidence due to excessive groundwater exploitation exacerbates the impact of sea level rise in these coastal cities. Coastal inundation due to rising sea levels will cause socioeconomic losses to coastal communities in the Indonesian archipelago.

Furthermore, rising sea levels have many adverse impacts, including inundation of coastal plains, increased beach and coastal erosion, removal of protecting sand dunes and vegetation, and intrusion of salt water into freshwater supplies. As the coastal population and economic assets increase, it will be essential to understand how they may be affected by natural hazards. The coastal areas are vulnerable to various natural hazards, including erosion, land subsidence, and changes in hydrology, and are often in areas with increasing population densities (Özyurt and Ergin, 2010). In this context, identifying the vulnerability of various coastal sectors to the impact of rising sea levels is indispensable for coastal zone management. Quantification is needed to determine the degree of vulnerability experienced by a coast (Sanchez-Arcilla et al., 1998) since measuring vulnerability is a fundamental phase towards effective risk reduction (Birkman, 2006). In addition, identifying shoreline changes early and understanding normal shoreline behavior is essential in recognizing ecological problems in coastal areas. Monitoring shoreline change over an extended period will result in a better understanding of its effect.

1.2. Research Problems

The coastal area considered the most vulnerable area affected by climate change, suffered a significant impact. A warning of this microclimate appears evident in symptoms such as drought, floods, and loss of marine habitat through coral bleaching and coastal erosion. Losing coastal ecosystems would also negatively affect tourism, infrastructure, freshwater supplies, biodiversity, and fisheries.

Climate change is predicted to severely impact its coastal area and small islands, such as Bali Island. Bali Island, the mainland of Bali Province, has a beach length of ~593 km, and about 18% are coral beaches with white sand. This small island makes up only 0.3% of Indonesia's landmass and is home to 1.4% of Indonesia's population - 80% of which rely on the tourism industry. However, about 86 km, or 20% of the length of the existing beaches, have been eroded (Government of Bali Province, 2015) due to natural factors and human activities (Figure 1-4). In addition, Bali has experienced severe environmental degradation due to changing land use and lifestyles (Sutawa, 2012) .



Gambar E.1. Pantai Tererosi di Pulau Bali

Figure 1-4. Coastal erosion in Bali Province.

The risks created by sea-level rise impact coastal erosion and flooding in some areas along Bali's coastline. It should be noted that flooding and coastal erosion also present a very serious risk to public assets, critical infrastructure, and transport.

- In August 2016, high waves and flooding struck Leping Beach. This submerged about 5 hectares of rice fields. It was inundated by seawater due to tidal waves.
- In January 2019, high waves and rob strikes struck Penimbangan Beach, Buleleng Regency, causing dozens of small traders' stalls on the beach area to be swept up by 5-meter-high waves. The high waves also damaged roads, around 6 meters long and 5 meters wide, broken due to being hit by the waves.
- In July 2019, the water overflowed and inundated the road when the high waves struck Kuta Beach.
- In July 2022, high tide and flooding occurred at Rangkakan Beach and Sangat Beach, Gianyar Regency. The water overflowed and inundated the road.



Figure 1-5. Coastal flooding events in Bali Province.

The various environmental problems are potentially increasing as climate change, associated with rising sea levels, occurs. Sea-level rise may lead to more risk and more damages

and losses. Therefore, vulnerability assessment of coastal areas and coastline change monitoring is necessary to understand better the impact of natural hazards in Bali Province, which is affected by sea-level rise, as well as the adaptive capacities of human and natural systems. This assessment can help evaluate whether the coastal area is resilient or susceptible to this hazard within a large domain and even at different time scales. Furthermore, this assessment is an approach to showing the potential negative impacts that may arise due to an existing potential disaster.

As a decision-maker in disaster risk reduction, the government has to accommodate the potential loss of natural hazards. The potential economic loss will be an entrance in appreciating the future damage as a negotiating factor in the disaster risk reduction action plan. On the other hand, in local communities, adaptation has been a great response to dealing with climate change, especially in coastal and low-lying areas vulnerable to its impact.

National assessment of coastal vulnerability has been carried out by the Marine Research Center - Ministry of Marine Affairs and Fisheries (2009) and Badan Perencanaan dan Pembangunan Nasional (Bappenas, National Development Planning Agency) (2018) using the Coastal Vulnerability Index (CVI). Despite the national assessments being done, data resolution used in the national assessment is low resolution with consideration and ranges nationally. This assessment might not be suitable for decision-making on a local or regional scale. Furthermore, Badan Nasional Penanggulangan Bencana (BNPB, National Agency for Disaster Management) has issued a disaster index using 2015 data and produced a disaster risk map with a scale of 1:250,000 for the national scale. Disaster risk assessment was calculated using a 1-hectare grid size and divided into three classes of risk rating, which are high, moderate, and low risk. Based on that assessment, 1,800 km of shoreline in Indonesia has a very-high vulnerability, with the total potential economic loss for the marine sector at 400.8 trillion Rupiah and the coastal sector at 6.7 trillion Rupiah.

In addition, based on the Regulation from the National Agency for Disaster Management (BNPB) of the Republic of Indonesia No. 2/2012 on the General Guidelines for Disaster Risk Assessment, the vulnerability assessment should ideally start from the district/municipality level. The results of all district/municipality studies are then compiled at the provincial level. The results of all provincial-level studies are then compiled at the national level. If this ideal condition is created, the effectiveness of disaster management for every disaster that threatens Indonesia will be obtained with appropriate support, both budgetary and technical, from the national to district/municipality level. The period of validity for a regional disaster risk assessment is five years. This is because one of the main functions of this study is to form the basis for preparing a Disaster Management Plan. As is well known, the period of disaster management planning is five years. Disaster risk assessment can be reviewed periodically every two years or at any time in the event of a disaster and extreme conditions that require revision and assessment of existing ones. Disaster risk assessment is an approach to show the potential negative impacts that may arise due to an existing potential disaster. The potential negative impacts are also calculated by considering the level of vulnerability and capacity of the area.

1.3. Research Objectives

General Objectives:

The primary purpose of this research is to investigate and assess the vulnerability of the Bali Province coast to the effect of coastal erosion.

Specific Objectives:

- To determine the physical and geological parameters in the area that are necessary for evaluating coastal zones vulnerable to SLR;
- To identify the area submergence in different sea level scenarios based on the derived annual SLR rates and actual tidal measurements;
- To analyze the dynamic changes in shoreline position from satellite images.

1.4. Dissertation Structure

This dissertation is divided into seven chapters and listed as follows:

- **Chapter 1 – Introduction**
This chapter explains the general overview of the research, comprising the rationale and background, objectives, and dissertation structure.
- **Chapter 2 – Literature Review and Methodology**
This chapter explores the extensive background of previous studies' theories, methods, and summary.
- **Chapter 3 – Coastline Change Detection**
This chapter evaluates the coastline change and coastal protection strategy in Bali Province.
- **Chapter 4 – Coastal Flood Impacts Detection**
This chapter examines the future coastal flooding from tide models.
- **Chapter 5 – Coastal Vulnerability in Bali Province from Physical Parameters**
This chapter determines the coastal vulnerability from the physical and geomorphological factors with the case study in Bali Province.
- **Chapter 6 – Accuracy Assessment of Coastline Extraction**
This chapter evaluates of automatically delineating sandy beaches coastline of five commonly techniques for coastline extraction.
- **Chapter 7 – Concluding Remarks and Outlook**
This chapter recapitulates the study results and offers suggestions for future studies.

CHAPTER 2. LITERATURE REVIEW AND METHODOLOGY

2.1. Literature Review

2.1.1. Definitions of Hazard, Vulnerability, and Risk

A hazard is a potential source of danger or harm within an environment or system (UNISDR, 2009a). Hazards can be natural, i.e., earthquakes, floods, hurricanes, or human-made, i.e., chemical spills, industrial accidents, or unsafe construction practices. The hazard represents the conditions or events that can potentially cause adverse effects, but the impact depends on the exposure and vulnerability of the affected entities.

There are varied definitions of vulnerability. Vulnerability is the extent of harm that can be expected under certain conditions of exposure, susceptibility, and resilience (Balica et al., 2012; Fuchs, 2010; Hufschmidt, 2011; Scheuer et al., 2011; Willroth et al., 2011). The Intergovernmental Panel on Climate Change (IPCC, 2001) defines vulnerability as a function of exposure, sensitivity, and adaptive capacity. Based on the Regulation from the National Agency for Disaster Management (BNPB) of the Republic of Indonesia No. 2/2012 on the General Guidelines for Disaster Risk Assessment, vulnerability is a condition of a community and/or society that leads or causes an inability to cope with the threat of disaster.

Risk is the potential for harm, damage, loss, or adverse consequences arising from an event or action (UNISDR, 2009a). It combines the likelihood of an event occurring with the potential impact or severity of the consequences. In other words, risk assesses the probability of an adverse outcome resulting from exposure to a hazard, considering the vulnerability of the exposed entities or systems.

According to the framework proposed by the UN International Strategy for Disaster Reduction (UNISDR, 2009b), the analysis of the likely impacts or risk related to hazards involves the evaluation of two main components: hazard (i.e., an event or phenomenon with the potential to cause harm, such as loss of life, social and economic damage or environmental degradation) and the system vulnerability (i.e., characteristic of a system that increases its susceptibility to the impact of climate-induced hazards). In this context, vulnerability is often expressed in several qualitative indexes and is a key step toward risk assessment and management (Romieu et al., 2010).

$$Risk = Hazard \times Vulnerability$$

Recognizing vulnerability as a critical element in the risk context has also been accompanied by growing interest in understanding and enhancing the positive capacities of people to cope with the impact of hazards. Furthermore, assessing the vulnerability is extremely important in assessing the potential consequences of an event and for mainstreaming disaster risk reduction into the local development planning processes.

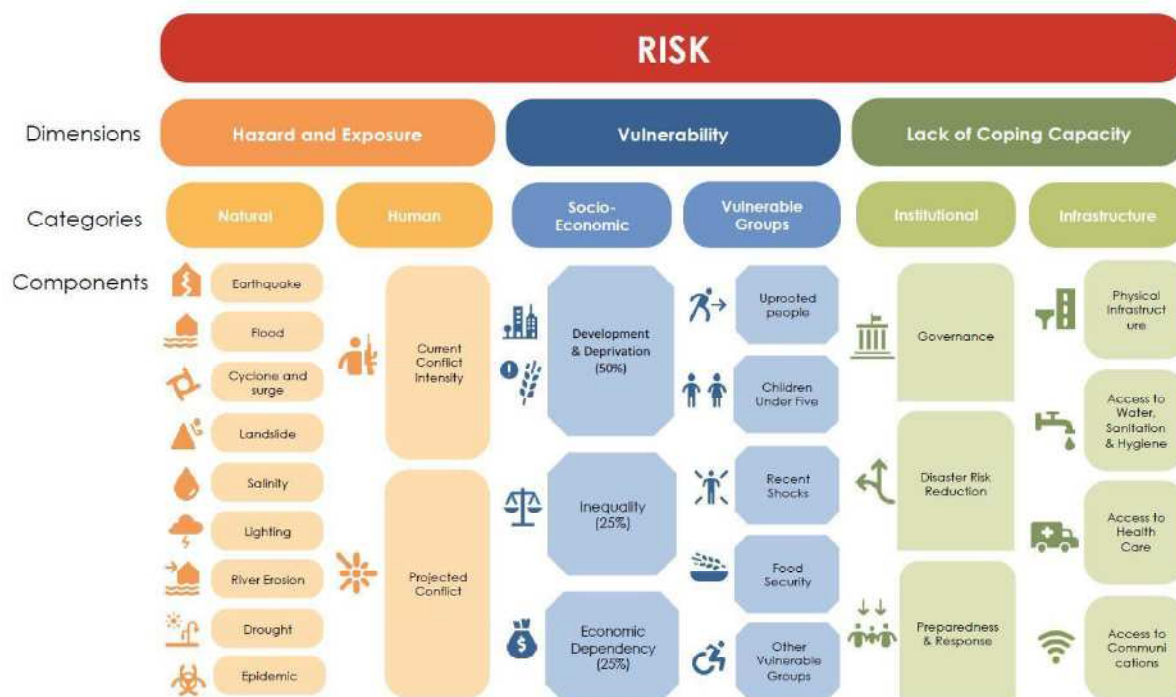


Figure 2-1. Risk dimension, categories, and components retrieved from Bangladesh INFORM Sub-National Risk Index 2022 (UNDRR, 2022).

To illustrate the relationship between these terms, a hazard like rising sea level (including coastal flooding, erosion, saltwater intrusion, etc.) poses a risk to buildings and infrastructure in coastal zones. The level of risk depends on the vulnerability of the physical conditions (geographical location, ecosystems, and habitats, etc.) and the population’s vulnerability (their preparedness, socioeconomic conditions, etc.) to withstand and recover from the rising sea level’s impact. In risk assessment and management, these concepts are used to make informed decisions and take actions to reduce or mitigate potential adverse outcomes.

2.1.2. Coastal Zone

The coastal zone is an area of transition between the purely terrestrial and purely marine components (Crossland et al., 2005) and the most dynamic interfaces on Earth’s surface. The coastal zone, also referred to as the littoral zone, is the area where land and ocean meet, typically encompassing the region from the high-tide mark on the landward side to the outer limit of marine influence, which can extend seaward to include nearshore waters and submerged land features like sandbars and reefs.

The coastal area is difficult to define due to its dynamic and ever-changing zone and depends on the jurisdiction or intended use (Finkl, 2016). Based on Law of the Republic of Indonesia No. 1/2014 amending Law No. 27/2007 on the Management of Coastal Zones and Small Islands, coastal areas are defined as the transitional area between land and marine ecosystems influenced by land and sea changes. In addition, that definition was also enacted in the Regulation of the Minister of Marine Affairs and Fisheries of the Republic of Indonesia No 23/Permen-KP/2016 concerning Coastal Area and Small Islands Management Planning.

These zones are important because most of the world's population inhabits such zones. It is an ecologically and economically significant area supporting many habitats, communities, and activities. Coastal zones are continually changing because of the dynamic interaction between the oceans and the land. Waves and winds along the coast erode rocks and deposit sediment continuously, with erosion and deposition rates varying considerably from day to day along such zones. The energy reaching the coast can become high during storms, and such high energies make coastal zones highly vulnerable to natural hazards. Thus, understanding the interactions of the oceans and the land is essential in understanding the hazards associated with coastal zones.

2.1.3. Coastal Vulnerability

Coastal vulnerability is the degree to which a system is susceptible to or unable to cope with natural hazards and is mainly dependent on the extent of development within the coastal zone (Cooper and McKenna, 2008; Gornitz et al., 1991; O'Connor et al., 2009). Vulnerability evaluates the combination of sensitivity and exposure to an impact (Abuodha and Woodroffe, 2006) and determines the impact probability by classifying vulnerability according to various intensities. The vulnerability of a coastal area is distinct to a given location, group, or sector and, therefore, is dependent upon socioeconomic (Hinkel and Klein, 2009) and ecological characteristics of the area (Gornitz et al., 1991; Tragaki et al., 2018).

Coastal zones are highly vulnerable to the impacts of human activities, land cover change, sea level rise, and climate extremes. Coastal vulnerability is a spatial concept that identifies people and places susceptible to disturbances resulting from coastal hazards. Hazards in the coastal environment, such as coastal storms, sea level rise, and erosion, pose significant threats to coastal physical, economic, and social systems.

Coastal vulnerability assessment is the result of identifying, quantifying, and prioritizing (or ranking) the vulnerabilities in the coastal systems. This involves social, economic, and environmental aspects and the institutional context. The coastal vulnerability assessment is carried out to ensure the risk of susceptibility to anthropogenic assets and infrastructure, with its primary purpose being to provide information to guide the process of adaptation and enhance society's adaptive capacity (Kelly and Adger, 2000).

2.1.4. Coastal Flooding

Coastal flooding is where any part of the land becomes inundated by seawater, contrary to normal conditions. This can be by storm surges, breaching, overtopping, sea level rise, or tsunamis. When one of these components is at an extreme level, it can temporarily push water levels across a threshold or cause a breach/failure of a coastal defense structure, resulting in significant inundation of coastal areas.

Coastal flooding often occurs when seasonal high tides and storms push water ashore. However, as sea levels rise, flooding in coastal communities increasingly occurs on less extreme tides or weak winds, even on sunny days. Coastal flooding is largely a natural event. However, human influences on the environment can exacerbate this. Engineered protection

structures along the coast, such as a seawall, alter the natural processes of the beach, often leading to erosion on an adjacent stretch of the coast, which also increases the risk of flooding. Sea level changes and the extreme weather caused by climate change have increased the intensity and occurrences of storms, coastal flooding, and inundation of low-lying areas (Oppenheimer et al., 2019). Sea level rise is an example of the long-term impact of global climate change on the coastal area.

There are several stages of coastal flooding to clarify the amount of water over normal tides:

- a. Minor: harmful coastal flooding in areas adjacent to the coast. Minor beach erosion may occur. Minor coastal flooding is not expected to block roads or cause major structural damage to homes and other buildings.
- b. Moderate: coastal flooding is more severe, threatening life and property. Some roads may be impassable due to flooding. Moderate beach erosion and damage to some homes, businesses, and other facilities will occur.
- c. Major: a serious threat to life and property. Many roads may be flooded. Many homes and businesses along the coast will suffer significant damage. Everyone should consider safety precautions and prepare to evacuate if necessary. Significant beach erosion is also expected.

Coastal flooding is something that can happen anywhere along a coastline. Especially the last few decades have proven significant as it appears to happen more often, and coastal areas attract more people, tourists, and locals alike. The latter could potentially lead to more casualties when coastal flooding happens. Coastal flooding impacts include frequent road closures, reduced stormwater drainage, infrastructure deterioration, and saltwater intrusion. These impacts can also affect human health: for example, deterioration of water infrastructure and saltwater intrusion can expose people to pathogens and toxic chemicals.

2.1.5. Shoreline Change

Shoreline change refers to the loss or gain of land area or changes to the landscape on the marine edge. It is an important indicator of environmental threats in beach areas. It is a problem because natural habitats are altered as shorelines change and may destroy cultural resources, facilities, and other infrastructure.

Shoreline change is a potential consequence of climate-change-driven sea-level rise due to permanent passive submersion and coastal erosion (Ranasinghe et al., 2012; Yang et al., 2013; Zhang et al., 2004). Additionally, increasing anthropic activities in coastal areas, such as beach nourishment, port construction, and tourism development, tend to change the coastal environment and reshape the coastline (Jennings, 2004; Peterson and Bishop, 2005; Syvitski et al., 2009; Tanaka and Sato, 1976).

2.2. Methodology

2.2.1. Remote Sensing and GIS Techniques for Disaster Management and Coastal Zone Monitoring

Remote sensing technology acquires and records information without direct contact with objects. Remote sensing has been refined as the science and technology of earth observation, including space-earth observation, airborne observation, and field monitoring.

GIS is an important and specific spatial information system. This technical is intended to collect, store, manage, exploit, analyze, display, and describe geographical distribution data of all or part of the Earth's surface (including the atmosphere). In addition, Husman and de By (2009) define GIS as a computer-based system that presents the following four sets of capabilities to handle georeferenced data: data capture and preparation, data management, including storage and maintenance, data manipulation and analysis, and presentation. Remote sensing and GIS technology help identify disasters before they occur, using forecast or risk zone maps. GIS has a role in disaster, as Figure 2-2 shows.

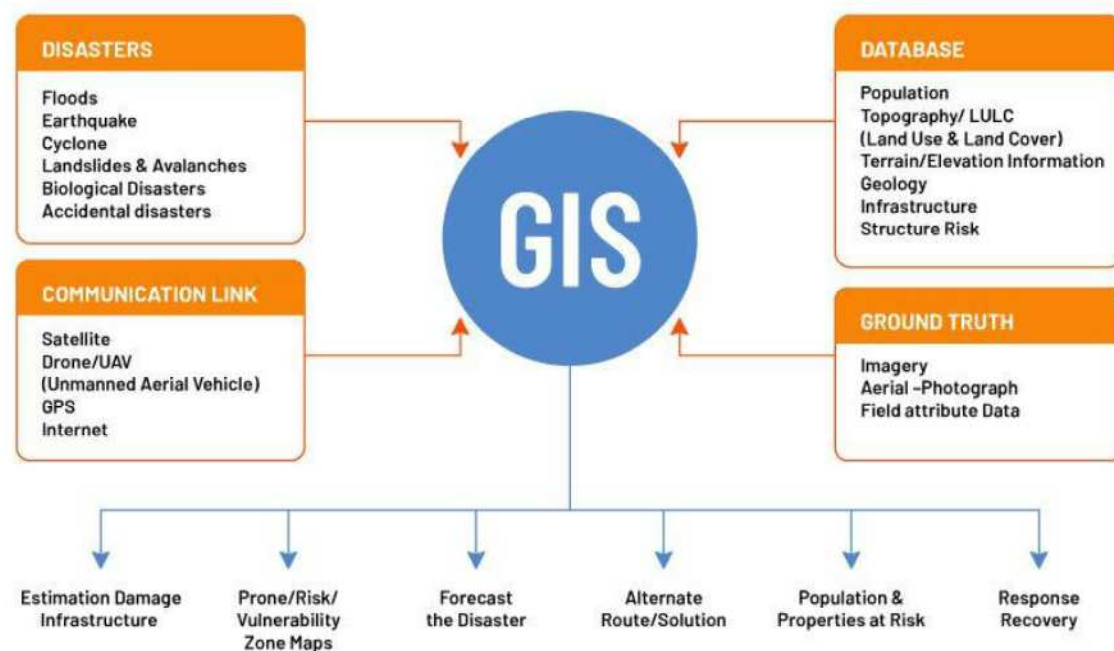


Figure 2-2. GIS for disaster management. (Source: Scanpoint Gematics Ltd., 2022)

Coastal zone monitoring primarily includes the content of the shoreline displacement, landscape change, ecosystem change, and environmental pollution. Traditional research methods in monitoring coastal areas have certain limitations. The intensity of monitoring and activity itself need help to meet the need for real-time monitoring due to coastal development, environmental changes, and natural disasters. Remote sensing is a modern technology for monitoring due to its ability to provide synoptic information over wide areas with high acquisition frequencies (Maselli, 2004). Remote sensing has been widely used in resource development, coastal planning and management, monitoring shoreline changes, and understanding physical processes in coastal environments using geographic information

systems (GIS) (Ghionis et al., 2014). With the development of remote sensing, monitoring of coastal zones is easily achieved by image processing. Satellite images play a significant role in spatiotemporal studies where the obtainable free satellite image facilitates the detection of changes.

2.2.2. Sentinel-2 Image

The Copernicus SENTINEL-2 mission comprises a constellation of two polar-orbiting satellites in the same sun-synchronous orbit, phased at 180° to each other. It aims at monitoring variability in land surface conditions and its wide swath width (290 km) and high revisit time (10 days at the equator with one satellite and 5 days with two satellites under cloud-free conditions, which results in 2-3 days at mid-latitudes) will support monitoring of Earth's surface changes. Sentinel-2 is a multispectral image with fine resolution provided by the European Space Agency (ESA), which has a mission to observe land, vegetation, water, and coastal areas. Sentinel-2 has 13 spectral bands: near-infrared and four bands at 10 m, six bands at 20 m, and three bands at 60 m spatial resolution (European Space Agency, 2018). Each of these bands has a function. For shoreline detection applications, the relevant spectral bands are the visible band (Blue, Green, Red), the near-infrared band (NIR), and the short-wave infrared band (SWIR).

Table 2-1. Spectral bands range and spatial resolution of Sentinel-2A and -2B

Spatial Resolution (m)	Bands	Sentinel-2A		Sentinel-2B	
		Central wavelength (nm)	Bandwidth (nm)	Central Wavelength (nm)	Bandwidth (nm)
10	Band 2—Blue	492.4	66	492.1	66
	Band 3—Green	559.8	36	559	36
	Band 4—Red	664.6	31	664.9	31
	Band 8—NIR	832.8	106	832.9	106
20	Band 6—Red edge	740.5	15	739.1	15
	Band 7—Red edge	782.8	20	779.7	20
	Band 8A—Narrow NIR	864.7	21	864	22
	Band 11—SWIR	1613.7	91	1610.4	94
	Band 12—SWIR	2202.4	175	2185.7	185
60	Band 1—Coastal aerosol	442.7	21	442.2	21
	Band 9—Water vapour	945.1	20	943.2	21
	Band 10—SWIR—Cirrus	1373.5	31	1376.9	30

2.2.3. PlanetScope Image

The PlanetScope satellite constellation consists of multiple launches of groups of individual cubesats (Doves and SuperDoves). These constellations comprise hundreds of satellites equipped with RGB and infrared sensors. Introduced in March 2016, the PlanetScope constellation consists of more than 130 satellites operating in a sun-synchronous orbit around the Earth, featuring a swath size ranging from 24 to 32.5 km. The PlanetScope Dove constellation has a daily or sub-daily temporal resolution, with pixel size or spatial resolution of 3.7 m at the nadir and resampled to a 3 m fixed resolution, which is significantly higher than the 10–30 m resolution of Landsat and Sentinel-2 imageries (Doherty et al., 2022; Mansaray et al., 2021). PlanetScope imagery products are derived from three cohorts of satellites, with

instruments IDs of *PS2*, *PS2.SD*, and *PSB.SD*. Depending on the scene product requested—3-band, 4-band, or 8-band—imagery can come back from a combination of different sensors. Table 2-2 provides the frequencies of the imagery returned from the three sensors. Considering that PlanetScope is a new technology, researchers are still investigating its characteristics. A study on developing a user-friendly approach and toolkit has also been conducted.

Table 2-2. PlanetScope band order and sensor frequencies

Band Order and Sensor Frequency			
	Imagery Frequency of Order Returned from PlanetScope Sensors		
Bands Ordered	Imagery from PS2	Imagery from PS2.SD	Imagery from PSB.SD
3-band			
Band 1 = Red	Red: 590 - 670 nm	Red: 650 - 682 nm	Red: 650 - 680 nm
Band 2 = Green	Green: 500 - 590 nm	Green: 547 - 585 nm	Green: 547 - 585 nm
Band 3 = Blue	Blue: 455 - 515 nm	Blue: 464 - 517 nm	Blue: 465 - 515 nm
4-band			
Band 1 = Blue	Blue: 455 - 515 nm	Blue: 464 - 517 nm	Blue: 465 - 515 nm
Band 2 = Green	Green: 500 - 590 nm	Green: 547 - 585 nm	Green: 547 - 585 nm
Band 3 = Red	Red: 590 - 670 nm	Red: 650 - 682 nm	Red: 650 - 680 nm
Band 4 = Near-infrared	NIR: 780 - 860 nm	NIR: 846 - 888 nm	NIR: 845 - 885 nm
8-band			
Band 1 = Coastal Blue	n/a	n/a	Coastal Blue 431 - 452 nm
Band 2 = Blue			Blue: 465 - 515 nm
Band 3 = Green I			Green I: 513 - 549 nm
Band 4 = Green			Green: 547 - 583 nm
Band 5 = Yellow			Yellow: 600 - 620 nm
Band 6 = Red			Red: 650 - 680 nm
Band 7 = Red Edge			Red Edge: 697 - 713 nm
Band 8 = Near-infrared			NIR: 845 - 885 nm

2.2.4. Digital Elevation Model (DEM)

Digital Elevation Model (DEM) is a digital cartographic dataset model of the earth's surface in three (XYZ) coordinates and has been derived from contour lines or photogrammetric methods (Gandhi and Sarkar, 2016). DEM forms one of the most frequently used spatial data sources in GIS projects. They are also the basis for a large number of derivative information to be generated. Digital Elevation Models can either be stored in vector or raster format. DEM is commonly used interchangeably with the digital terrain model (DTM) and digital surface model (DSM) with slightly different surface representations. DEM data files that contain the elevation of the terrain over a specified area, usually at a fixed grid interval over the surface of the earth. The intervals between each grid point will always reference some geographical coordinate system.

Geospatial Information Agency (Badan Informasi Geospasial, BIG) provides a high spatial resolution of DEM. DEM data with 0.27 arcsecond (~8.1 m) resolution using the EGM2008 vertical datum available at tides.big.go.id/DEMNAS/ and built from several data

resources, including IFSAR (5 m resolution), TERRASAR-X (5 m resolution) and ALOS PALSAR (11.25 m resolution) data (BIG, 2020).

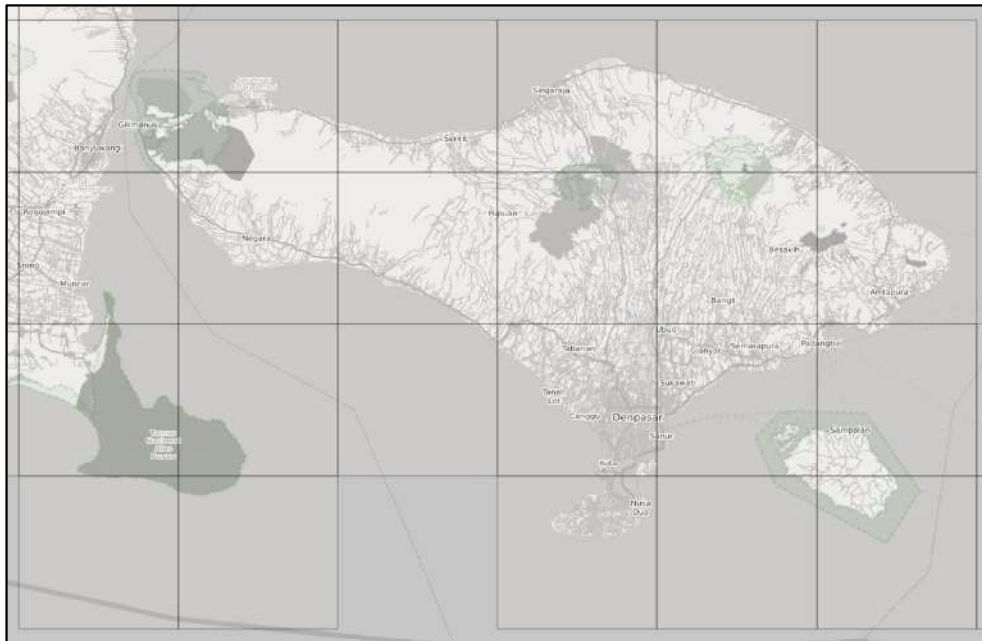


Figure 2-3. The interface of the BIG website provides the DEM tiles.

DEMs are distributed and packaged in small tiles to keep file sizes and processing times manageable. Before continuing to download, you need to determine which tile(s) you need. Figure 2-3 shows the tile of DEM data, which has a number ID to download and is available in *.tif format. After data is downloaded, the next step is merging two or more DEM tiles. When the DEMs are merged, they are combined into a single new DEM that can be used for contour generation or other analysis without modifying the original DEM.

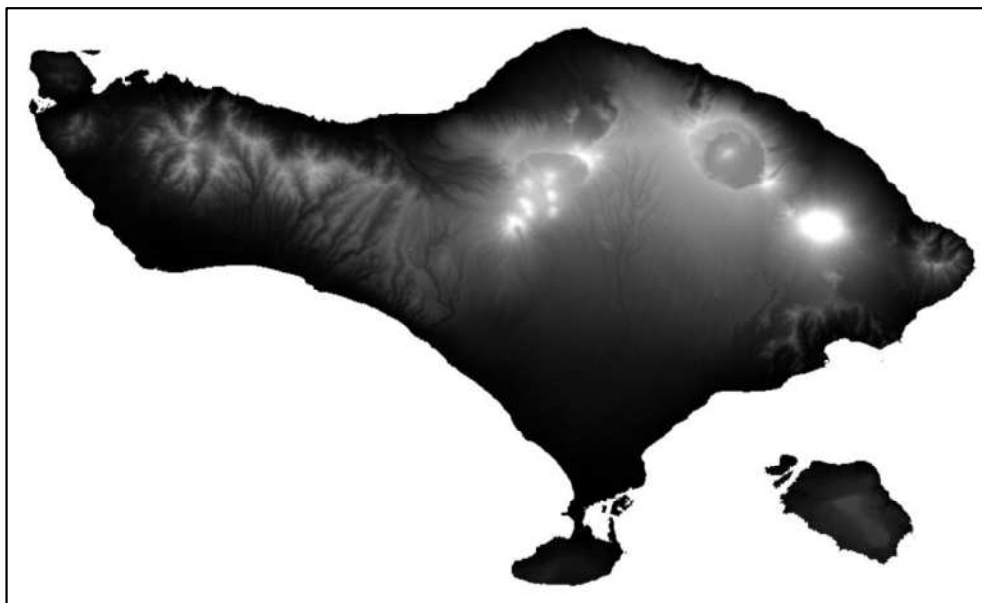


Figure 2-4. The gray-level DEM imagery data of Bali Province has been merged from 19 tile images.

2.2.5. Overview of The Study Area

This study was carried out along the shoreline of Bali Province, Indonesia. Bali is located between the islands of Java and Lombok and is located at 8°03'40"–8°50'48" S and 114°25'53"–115°42'40" E. Bali is part of Lesser Sunda, which stretches approximately 153 km from west to east and 112 km from north to south and has a total land area of 5,590.15 km², accounting for 0.29% of Indonesia. Bali is bordered by the Bali Sea to the north, the Bali Strait to the west, the Lombok Strait to the east, and the Indian Ocean to the south.

The topography of Bali is defined by a mountain chain that stretches from west to east, dividing the island into two parts, north and south. Topography has played an important role in coastal evolution and control of present-day coastal morphologies and types of coastline by providing regional slope by establishing the initial orientation concerning prevailing winds and waves and through local variations such as embayment and headlands from valleys and interfluves (Belknap and Kraft, 1985; Dillenburg et al., 2000). Most beaches in Bali Province are characterized by sandy beaches composed of volcanic alluvial deposits. In contrast, the southern beaches of Bali and Nusa Island are composed of limestone formations (cliff coast) (Purbo-Hadiwidjojo et al., 1998). Moreover, some areas have mangrove-lines beaches, such as Benoa Bay, Gilimanuk Bay, and the northern part of Nusa Lembongan Island.

According to the bathymetry map, Bali Province's coastal waters are typically classified as deep and steep. This is because the seawater around Bali Island is a transition zone between the Sunda Shelf in the west and the Sahul Shelf in the east (Shipton et al., 2021). Bali Province experiences a mixed semi-diurnal tidal cycle, which means it has a cycle with two high and low tides of different sizes every lunar day (Berlianty and Yanagi, 2015a; Hanifa et al., 2020; Widiawan and Nurdjaman, 2018). Astronomical tides range from 2.133 to 3.265 m (Hastuti et al., 2022a) and can reach up to 5 m when combined with meteorological tides. Changes in sea depth and the rise and fall of tides, which distribute wave energy along the shore, can cause changes in the position of the shoreline (Pelling et al., 2013; Narayana, 2016).

The coastal zone plays a crucial role in driving the social and economic development of Bali Province. It serves as a human settlement center, with most of the island's population residing along the shore, significantly contributing to the region's economy and governance (Mujiburrahman et al., 2020). Coastal areas are the main tourist attractions; hence, the tourism sector contributes significantly to the economy of the Bali Province (Antara and Sumarniasih, 2017). Bali's coastal waters also support a robust industry, providing livelihoods for local communities (Rajendra, 2020a). The coastal plains of the Bali Province are fertile and suitable for agriculture (Widhianthini, 2022). Additionally, aquaculture activities such as fish and shrimp farming are carried out in coastal areas, contributing to the production and supply of seafood (Gusmawati et al., 2016; Oktopura et al., 2020). Bali's coastal areas are also used for salt production. Salt farms and salt pans are established along the shoreline, where saltwater evaporates to produce salt (Mujiburrahman et al., 2020). This industry provides employment and contributes to the local economy (Mahasin et al., 2020). Besides their economic significance, Bali's coastal areas are deeply rooted in Hinduism's culture, traditions, and religion (Bakker, 1997). Many religious ceremonies are held on the beach; hence, it is necessary to recognize that coastal areas are important in Balinese culture and contribute to the

people's cultural identity (Murni et al., 2018). As a result, the coastal region is important in terms of the socio-economic and cultural heritage of Bali Province.

2.2.6. Accuracy Assessment

Accuracy assessment is crucial for evaluating the reliability and precision of data and information generated from remote sensing and GIS technologies. It helps ensure that the data used for decision-making is trustworthy. This assessment is often assessed by comparing the classification with some reference data. The common methods to obtain the reference data for accuracy assessment are:

1. Field survey (ground truth): One of the most direct methods is to conduct a field survey, where ground truth data is collected to verify the accuracy of remotely sensed or GIS-derived information. Field surveys involved physical visits to locations, collecting data, and comparing it to the data obtained through remote sensing or GIS.
2. Control points: Control points are precisely located features with known coordinates. They serve as reference points for assessing the accuracy of remotely sensed data. Ground truth data is collected at these control points, and the results are compared to the remotely sensed data.
3. Root Mean Square Error (RMSE): Used to measure the difference between predicted and observed values in regression analysis. In remote sensing and GIS, it can be applied to assess the accuracy of continuous data, such as elevation models.
4. Image interpretation: This method involves visually comparing remotely sensed imagery to reference data or higher-resolution imagery, assessing the accuracy of feature identification.
5. Comparative analysis: This method involves comparing the results of different remote sensing or GIS methods or datasets to assess the relative accuracy and identify discrepancies.

Overall accuracy was used to assess the correctness or accuracy of a classification or mapping process. It represents the percentage of correctly classified or mapped pixels or features in relation to the total of pixels or features in the study area. Overall accuracy is calculated by comparing the classification or mapping results to a reference dataset (ground truth or validation data). The reference data contains known information about the features or land cover classes in the study area. The formula for overall accuracy is:

$$\text{Overall Accuracy (OA)} = \frac{\text{Number Correctly Classified Pixels (or Features)}}{\text{Total Number of Pixels (or Feature)}} \times 100\% \quad (2.1)$$

Overall accuracy is an important metric for evaluating the reliability and utility of remote sensing and GIS-based products, particularly in applications like land cover mapping, land use monitoring, and environmental change analysis.

To explain the suitability for qualitative items, the kappa coefficient of agreement was introduced to remote sensing in the early 1980s as an index to express the accuracy of an image classification (Congalton et al., 1983; Rosenfield and Fitzpatrick-Lins, 1986). Identically, Lillesand et al. (2004) expressed that the Kappa coefficient is widely used in remote sensing

as an accuracy assessment method to measure the agreement between interpretation and real conditions in the field. The Kappa coefficient of agreement, \widehat{K} , is estimated from (Cohen, 1960):

$$\widehat{K} = \frac{p_o - p_c}{1 - p_c} \quad (2.2)$$

Where p_o is the proportion of cases correctly classified (observed agreement) and p_c is the expected proportion of cases correctly classified by chance (chance agreement).

The magnitude of \widehat{K} lies on a scale from -1 to +1, but interest is typically focused only on positive values because negative values generally be interpreted as ‘no agreement’ (Sim and Wright, 2005).

CHAPTER 3. SHORELINE CHANGE DETECTION

3.1. Overview

A change in the location of the shoreline is an indication of the sensitivity of the coast to erosion. Coastal erosion is considered a risk because it threatens buildings and infrastructures, degrades and diminishes the beach's extent, and potentially impacts tourism negatively (Domínguez et al., 2005). This is unless the shoreline and beach are not obstructed from moving landward, which is often not the case in regions with a developed coast, such as tourist destinations.

Coastal erosion has been one of the significant environmental concerns in many parts of the world (Malini and Rao, 2004). The situation is dire for all coasts in Bali Province. Approximately 187 km of coastline in Bali Province is eroding. Bali Province has wind patterns similar to those in the Indian Ocean, where the monsoon influences wind, which causes an increase in current intensity and wave energy that affects coastal erosion and accretion. In addition, the development in coastal areas also causes changes in the direction of the waves. The longshore current is induced by waves that are able to transport the beach sediments. It potentially moves the sediments for many kilometers in the longshore direction and is called the littoral drift. Monitoring must be undertaken across the coastline to understand how sediment moves in a coastal compartment, as the coastline is the most critical and dynamic natural phenomenon (Almar et al., 2021; Barnard et al., 2019; Nicholls et al., 2007).

Monitoring and evaluating shoreline changes is crucial due to the importance of the shoreline to coastal ecosystems and marine environments. Thanks to this process, future generations will benefit from the visual, cultural, and sociological resources of coastal areas, which is essential for spatial planning and sustainable development (Boussetta et al., 2022; Zambrano-Medina et al., 2023). Adopting the latest technology for coastal monitoring is important for preserving these vulnerable areas. Remote sensing technology is fundamental in monitoring and detecting coastal changes over time (Fraiola et al., 2023; García-Sánchez et al., 2021). Monitoring a wide coastal area at a relatively low cost is now feasible using high-resolution satellite images from the latest generation.

The most common methods for monitoring coastline change are fieldwork or aerial photographs (Boak and Turner, 2005; Gens, 2010; Mills et al., 2005). Coastline maps were generated through ground surveying from 1807 to 1927 (A A Alesheikh et al., 2007). Once the airplane was invented in the early 1900s, aerial photography had a new and ideal platform. In 1927, aerial photography was recognized as a valuable tool for mapping the coast (A A Alesheikh et al., 2007). This continued until the 1980s, so it was notable as the only source for coastal mapping. However, these methods are, by definition, subjective and depend on the interpreter's abilities. For over 30 years, scientists have utilized satellite imagery for topographic mapping by digitally overlaying the satellite imagery on the charts, and changes in shoreline features can be easily detected.

The patterns of shoreline change and its dynamics within a specific time in Bali are less constrained. The main objective of this study was to investigate shoreline changes along the Bali Province coast of Indonesia within a defined timeframe employing high-resolution satellite images. This study attempted to comprehensively analyze rapid shoreline change with a focus on the ability of coastal areas to respond, adapt, and withstand the challenges posed by the dynamic shorelines and anthropogenic activities. We coupled GIS approaches using high-resolution satellite images from PlanetScope. By applying these advanced methods and data, we seek to gain a better understanding of the dynamics of shoreline change in Bali Province and contribute valuable insights to coastal management and planning efforts for a sustainable and resilient coastal future

3.2. Materials and Methods

3.2.1. Data Sources

Multitemporal image data is needed to monitor the coastline change. Multitemporal image means that some image has time differences, with a significant interval. Multitemporal satellite data from the study area were acquired from PlanetScope imagery, covering 2016 and 2021. An analytical orthographic scene product with a 4-band multispectral (Blue: 455–515 nm, Green: 500–590 nm, Red: 590–670 nm, NIR: 780–860 nm) was chosen as the most suitable alternative for accurate shoreline mapping (Tu et al., 2022). These scenes were derived using raw sensor-captured data with an average ground sample resolution of 3.125 meters (Shendryk et al., 2019). Images with a 30% cloud cover were manually downloaded from the Planet Explorer website (available at <https://www.planet.com/explorer>). Subsequently, these images underwent orthorectification, geometric, radiometric, and atmospheric correction.

This study was not expected to obtain multi-satellite images with similar conditions. In this case, shoreline data must be corrected to reduce the influence of the tide on the shoreline positions (Hoang et al., 2017). The shoreline shift calculation in different tide levels (Table 3-1) used the triangular theory between water levels and beach slopes. According to the tidal correction measurement, no section of the shoreline experiences a shift in position due to tidal influences greater than one pixel of PlanetScope imagery. The shoreline shift position ranges from 0.22 m to 2.02 m. Hence, this study determined that tidal correction can be abandoned since the shift in shoreline position by tidal influence was not visible in satellite images. The data were provided in the WGS84 Universal Transverse Mercator coordinate system (zone 50S for the study area). This approach adopted in this study is widely accepted for processing temporal satellite images for shoreline extraction. For temporal satellite image processing, an open-source GIS program and image processing software, such as QGIS 3.28 LTR, were employed (QGIS Development Team, 2022).

Wave and current data were collected as supplementary information from the Copernicus Marine Environment Monitoring Service (CMEMS) (available at: <https://doi.org/10.48670/moi-00022> and <https://doi.org/10.48670/moi-00021>). CMEMS, a European Earth observation and monitoring program, provides oceanographic products and services ranging from in situ measurements to remotely sensed images and model output (Jutz and Milagro-Pérez, 2018). The data set included daily and monthly average files with a 1/12°

horizontal resolution for ocean currents and a 1/5° grid for ocean waves (Jean-Michel et al., 2021).

Table 3-1. Astronomical Tide Level Information

Acquisition Date	Astronomical Tide Level (m)
6 August 2016	1.21
28 August 2016	1.23
6 September 2016	1.13
21 September 2016	0.88
27 September 2016	1.13
19 October 2016	1.31
20 November 2016	0.85
3 April 2021	0.96
19 April 2021	0.73
23 April 2021	1.62
21 June 2021	1.23
27 June 2021	1.42
30 June 2021	0.73



Figure 3-1. Location map of the study area.

A field survey was also undertaken along the shoreline of Bali Province to collect shore-type information and conduct the validation study. The field survey was conducted on 10–19 March 2023, with validation stations chosen by systematic random sampling method for natural and artificial shorelines. 75 sampling points were collected (Figure 3-1). Each sampling location had a database containing all information related to physical aspects (shore type and/or

substrate, land use and/or geomorphology, elevation, and coastal condition). Data and information were collected by visual observation and aerial photographs to determine the coastal condition. In this case, an aerial drone (DJI Mavic 2) was employed to capture aerial images. Furthermore, the Kappa coefficient and confusion or error matrix were used to express the accuracy of an image classification.

3.2.2. Extraction and Classification of Shoreline

The Normalized Difference Water Index (NDWI) was utilized to effectively distinguish water and non-water areas using analysis of the green (Band 2) and near-infrared (NIR) (Band 4) bands of PlanetScope imagery. The NDWI reduces the reflectance of non-water features through the use of the NIR band while simultaneously maximizing the reflectance of water through the green band (Abdelhady et al., 2022; Darwish and Smith, 2021; McFeeters, 1996). The formulation of the NDWI can be expressed using Eq. (5.1).

$$NDWI = \frac{Green - NIR}{Green + NIR} \quad (3.1)$$

Image digitizing was applied to obtain the coastline. Then, the coastline in 2016 and 2021 were compared using the overlay method to acquire the displaced coastline. This overlay method is commonly used to detect longer-term coastline changes. The displaced coastline is then calculated to get the information of coastline changes.

The shoreline of Bali Province is diverse and may be classified into two main categories: natural and artificial shores (Sui et al., 2020). The natural shore category includes bedrock, mangrove, sandy, and silty shorelines. The artificial shore category is further subdivided into the farm (used for agriculture and/or aquaculture), embankment, and man-made infrastructure (including harbors, wharves, and airports), resulting in a total of seven distinct secondary category types (Table 3-2).

Table 3-2. Shoreline categories.

Primary Categories	Secondary Categories	Description
Natural shoreline	Bedrock shoreline	The shoreline is tortuous and covered with pebbles or rocks with zigzag shapes and evident contours. The waterway is demarcated, and the tone is darker, with steep structures, including cliffs.
	Mangrove shoreline	Characterized by dense vegetation forest lining the coast, primarily branch-like water systems with regular shapes and sharp edges, and a reddish hue in the satellite image.
	Sandy shoreline	Generally composed of loose particles of sediment, such as granules, pebbles, or larger grains of sand, and deposits of volcanic eruptions, consisting of relatively straight and wide shorelines. Occur at high brightness parallel to the seashore.
	Silty shoreline	Beach's broad, smooth surface, to the roadside vegetation's lush, sparse vegetation on the seaward side. Occur in a darker texture and gray or off-white in satellite images, with the effect of increasing cohesive properties and water content depending on the fine grain diameter.
Artificial shoreline	Farm	A rectangular grid arrangement, uniform texture, darker hues to lighter shades (aquaculture), and red color (agriculture).
	Embankment	Adjacent infrastructure, the boundary between the outer edge of the sea, such as ports, docks, storage land, towns, and industrial land, and

	the waterway of the ocean, is generally distributed on a large scale with a certain brightness, but this is not uniform.
Man-made infrastructure (harbor, wharf, and airport)	Convex embankment, harbor pool markers, concrete texture, smooth geometries, linear structure, adjacent infrastructure.

Source: Modification from Sui et al. (2020).

To accurately classify and locate various shore types, a set of remote sensing indices was developed based on color, texture, and feature adjacency information extracted from both satellite images and field surveys of the coastal zone (Sui et al., 2020). Combining these indices facilitated the classification of shores in false-color images generated by combining the near-infrared, red, and green bands (Figure 3-2).

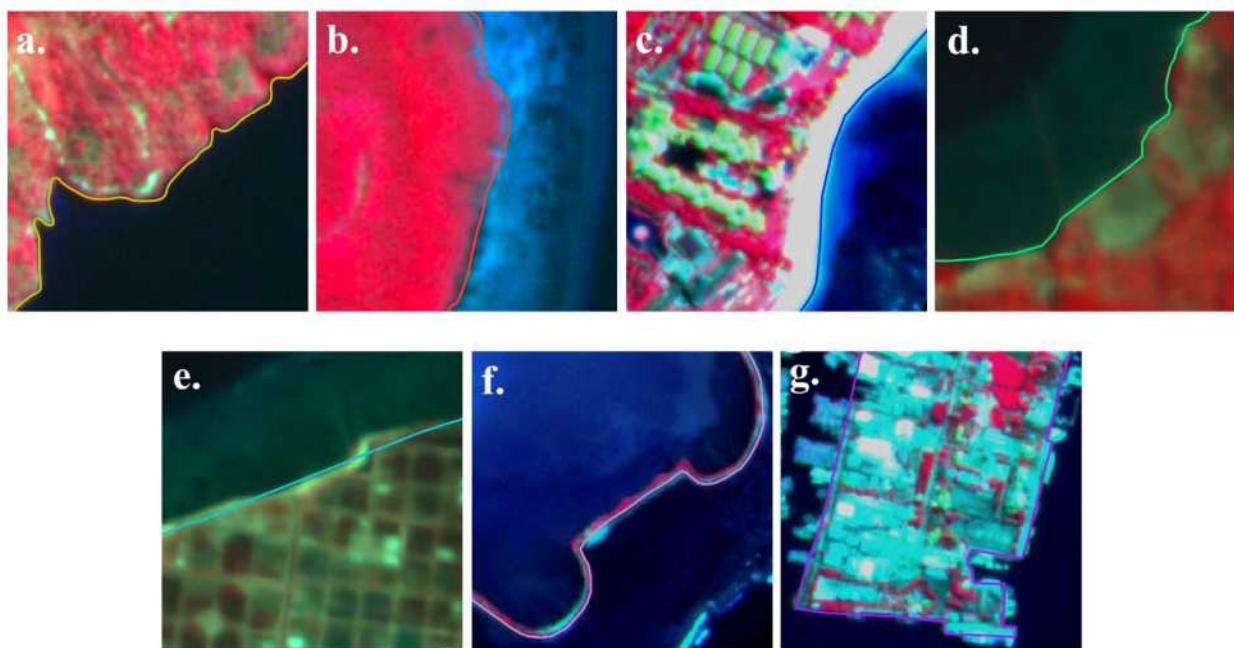


Figure 3-2. The interpretation of PlanetScope images shows the diverse shoreline types of Bali: (a) Bedrock shoreline, (b) Mangrove shoreline, (c) Sandy shoreline, (d) Silty shoreline, (e) Farm shoreline, (f) Embankment, (g) Man-made infrastructure.

3.2.3. Analysis of Shoreline Change

In order to estimate the shoreline change rates, an analysis was conducted using measured distance differences between shoreline positions over time along transects. A total of 12,052 transects were created, each oriented perpendicularly between two shorelines and spaced at 50 m intervals, with a consistent length of 1000 m. The distance between two shorelines on each transect represents the extent of shoreline change between the corresponding time points. The end point rate (EPR) approach was employed in this study to determine the shoreline change rate. The shoreline change rate was calculated by dividing the perpendicular distance between the two shorelines by the time difference between the measurements (De Lima et al., 2021).

3.2.4. Analysis of Land Area Change

The term "land area change" refers to changes in the coastal land area resulting from shifts in the shoreline position in this study. When the shoreline extends seaward, it expands the land area, and when the shoreline moves towards the land, it causes a reduction in land area due to retreatment. To assess these changes, shorelines from two distinct periods were overlaying in QGIS 3.28 LTR, and topological analysis was performed to generate polygons representing the differences between these shorelines and their corresponding land areas. Each polygon was categorized based on whether it represented an increase or decrease in land area (Griffiths et al., 2019; Smith and Cromley, 2012). Subsequently, the net change in land area was determined by summing the increases and decreases in land area, providing a comprehensive understanding of how the coastal landscape evolved over the specified timeframe. This method allowed us to measure and analyze the dynamics of land area changes, shedding light on the impacts of shoreline advancement and retreatment on the coastal region (Gao et al., 2023).

3.3. Result and Discussion

3.3.1. Shore-type Changes

The analysis of shore-type changes in Bali Province from 2016 to 2021 revealed substantial changes in shoreline characteristics. In 2016, the total shoreline length of Bali Province measured 668.64 km, with different types of shores distributed as follows (Table 3-3): bedrock covering 177.00 km (26.47%), mangrove 68.40 km (10.23%), sandy 378.00 km (56.53%), silty 18.28 km (2.75%), farm 3.49 km (0.52%), embankment 10.42 km (1.56%), and man-made infrastructure shores 13.05 km (1.95%). Natural shoreline retention accounted for 641.68 km (95.97%). However, by 2021, the total shoreline length of Bali Province decreased to 662.59 km. The distribution of shore types in 2021 was as follows: bedrock covering 176.53 km (26.64%), mangrove, 62.25 km (9.39%), sandy 374.70 km (56.55%), silty 20.69 km (3.12%), farm 1.71 km (0.26%), embankment 8.81 km (1.33%), and man-made infrastructure shores 17.90 km (2.70%). Natural shoreline retention accounted for a total of 634.17 (95.71%).

Between 2016 and 2021, the total shoreline length of Bali Province experienced a reduction of 6.04 km, resulting in a new length of 662.59 km, which corresponded to an annual change rate of -1.21 km/yr. Over this study timeframe, specific shore types underwent distinct alterations. Bedrock shores decreased by -0.47 km at -0.09 km/yr, and the annual change rate of mangrove shores decreased by -6.16 km at a -1.23 km/yr annual change rate. Sandy shores decreased by -3.30 km at an annual rate of -0.66 km/yr, and farm shores decreased by -1.78 km at an annual rate of -0.36 km/yr. Similarly, embankment shores experienced a reduction of -1.60 km, with an annual change rate of -0.32 km/yr.

Man-made infrastructure and silty shorelines increased by 4.85 km and 2.41 km, respectively, with change rates of 0.97 km/yr and 0.48 km/yr. Remarkably, man-made infrastructure shorelines, such as airports and harbors, expanded significantly between 2016

and 2021 (Figure 3-3). In contrast, the natural shoreline experienced a significant decrease of 7.51 km, reflecting a reduction of 0.26% over the examined period.

Table 3-3. Length ratio and change rate of different coastline types from 2016 to 2021

Type of Coastline		Extent	2016	2021
Natural Coastline	Bedrock	Length (km)	177.00	176.53
		Length ratio (%)	26.47	26.64
		Change rate (km/yr)		-0.09
	Mangrove	Length (km)	68.40	62.25
		Length ratio (%)	10.23	9.39
		Change rate (km/yr)		-1.23
	Sandy	Length (km)	378.00	374.70
		Length ratio (%)	56.53	56.55
		Change rate (km/yr)		-0.66
	Silty	Length (km)	18.28	20.69
		Length ratio (%)	2.73	3.12
		Change rate (km/yr)		0.48
	<i>Subtotal</i>	Length (km)	<i>641.68</i>	<i>634.17</i>
		Length ratio (%)	<i>95.97</i>	<i>95.71</i>
		Change rate (km/yr)		<i>-1.50</i>
Artificial Coastline	Farm	Length (km)	3.49	1.71
		Length ratio (%)	0.52	0.26
		Change rate (km/yr)		-0.36
	Embankment	Length	10.42	8.81
		Length ratio (%)	1.56	1.33
		Change rate (km/yr)		-0.32
	Man-made infrastructure	Length (km)	13.05	17.90
		Length ratio (%)	1.95	2.70
		Change rate (km/yr)		0.97
	<i>Subtotal</i>	Length (km)	<i>26.96</i>	<i>28.42</i>
		Length ratio (%)	<i>4.03</i>	<i>4.29</i>
		Change rate (km/yr)		<i>0.29</i>

These findings highlight the significant changes and diverse trends in the distribution of shore types in Bali Province, characterized by a decline in natural shorelines and a corresponding increase in man-made coastal structures during the investigated timeframe. Shorelines are subject to changes driven by a combination of natural processes and human activities, with coastal development being a prominent factor contributing to alterations in natural shorelines in Bali Province. Such changes' impact on the coast's natural shape can be profound, leading to the degradation of various coastal habitats (Ge and Zhang, 2011; Gittman et al., 2016). Moreover, these changes can also have implications for the socio-economic aspects of coastal communities reliant on the health of these habitats (Mishra et al., 2021). It is worth mentioning that almost half of Bali Province's total coastal length is categorized as high to very highly vulnerable to shoreline changes (Hastuti et al., 2022a). In response to this vulnerability, it becomes important to conduct regular shoreline monitoring and develop effective coastal management strategies to protect the sustainable use of the coastal zone in Bali Province.

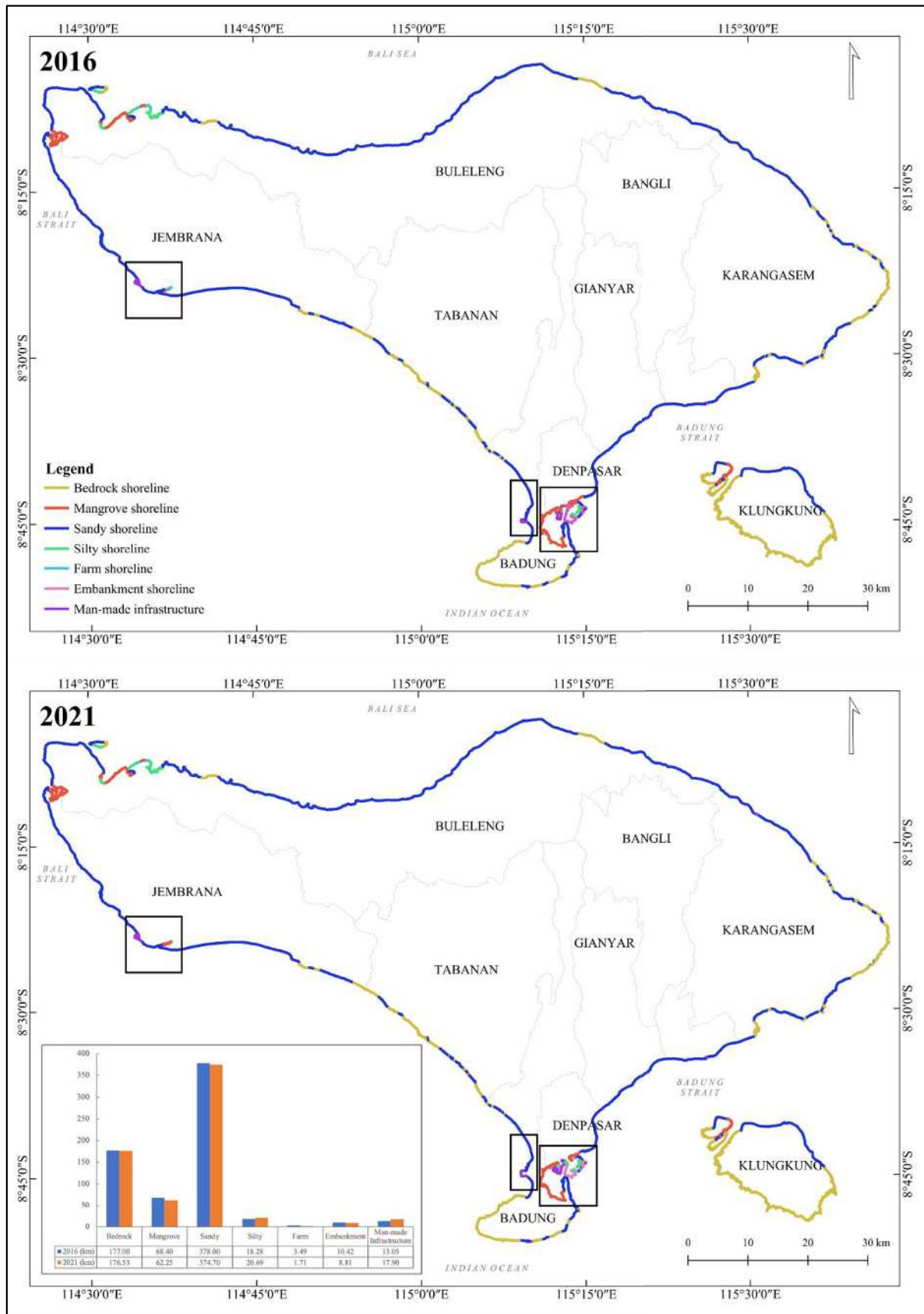


Figure 3-3. Bali Province shoreline lengths were defined by type between 2016 and 2021. (Note: The black boxes mark the significant changes in the two periods).

3.3.2. Shoreline and Coastal Area Change Rates

Based on a comprehensive analysis of the shoreline changes at the 12,052 transects, the average rate of shoreline changes in Bali Province from 2016 to 2021 was determined to be 0.07 m/yr. This finding highlights the continuous and dynamic fluctuations as shorelines constantly change and move either landward (retreat) or seaward (advance) in general (Figure 3-4). Among these transects, 5577 (46.38%) exhibited shoreline retreatment, showing an average rate of -1.97 m/yr. These specific transects were predominantly located on sandy and silty shores. Notably, the most significant retreat occurred near the mouth of the Telaga Waja River, specifically at Karangdadi Beach, Klungkung Regency, with a notable shoreline retreat rate of -19.07 m/yr (transect no. 11) (Figure 3-4).

Among the analyzed transects, 4771 (39.68%) demonstrated shoreline advancement, exhibiting an average rate of 2.47 m/y. These specific transects were primarily observed in areas characterized by newly constructed artificial shores, representing man-made infrastructure development and silty shores, particularly at transects no. 1, 6–7, and 9 (Figure 3-5). Notably, the shores of Pengambangan Beach (transect no. 1), Ngurah Rai Airport (transect no. 6), and Benoa Bay (transect no. 9) prominently showed shoreline advancement.

Of the analyzed transects, 1704 (14.17%) were identified as stable, indicating shorelines that experienced minimal changes over the studied period. The majority of these stable transects were located at artificial and bedrock shores, particularly the rocky shorelines in the southern part of Bali Island (Badung Regency), Nusa Penida Island (Klungkung Regency), and certain artificial shores in Badung and Denpasar Regencies.

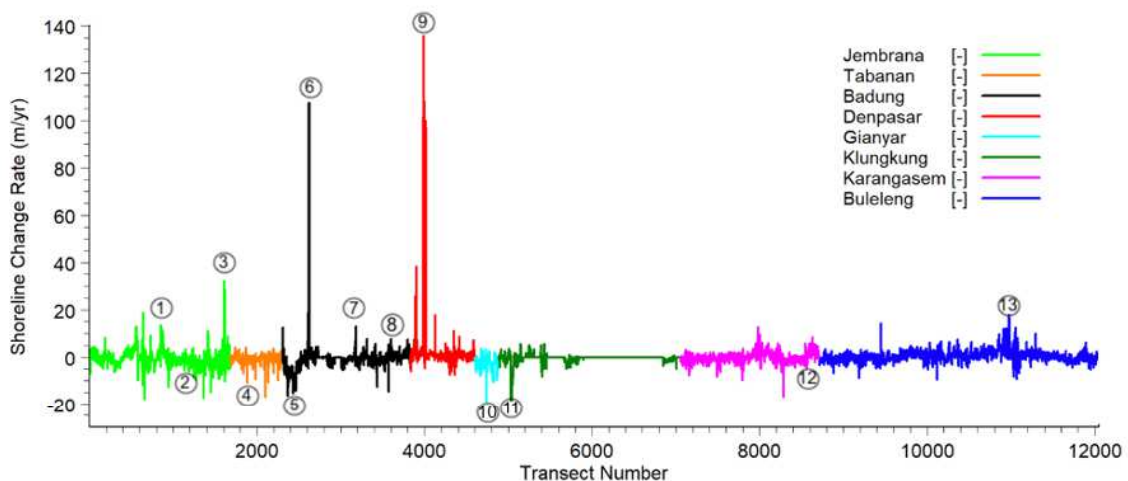


Figure 3-4. Shoreline change rate in Bali Province from 2016 to 2021. The color bar represents the regency.

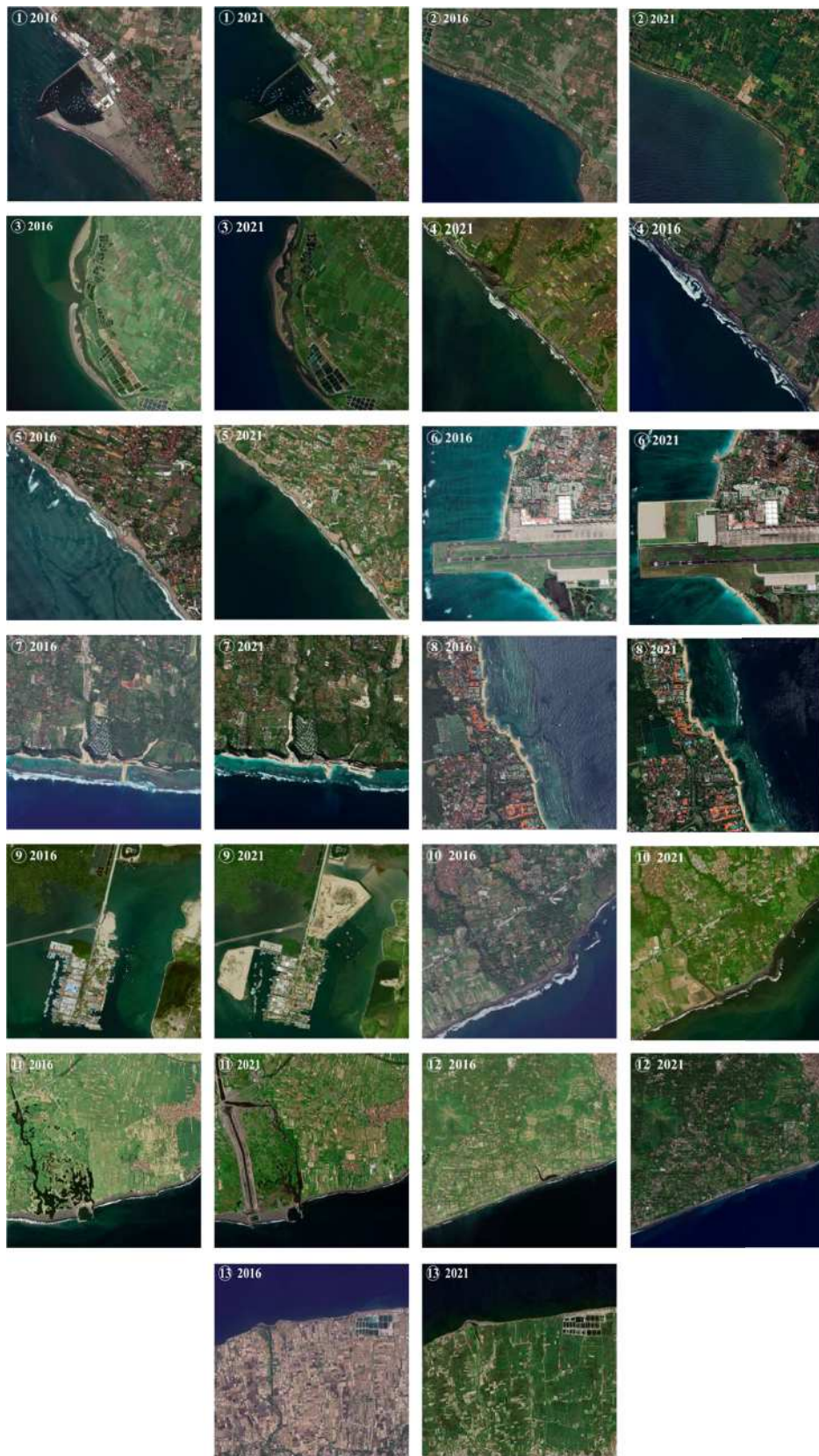


Figure 3-5. Examples of shoreline change between 2016 and 2021 were captured in remote sensing images.

The analysis of land area changes corresponding to shoreline advancement and recession revealed an increase of 4.01 km² and a decrease of 2.76 km², respectively, resulting in a net increase of 1.25 km² and an average land area change rate of 0.25 km²/yr. The most significant increase in land occurred at Tuban, Badung Regency (transect no. 6), and Benoa Bay, Denpasar Regency (transect no. 7) (Figure 3-6), attributed to land reclamation for the expansion of Ngurah Rai Airport and Benoa Port. Conversely, shoreline retreatment was primarily observed at Pebuahan Beach, Jembrana Regency (transect no. 2) (Figure 3-6) and Karangdadi Beach, Klungkung Regency (transect no. 11) (Figure 3-6). The observed changes can be attributed to the construction of a port, which interferes with the natural littoral drift, causing erosion in the affected beach areas.

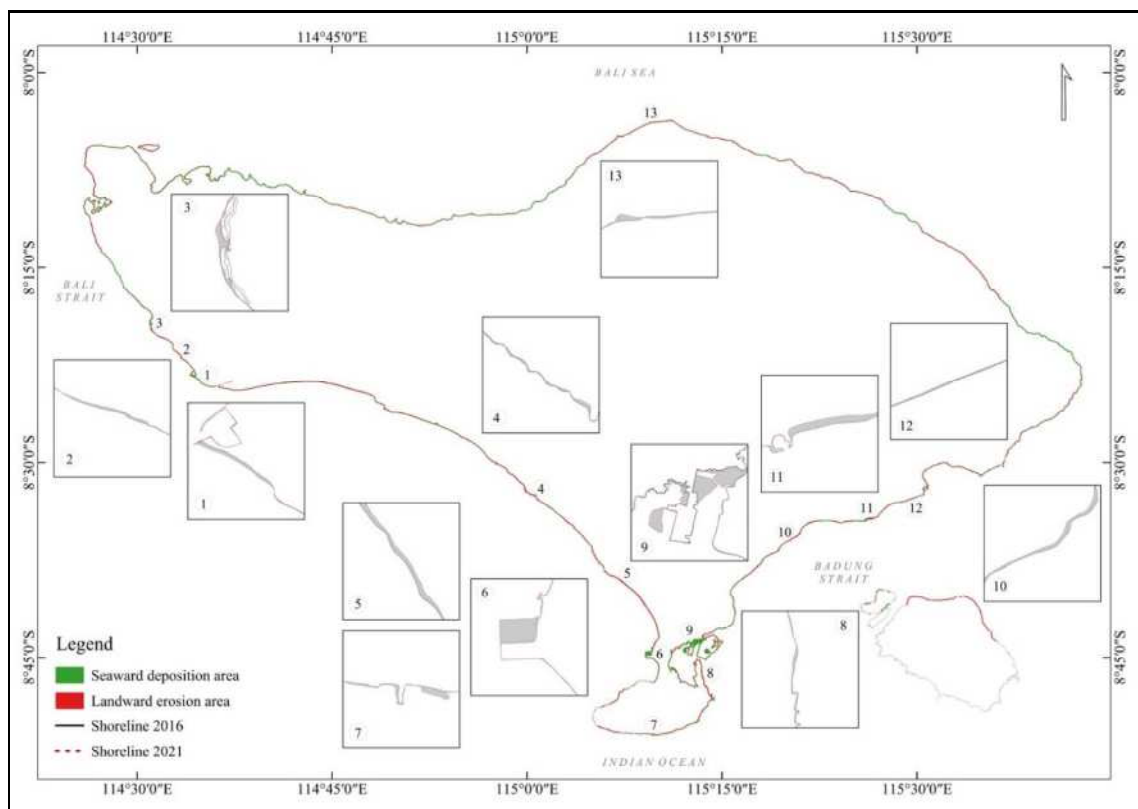


Figure 3-6. Land area changes in the coastal area of Bali Province between 2016 and 2021.

These results highlight the dynamics and ever-changing nature of Bali's shorelines, showing considerable variation across different regions throughout the study period. This study's results align with previous studies conducted in the region (Rahmawati et al., 2021; Triwahyuni and Asai, 2014; Uda et al., 2015). Coastal retreatment emerged as the predominant process, leading to a notable annual erosion rate, particularly affecting sandy and silty shores in Bali Province. The retreatment in these areas can be attributed to an imbalance in sediment transport along the coast, resulting from natural processes and human interventions. On the other hand, coastal advancement is also evident, with a significant shoreline advancement in Bali Province. While the rate of shoreline advancement surpasses the erosion rate, it is important to approach coast development cautiously to prevent erosion impact on other areas. The impact of human activities, coastal engineering, and land reclamation on the advancement of certain shorelines in Bali Province is evident. Likewise, similar studies have highlighted

how human activities, particularly coastal development, have contributed to coastal advancement in other coastal cities worldwide (Y. Chen et al., 2019; Gao et al., 2023; Lim et al., 2021; Masucci and Reimer, 2019; Wang et al., 2021). These findings emphasize the significance of adopting responsible coastal management strategies to balance development and environmental preservation on Bali's shorelines.

The resolution of the images significantly impacts the evaluation of coastal morphological changes through satellite-based imagery. The utilization of higher-resolution imagery, such as the one provided by PlanetScope, results in more detailed and precise measurements of coastal dynamics. The capacity to capture finer details with higher-resolution imagery enhances our understanding of the changes occurring along the shoreline, contributing to more precise analyses and informed decision-making in coastal management and planning efforts (Abdelhady et al., 2022; Darwish and Smith, 2021; Doherty et al., 2022).

3.3.3. Significant Wave Height Analysis

The variation in wave height in Bali's waters results from multiple interrelated factors, including weather conditions (wind speed), oceanic currents, and local geographical features (seabed topography). These factors interact dynamically, creating a constantly changing wave environment in the region. Also, the monsoon winds, which change direction throughout the year, significantly impact wave height (Rachmayani et al., 2018; Rizal et al., 2019). Weather conditions, particularly strong winds, are significant in determining wave height, as they can generate more extensive and powerful waves. Winds blowing toward the shore drive the formation of larger waves, while offshore winds cause waves to break and reduce in size (Kuntoro et al., 2020). The interaction between wind and waves is a complex process influenced by wind speed and duration (Lira-Loarca et al., 2019; Wu et al., 2016). Higher wind speed transfers more energy to the water, producing more extensive and powerful waves. Moreover, sustained wind over longer periods generate larger waves than a brief burst of wind. The complex relationship between these factors contributes to the dynamic wave characteristics in Bali's waters.

A complex interplay of various factors shapes the wave characteristics in northern and southern Bali. Bali's geographical location, where the Indian and Pacific Oceans converge, gives rise to distinct wave patterns contributing to the region's uniqueness. The island's landmass protects the northern waters, resulting in relatively lower wave heights. Conversely, more exposed to external forces, the southern waters exhibit higher wave heights. The interaction of these factors results in diverse and dynamic wave environments along the Bali coast.

In the southern Bali waters, the significant wave height, defined as the mean wave height of the highest one-third of the waves, can reach remarkable heights up to 2.8 meters during the dry season, which runs from May to October (Figure 3-8). The prevailing winds during this period, primarily from the east and southeast, generate considerable wave activities. When combined with strong oceanic currents, these winds contribute to the formation of higher wave heights. On the other hand, the northern Bali waters experience lower wave heights, typically less than 1 meter (Figure 3-7). The wave patterns in these waters are predominantly influenced

by the local wind conditions and the underwater topography, which can cause variations in the wave height. However, it is essential to note that the wave height in northern and southern Bali waters is subject to seasonal variations. For instance, during the dry season, also known as the Australian monsoon, which occurs from June to August (Figure 3-8), the winds blow from Australia towards Asia, causing the waves to build up in the Indian Ocean. During this season, the wave height tends to increase due to the increased wind speed. This can lead to high waves observed in Bali's waters, especially along the southern coast. These seasonal variations in wave height have a significant impact on coastal conditions in Bali.

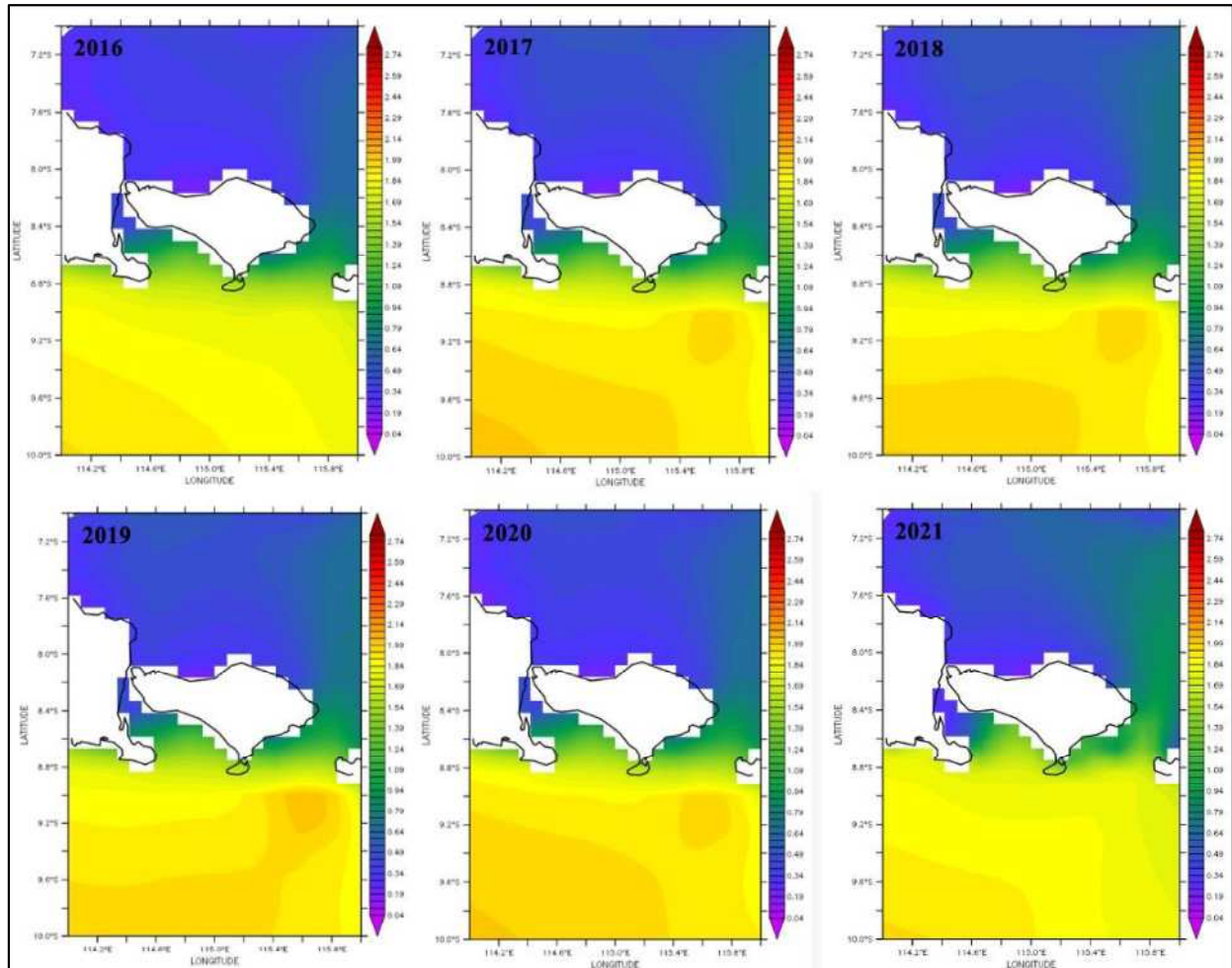


Figure 3-7. Yearly average distribution of simulated significant wave height in Bali Province between 2016 and 2021. (Data source: E.U. Copernicus Marine Service Information; Global Ocean Waves Analysis and Forecast).

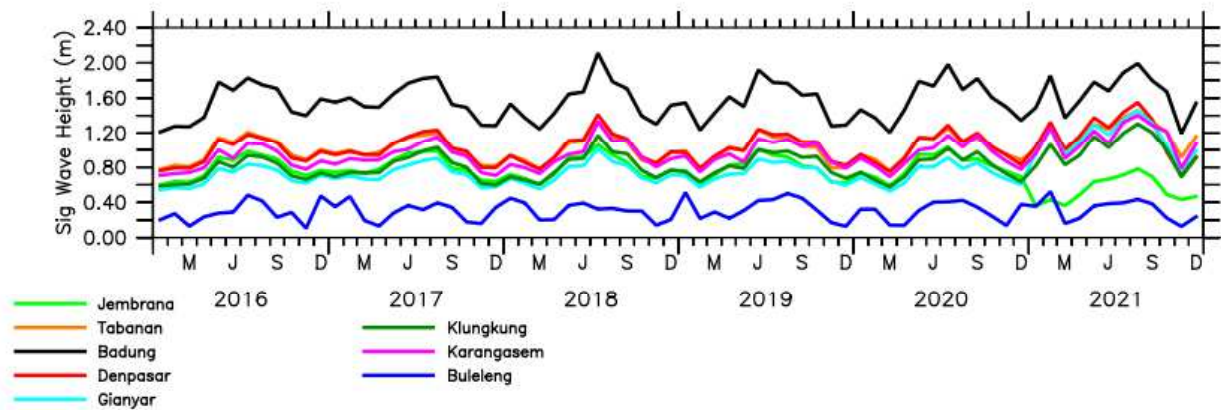


Figure 3-8. Monthly average of simulated significant wave height in Bali Province from 2016 to 2021. (Data source: E.U. Copernicus Marine Service Information; Global Ocean Waves Analysis and Forecast).

The relationship between wave height and shoreline change on Bali Island is a complex issue, and no one-size-fits-all answer applies uniformly to all island regions. However, studies indicate a general trend of increased wave height contributing to increased shoreline erosion in Bali (Dimiyati et al., 2022; Triwahyuni and Asai, 2014). The correlation can be attributed to the higher energy levels of waves, making them more effective at eroding shorelines. The relationship between wave height and shoreline alterations is more pronounced in certain places of Bali than in other counterparts (Uda et al., 2015). For instance, the southern coast of Bali is more exposed to high waves from the Indian Ocean, making this area more prone to erosion (Putro and Lee, 2020; Rahmawati et al., 2021). In contrast, the northern coast of Bali is protected by the island of Menjangan, and as a result, this area is less prone to erosion. The complex interaction between wave dynamics and coastal characteristics adds to the complexity of this connection. Consequently, it becomes crucial to consider local factors when examining the influence of wave height on shoreline change in Bali.

3.3.4. Ocean Current Analysis

The annual average current speed from 2016 to 2021 in the study area ranged from 0.1–1.5 m/s (Figure 3-9). The direction of the surface current is predominantly towards the south. The strait area, Bali Strait, and Lombok Strait exhibited higher current speeds. These straits serve as the main channels of the Indonesian throughflow (ITF), which connects the Pacific Ocean with the Indian Ocean via the Indonesian Seas (Gordon, 2005). The ITF and other factors, such as monsoon winds and seafloor topography, collectively significantly impact the dynamics and properties of the ocean currents around Bali (Gordon and Susanto, 1998).

The ocean currents surrounding Bali are subject to intricate seasonal variations in their patterns and trends, presenting a dynamic marine environment. The ocean currents in this area are primarily driven by monsoon winds, which also produce the seasonal reversal of the currents. In Bali's northern and southern waterways, the currents move from west to east during the northwest monsoon (November to April) and east to west during the southeast monsoon (May to October). These monsoon-driven currents significantly shape the hydrodynamic conditions in Bali's waters (Siswanto, 2010). The currents are often stronger during monsoon

seasons than inter-monsoon ones (Figure 3-10). This increased strength is a characteristic feature of the monsoonal influence on the oceanic circulation in the region. Moreover, the strait's currents consistently demonstrate a stronger pattern than those in the adjacent waters (Figure 3-9). This phenomenon is due to the narrow and confined nature of the straits, which channels and accelerates water flow. Furthermore, the combination of seasonal variability and spatial differences in current strength contributes to the dynamics and diverse water processes surrounding Bali.

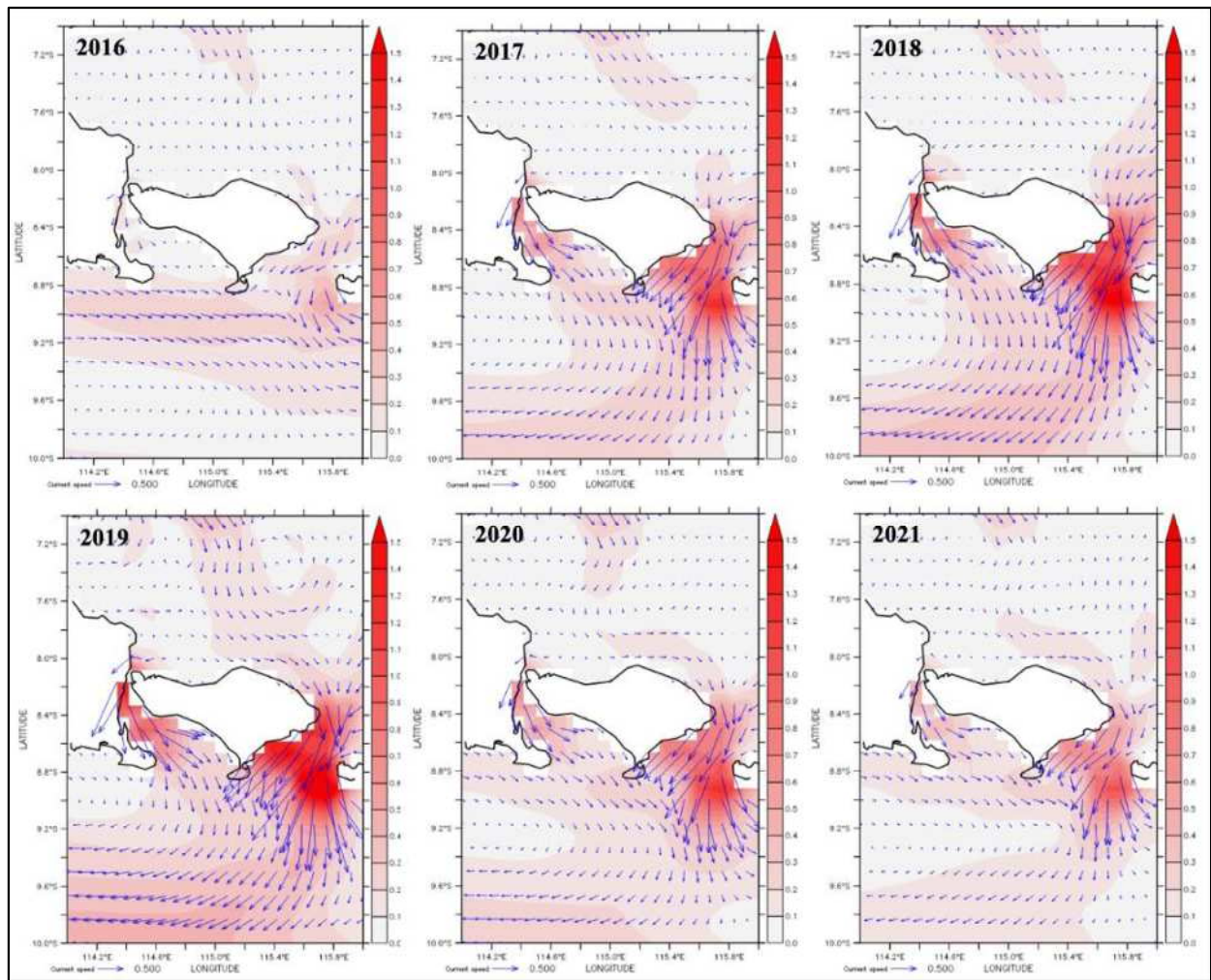


Figure 3-9. Yearly averaged of simulated current speed distribution in Bali Province from 2016 to 2021. (Data source: Copernicus Marine Service; Global Ocean Physics Reanalysis).

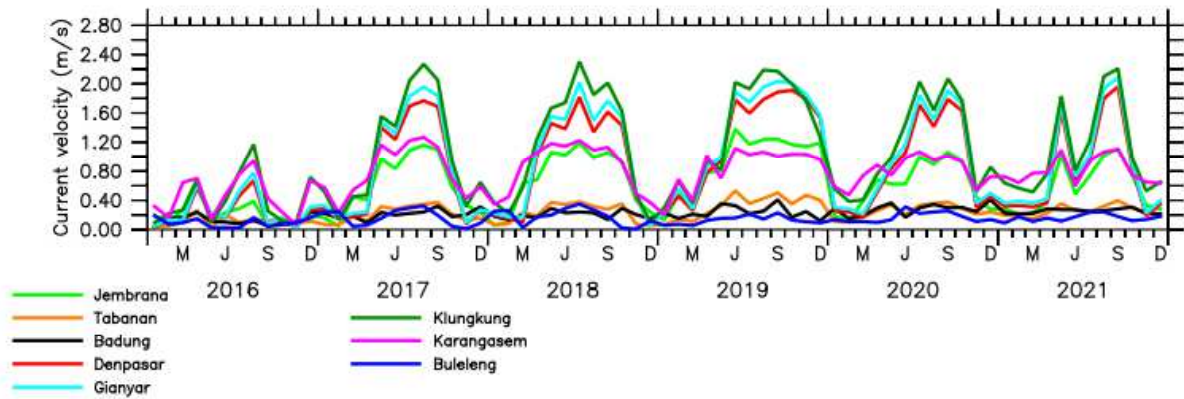


Figure 3-10. Monthly average of simulated surface current in Bali Province from 2016 to 2021. (Data source: Copernicus Marine Service; Global Ocean Physics Reanalysis).

Ocean currents have a significant impact on the dynamic shoreline of Bali in various ways. Strong currents have the potential to erode the shoreline by washing away sand and other debris, which can harm the shoreline and lead to the formation of cliffs, beaches, and other coastal features. Conversely, ocean currents can also lead to accretion, where sand and sediments accumulate along the shoreline, forming new beaches or expanding existing ones. Shoreline migration is a combined process driven by ocean currents, leading to the gradual shifting of the shoreline over time. Along with other factors like rising sea levels, this migration can be caused by accretion and erosion—this dynamic process of Bali’s shoreline results from continuous interactions between natural forces and coastal features.

Bali’s southern coast, including the southeast and southwest coast, is more affected by erosion than the northern coast. This might result from the southern coast being more exposed to strong Indian Ocean currents (Figure 3-9). In contrast, Menjangan Island on the northern coast provides natural protection, which mitigates the influence of strong currents. Strong currents from the Indian Ocean are causing major erosion along Bali's southern shore. This continuous erosive force has reduced the shoreline extent due to erosion, resulting in the construction of cliffs and other coastal features. In contrast, the presence of Menjangan Island serves as an effective barrier that protects Bali's northern shore from the erosive impact of strong ocean currents. Despite being exposed to currents from the Makassar Strait and the Java Sea in the northern and western parts, this natural protection has contributed to the relative stability of the northern coast compared to the more eroded southern coast of Bali (Dimiyati et al., 2022; Husrin et al., 2016).

3.3.5. Shoreline Changes Associated with Human Activities

Bali Island, renowned as Indonesia’s most popular tourism destination, attracts a substantial number of domestic and international tourists annually, establishing a region defined by anthropogenic activities. The impacts of urbanization and a dense population are evident in coastal areas of Bali. The rapid development of residential, commercial, and infrastructure to support the tourism sector has contributed to the transformation of the coastal landscape in Bali. Moreover, the construction of harbors and jetties has been observed further to modify the natural shorelines in certain coastal areas. These combined human interventions,

collectively known as “anthropogenic factors,” are the primary drivers that accelerated the erosion rates along Bali’s coastal area.

The combination of urban growth, tourism, and infrastructure developments has disrupted the coastal natural processes, leading to heightened vulnerability to erosion and coastal degradation. For instance, Candidasa Beach in Karangasem Regency has been exposed to beach erosion since the 1980s, primarily driven by the development of tourism facilities and exacerbated by extensive coral mining activities. The rapid expansion of tourist infrastructure and the depletion of coral reefs have disrupted the natural sediment dynamics, leaving shorelines exposed to erosive forces. Consequently, the formerly pristine beaches of Candidasa Beach have undergone significant degradation due to human activities in the area over the years.

The shoreline type presents a major constraint to coastal development, leading to the adoption of land reclamation as a prevalent solution. This approach involves the construction of artificial land along the shoreline to meet the increasing demands of various sectors. The rapid development along the coast has led to a significant expansion of the artificial shoreline, characterized by human-made structures and infrastructure. In contrast, natural shorelines have been gradually diminishing due to accelerated erosion processes. Notably, the artificial shoreline increased from 4.03% to 4.29% of the total shoreline length between 2016 and 2021, indicating the growing effect of human activities on Bali’ coastal areas (Figure 3-3).

Natural shoreline conversion to artificial shorelines has serious implications for coastal ecosystems, environmental quality, and ecological balance. One notable repercussion of reclamation is the potential increase in water turbidity and subsequent sedimentation (Tanto et al., 2017; Maharta et al., 2019; Wisha et al., 2019). Benoa Bay, Badung Regency, a semi-enclosed water area, has experienced land reclamation activities associated with port expansion, which presents a potential risk to the bay’s environment (Dewi, 2019; Putra et al., 2021). Observation in the area reveals the impact of reclamation, with the rise in silty shorelines increasing by 13.18% (Figure 3-3). This sedimentation is indicative of the potential harm caused to the bay’s coastal ecosystems. In consequence, aquatic ecosystems such as coral reefs (Kleypas, 1996; Larcombe et al., 2001; Palmer et al., 2010; Sanders and Baron-Szabo, 2005), seagrass beds (Hossain et al., 2018; Xu et al., 2021) and mangroves (Ellison, 1999; Nardin et al., 2021; Sayers and Reef, 2022) may encounter significant damage due to sedimentation, disrupting their ecological functions and biodiversity.

Land reclamation frequently harms mudflats, mangroves, and fisheries activities in Bali Provinces (Dewi, 2019; Putra et al., 2021). Mudflats, vital habitats for numerous species, face degradation and loss due to converting these areas into developed land. Mangroves, with their ecological significance in coastal protection and supporting biodiversity, are also affected as they are often cleared for reclamation purposes, diminishing their protective role against erosion and storm surges. Sediment deposition in the mangrove ecosystem causes destruction, burying or covering the pneumatophores of breathing roots mangroves (Ellison, 1999). Moreover, fisheries activities, a crucial economic activity for coastal communities, encounter challenges when reclamation disrupts traditional fishing grounds, spawning areas, and fish migration routes, reducing catch and livelihood insecurity for fishermen.

The shoreline retreatment and recession analysis are essential studies for identifying the areas of significant erosion that require protection to avoid the beach's land loss. Two prominent locations exhibiting shoreline retreatment are Pebuahan Beach, Jembrana Regency (transect no. 2) (Figure 3-6), and Karangdadi Beach, Klungkung Regency (transect no. 11) (Figure 3-6). The primary driver of this retreatment can be attributed to the construction of the port, which interrupts a large volume of littoral drift and causes erosion of beaches. These man-made constructions considerably influence the shoreline's position, reducing land area as the eroded sediment is carried away from the affected beaches. Such modification to the shoreline not only impacts the coastal environment but also raises concern for the welfare of communities and infrastructure situated in these vulnerable areas. Coastal erosion results in economic losses in various sectors, affecting agricultural lands and public facilities, including access roads, schools, and settlement areas. These challenges pose challenges to local communities and impede their livelihoods. Furthermore, this phenomenon harms tourism facilities, particularly beach temples essential to Bali's cultural and recreational appeal.

3.3.6. Shoreline Change Associated with Global Climate Change

Based on the findings of this study, from 2016 to 2021, the shoreline in Bali Province experienced continuous landward (retreat) and seaward (advance) erosion, with erosion predominantly occurring (Figure 3-4). Erosion can be measured regarding landward shoreline movement or a reduction in beach volume. This phenomenon of beach erosion poses significant challenges to coastal assets. It directly exposes these assets to the relentless impact of waves, resulting in potential damage or loss. Moreover, erosion may approach coastal land close enough to reduce its foundation capacity, posing a threat to the stability of built structures and infrastructure. In some cases, the proximity of beach erosion can lead to these assets' undermining and eventual collapse.

Various factors drive shoreline change; however, sea level change directly correlates with this phenomenon (Nidhinarangkoon et al., 2023). The rising sea level, attributed to global climate change, significantly risks Bali's coastal areas (Hastuti et al., 2022a). As sea level rises, high-energy waves can reach farther inland, redistributing sand offshore, especially sandy shores, most vulnerable to sea level changes. The balance of natural ecosystems, particularly mangrove forests, which serve as essential buffers against coastal erosion and storm surges, is also adversely affected by this process. Moreover, coastal infrastructure is at risk due to the incursion of high-energy waves generated by sea level rise (Figure 3-11). Structures along the coast are increasingly vulnerable to the force of waves, resulting in the degradation and destruction of vital infrastructure such as roads, buildings, and utilities.



Figure 3-11. Destroyed coastal infrastructure in Bali Province due to erosion in sandy shores in Jembrana and Badung Regencies. (Source: field survey, 10—19 March 2023).

Sea level changes play an essential role in governing shoreline movement, resulting in wave-induced erosion of coastal landforms. This study indicates a noticeable decline, particularly in the natural sandy shoreline (Figure 3-3). Erosion of the sandy shoreline occurs through the combined effects of waves and currents due to longshore sediment transport or littoral drift. The continuous erosion raises concern about the potential consequences of rising sea levels. The rising sea level poses a high risk of more frequent and severe storms, exacerbating coastal flooding and erosion. Vulnerable coastal regions will encounter amplified challenges as the erosive forces of waves and currents intensify, posing threats to ecosystems, infrastructure, and coastal communities.

Studying the historical changes in shoreline positions over extended periods offers researchers and coastal managers valuable insights into the dynamic evolution of coastal areas. This knowledge is a foundation for developing effective adaptation and mitigation strategies for future sea-level rise (Mentaschi et al., 2018; Nidhinarangkoon et al., 2023; Ribas et al., 2023). As sea levels rise, posing significant threats to coastal regions worldwide, the long-term shoreline change analysis becomes even more crucial. By understanding how coastlines have evolved, communities can build resilience, implement sustainable coastal management practices, and protect valuable ecosystems and infrastructure from the increasing risks posed by climate change.

3.3.7. Existing Coastal Protection Strategy

Coastal erosion poses a significant challenge for Bali Province and other coastal regions. To address and mitigate this issue, the local government has implemented measures such as constructing seawalls, sandbags, breakwaters, and groins to protect the coastal area (Figure 3-12). A field survey conducted in March 2023 shows that the local authorities have adopted various approaches to adapt to climate change (Figure 3-12). Prioritizing the installation of coastal protections to mitigate the impact of erosive waves and ongoing efforts are being made to establish these protective structures. Since each coastal area has unique characteristics, selecting appropriate coastal protection measures should be based on carefully assessing local conditions, encompassing factors such as wave energy, sediment dynamics, and environmental considerations. Bali Province can mitigate and prevent further coastal erosion by implementing site-specific strategies and protecting valuable coastal ecosystems and vital infrastructure.



Figure 3-12. Various coastal protection structures in the study area: (a) Seawall with stone-filled gabions combined with revetment; (b) Sandbag at Kuta Beach, Badung Regency; (c) Seawall at Perancak Beach, Jembrana Regency; (d) Seawall at Pererenan Beach, Badung Regency; (e) Groins and (f) Offshore breakwater at Samuh Beach, Badung Regency; (g-h) Groins at Candidasa Beach, Karangasem Regency; (i) Offshore breakwaters at Jerman Beach, Badung Regency; (j-k) Groins at Sanur Beach, Denpasar City (Source: field survey, 10—19 March 2023).

A seawall is a direct method of coastal protection, constructed parallel to the shoreline between the high and low tide levels (Negm and Nassar, 2016). Its design is optimized to accommodate the maximum breaking wave force, which correlates with the water depth available at its toe. As a barrier, seawalls can be constructed parallel to the shoreline using various materials, ranging from concrete to sandbags, and can vary in design (Balaji et al., 2017; Zhu et al., 2010). Seawalls can effectively defend against flooding and erosion, immobilizing the adjacent beach sand. However, the cost and effectiveness of seawalls depend on their shape and size. Moreover, when combined with rock revetments, seawalls dissipate wave energy and prevent further recession of the backshore. Unlike seawalls, rock revetment features a distinct slope, while seawalls typically have a near-vertical design.

Groins are shoreline structures built perpendicular to the shoreline, often constructed using rocks or other materials. In sandy coastal areas, groins play a crucial role in sediment management by trapping sediment carried by longshore currents, leading to beach nourishment and expansion. The groin system serves as a breakwater; the presence of groins interrupts the water flow and reduces sand movements, thus mitigating erosion. As a result, groins significantly influence shoreline changes (Heikal et al., 2023). Sand accumulates on the up-current part of the groin, leading to beach growth, while erosion occurs in the down-current area due to reduced sediment supply. This combination of sediment trapping and erosion prevention makes groins effective coastal management tools for maintaining and enhancing beach stability and resilience. Beach nourishment combined with detached breakwaters in Samuh Beach, Badung Regency (Figure 3-12-f) effectively prevents the shoreline with no

significant retreat. This defense system limits the loss of sediments from sandy beaches and allows better protection to control shoreline erosion. However, there is a possibility for sediment loss in the future (Onaka et al., 2013).

Moreover, prioritizing protecting and restoring vital ecosystems such as mangroves, salt marshes, and seagrass beds can provide natural protection against erosion. Mangrove ecosystems provide valuable ecosystem services, making them indispensable for coastal regions. These habitats significantly improve coastal water quality by acting as natural filters, removing pollutants, and enhancing water clarity. Furthermore, mangroves serve as crucial wildlife habitats, supporting various plant and animal species, including migratory birds, fish, and marine invertebrates. Additionally, these resilient ecosystems possess the capacity to absorb wave energy and stabilize sediments, effectively reducing the impact of erosive forces from erosion, tsunamis, and storm surges by dissipating wave energy and stabilizing shorelines.

The interplay between development and shoreline erosion is significant to the Balinese, as the beach carries more than just economic benefits; it holds a deep cultural and religious significance. Beaches in Bali are not only a source of livelihood through tourism and fishing but also serve as sacred spaces for traditional ceremonies, rituals, and spiritual practices. The connection between Balinese culture and the coastal environment is deeply rooted, and many religious ceremonies and cultural festivals are conducted on the shores. The erosion of these precious coastal areas can disrupt the culture of the local communities and impact their spiritual connection to the land and sea. As development and urbanization continue to shape the coastal area, it becomes crucial to find a balance that preserves traditional values and cultural heritage while addressing the challenges posed by shoreline erosion to ensure the sustainable future of Bali's coastal communities.

3.3.8. Accuracy Assessment of The Proposed Method

This study emphasizes the significance of data quality in determining the accuracy of the results. Utilizing PlanetScope images, which offer a high spatial and temporal resolution, proved valuable for studying shoreline changes. Detailed assessments were conducted using grid cells with 50 m spacing and validated at 70 points. The Kappa Coefficient analysis revealed a moderate agreement of 0.50 between the field survey and shoreline type, with an overall accuracy of 78.38%. However, it is important to consider the time difference between the remotely sensed image for classification and validation data, as the shoreline type may change the time difference. The current study's findings are comparable to the previous studies (Hastuti et al., 2022). However, slight differences exist due to variations in transect locations and utilization of high-resolution satellite images. The enhanced spatial resolution of these satellite images facilitated a more precise analysis of the shoreline change, ultimately reducing forecast errors and increasing the reliability of future change predictions. These advancements contribute to a more comprehensive understanding of shoreline change studies.

3.4. Conclusion

This comprehensive study focuses on the dynamic changes occurring along the shoreline of Bali Province between 2016 and 2021. This study attempts to comprehend and analyze the complicated movement of shoreline changes in the dynamic coastal areas of Bali. The study effectively quantifies multitemporal shorelines using the NDWI and EPR model using advanced remote sensing and GIS technologies with high-resolution PlanetScope imagery data. The results show significant variations in shoreline positions, with rapid erosion emerging as a major concern for Bali Province. The southern part of Bali is more vulnerable to erosion than the northern part due to human activities and coastal hydrodynamics. These are recognized as primary drivers of erosion, leading to a decrease in the natural shoreline. However, artificial shorelines have increased net land due to human interventions such as land reclamation and infrastructure development. Despite efforts to manage coastal erosion using hard structures, the response has been restricted due to insufficient ecological assessment. The findings have significant implications for coastal planning and management, providing useful insights for informed decision-making and sustainable development in the coastal area of Bali Province. Addressing the issues provided by shoreline changes is essential to protecting coastal ecosystems, supporting economic growth, and preserving the cultural significance of the region for future generations. Moreover, a comprehensive analysis of shoreline changes, including a detailed assessment of the cost and benefit associated with potential adaptations and mitigation, should be undertaken to evaluate the possible actions for coastal protection strategies.

CHAPTER 4. COASTAL FLOOD IMPACT DETECTION

4.1. Overview

Sea-level rise will increase the risks for coastal communities, but these threats from rising seas are by no means new. Over the last decades, research on sea level rise has increasingly demonstrated, contributing to our understanding of its processes and possible impact. One of the references globally is the IPCC reports. Several studies have been devoted to projecting the potential impacts of sea level rise at a regional and local level. Dasgupta et al. (2009) analyze the global sea level rise impacts for 84 coastal developing countries using a spatially disaggregated global database. More specifically, Kuleli et al. (2009) utilized high-resolution SRTM topographic, orthorectified Landsat Thematic Mapper Mosaics, and census data to investigate the sea level rise impact on the 0-10 m elevation of the Turkish coastal zone. Ward et al. (2011) simulated coastal inundation and analyzed their potential damage to northern Jakarta, Indonesia. Meanwhile, Malik and Abdalla (2016) developed a geospatial model to analyze the potential impacts of the sea level rise on the coast of Richmond, British Columbia, Canada, based on a digital elevation model (DEM). These studies utilized the digital elevation model (DEM) and spatial population datasets such as land use.

The impacts of flooding events can encompass loss of life, damage to buildings and natural environments, and extreme disruption to the lives of the population affected. However, in the long term, the immediate and post-recovery phases can cause disruption, distress, health problems, and financial hardships that can last many years. Meteorological events cannot be changed, but the manifestation of a flood event as a result of weather extremes is, to some extent, mitigated. The land, built environment, and society can significantly contribute to our vulnerability to such events. Therefore, understanding the vulnerability level in an area with a high probability of hazard events is critical to mitigating and increasing resilience, thereby reducing the risk. Climate change is expected to increase the frequency and magnitude of storms and flood events, with coastal communities bearing the brunt of those impacts.

Flooding does not just impact areas within flood zones. It can often impact much wider than that. Much of the infrastructure that supports the region and communities is located in the floodplain, whether telecoms, water or power supply, or transport networks. This risk is poorly understood, as is the interdependency of the infrastructure system on one other.

This study aims to address the gap and analyze the regional impacts of climate change and sea level rise on the coastal areas of Bali Islands, Indonesia. We simulated coastal inundation due to rising sea levels in multiple scenarios of projected sea level heights in 2025, 2030, 2070, and 2100. Also, we estimated the potential impacts of coastal inundation on land use in the Bali Islands due to sea level rise. The study results are then visualized using inundation maps. The present study addresses the need to develop adaptation and mitigation to climate change impacts.

4.2. Data Collection and Methods

The study was conducted in Bali Province. Based on the 2022 census, the population of Bali Island was estimated at 4,317,404, making up 2% of the Indonesian population. Since the Bali Islands are a top tourist destination in Indonesia and Southeast Asia, most of the population relies on marine and coastal resources. Besides tourism and agriculture, services and trade are among the important economic support sectors in the islands. As expected (Table 4-1), the coastal area in Denpasar, Badung, and Buleleng Regency, which is also the center of Bali's tourism sector, is the most densely populated (Badan Pusat Statistik - Statistics of Bali Province., 2022). Moreover, public facilities and infrastructure, including national toll roads, were built in coastal areas. The southern coastal area of Bali, where most of the tourism centers were built, is the area that is under the most anthropogenic pressures. Not to mention coastal hard erosion and land subsidence due to excessive coastal resource exploitation in the region (Rajendra, 2020b; Triana and Wahyudi, 2020a). Bali's climate is defined by the rainy season, around November to April, and the dry season around May to October. The Indian Ocean strongly influences tides in Bali with mixed semi-diurnal type with two high and low peaks tides. The maximum tide range is approximately 2.24 m. During the high seasonal tides, coastal flooding often occurs in the Bali Islands, inundating low-lying areas (BMKG, 2020; Hastuti et al., 2022b; Rajendra, 2020b).

Table 4-1. Population characteristics of Bali Province.

Regency	Area (km2)	Population	Density per km2
Bangli	490.71	258,721	527
Denpasar	127.78	725,314	5,676
Badung	418.62	548,191	1,310
Tabanan	1013.88	461,630	455
Jembrana	841.80	317,064	377
Buleleng	1364.73	791,813	580
Karangasem	839.54	492,402	587
Klungkung	315.00	206,925	667
Gianyar	368.00	515,344	1,400
Total	5780.06	4,317,404	747

Source: (Badan Pusat Statistik - Statistics of Bali Province, 2022)

To study and analyze the potential impacts of sea level rise in Bali Province, a combination of the Digital Elevation Model (DEM) and regional sea-level change data was utilized to build a potential risk map in multiple scenarios. This study calculates the sea level rise trend from tidal observation of tide gauge and sea level anomaly observation of satellite altimetry. The framework of this study consists of two stages: mapping the potential inundation area and analyzing the impact of damage due to coastal inundation (Figure 4-1).

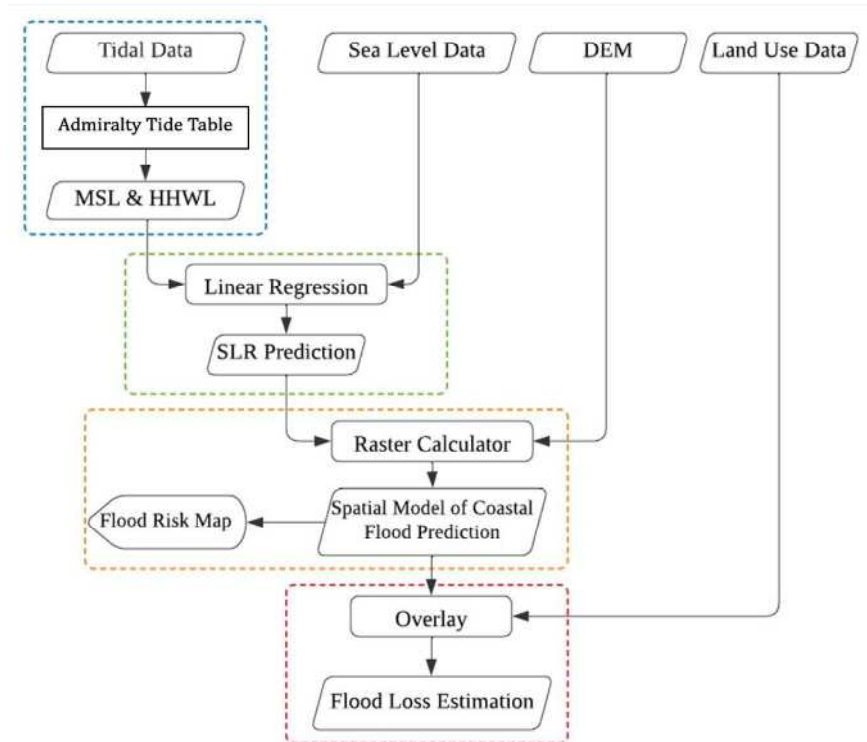


Figure 4-1. Flow chart showing the methodology.

Data needed as follows:

1. Hourly tides data
2. Sea level rise data
3. Digital Elevation Model (DEM)
4. Land use and land cover of Bali Province

Tide gauges and satellite altimetry data were utilized to generate regional sea level change data. Regional sea level change data were derived from altimetry data and tide gauges. Tidal data in Benoa Port was downloaded from the Geospatial Information Agency (BIG), Republic of Indonesia. Tidal data used is 2020 and processed with the admiralty method to obtain the Mean Sea Level (MSL) and Highest High-Water Level (HHWL). The admiralty method also predicts hourly heights of high and low water levels. Historical tide gauges in Benoa Port provide invaluable information on coastal sea level change relative to the ground from January 2006 to December 2020.

Sea level rise data from satellite altimetry downloaded from Jet Propulsion Laboratory (PODAAC) for the successive TOPEX/Poseidon, Jason-1, Jason-2, and Jason-3 missions with coordinates 8.75S and 115.25W for 26 years. This PODACC offers gridded altimetry measurements of sea surface height anomalies (SSHA) above a mean sea surface on 5-day increments at 1/6th degree resolution (~ 18.5 km). The future sea level rise (SLR) which is

defined as SL_{max} was obtained using Eq. (4.1) from the linear regression relationship between sea level and tidal data.

$$SL_{max} = HHWL + (SLR (Y_p - Y_b)) \quad (4.1)$$

SL_{max} = highest water level in prediction year (cm)

$HHWL$ = Highest High-Water Level in 2020

SLR = Sea Level Rise (cm)

Y_p = Prediction year

Y_b = Base year

Furthermore, the flood prediction is carried out by mapping the predicted sea level rise on the Digital Elevation Model (DEM). The coastal areas with the same height as the sea level rise will be determined as the inundated area. DEM of Bali Province with 0.27 arcsecond (~8.1 m) resolution using EGM2008 vertical datum was obtained from The Geospatial Information Agency (BIG), Republic of Indonesia. These data were built from several data resources, including IFSAR (5 m resolution), TERRASAR-X (5 m resolution), and ALOS-PALSAR (11.25 m resolution). In addition, to examine the extent of losses from the coastal flooding effect, land use data was also applied in this study with the assumption that there are no land use changes throughout the study. The land use of Bali Province obtained from the Geospatial Information Agency (BIG), Republic of Indonesia, as shown in Figure 4-2 and was delineated into seven LULC categories, i.e., water bodies, vegetation, flooded vegetation, agricultural land, aquaculture land, built-up areas, and bare ground. Moreover, Table 4-2 shows the LULC classification adopted by Brown et al. (2022).

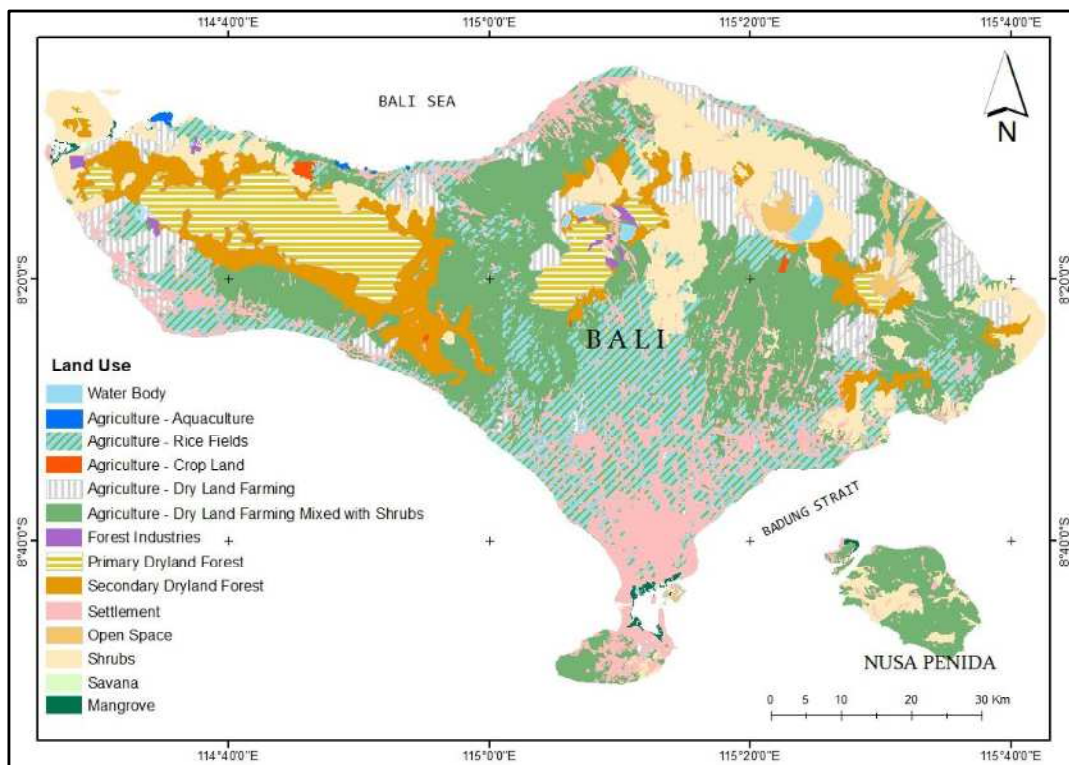


Figure 4-2. Land use and land cover in Bali Province.

Table 4-2. Description of LULC classification taxonomy.

Type of LULC	Description	Examples
Water bodies	<ul style="list-style-type: none"> – water is present in the image – contains little-to-no sparse vegetation, no rock outcrop, and no built-up features like docks – does not include land that can or has previously been covered by water 	<ul style="list-style-type: none"> – rivers – lakes – ocean
Vegetation	<ul style="list-style-type: none"> – any significant clustering of dense vegetation, typically with a closed or dense canopy – taller and darker than surrounding vegetation 	<ul style="list-style-type: none"> – wooded vegetation – dense green shrubs
Flooded vegetation	<ul style="list-style-type: none"> – areas of any vegetation with obvious intermixing of water 	<ul style="list-style-type: none"> – mangroves
Agricultural land and agroforestry	<ul style="list-style-type: none"> – area containing annual crops and vegetation planted by human 	corn, sugar cane, paddy, palm trees, cacao, coffee, tea
Aquaculture land	<ul style="list-style-type: none"> – water is present in the image 	<ul style="list-style-type: none"> – ponds – flooded salt pans
Built-up area	<ul style="list-style-type: none"> – human-made structures either in clusters or one single large structure – area with industrial, commercial, and private buildings, including the parking lots – a mixture of residential buildings, streets, lawns, trees, isolated residential structures, or buildings surrounded by vegetative land covers – major road and rail networks outside of the predominantly residential areas – artificial structures and man-made piles of boulders or concrete that are built on either side of a coastal inlet 	<ul style="list-style-type: none"> – cluster of houses, can include small lawns or small patches of trees included – dense villages, towns, and cityscapes (buildings and roads together) – cluster of paved roads and large highways – asphalt and other human-made surfaces – seawalls, jetties, groins, and breakwaters
Bare ground	<ul style="list-style-type: none"> – areas of rock or soil containing very sparse to no vegetation – large areas of sand with little to no vegetation 	<ul style="list-style-type: none"> – exposed soil – exposed rock – sand dunes – marine deposition (sediment)

4.3. Result

4.3.1. Sea Levels

Tidal constituents (or tidal components) are the net result of multiple influences impacting tidal changes over certain periods of time. Table 4-3 presents the principal tidal

constituents. The influence of the sun is characterized by the letter *S*, while the influence of the moon is characterized by the letter *M*. Index 2 refers to phenomena that occur twice daily.

Table 4-3. Tidal constituents.

	S0	M2	S2	N2	K1	O1	M4	MS4	K2	P1
A (cm)	206.94	64.92	37.47	12.28	26.33	13.78	0.99	0.67	10.12	8.69
g°		49.96	108.49	21.53	177.04	172.44	148.99	251.83	108.49	177.04

From Table 4-3, the Formzahl Number could be calculated. The Formzahl Number in Bali Province is 0.39, which means the tidal is mixed semi-diurnal tide, having two high tides and two low tides per day, but the heights of each tide differ, as shown in Figure 4-3. The Mean Sea Level (MSL) was obtained at 207.20 cm. MSL is caused by water conditions, coastlines, and bathymetry, the gravitational forces of the moon and sun. The amplitude of the Highest High-Water Level (HHWL) reached 361.98 cm.

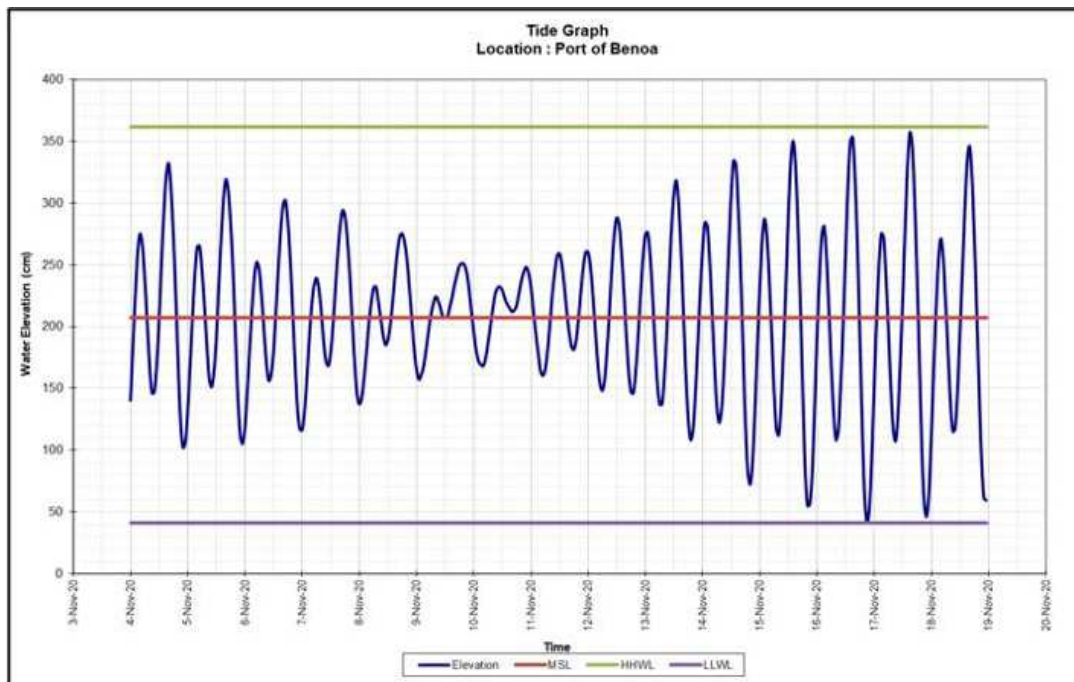


Figure 4-3. Sea level data from altimetry and tide gauge.

Figure 4-4 shows the correlation between the tide gauge and altimetry observations. It gives an insight into how altimetry observations can represent sea level variability close to the coast.

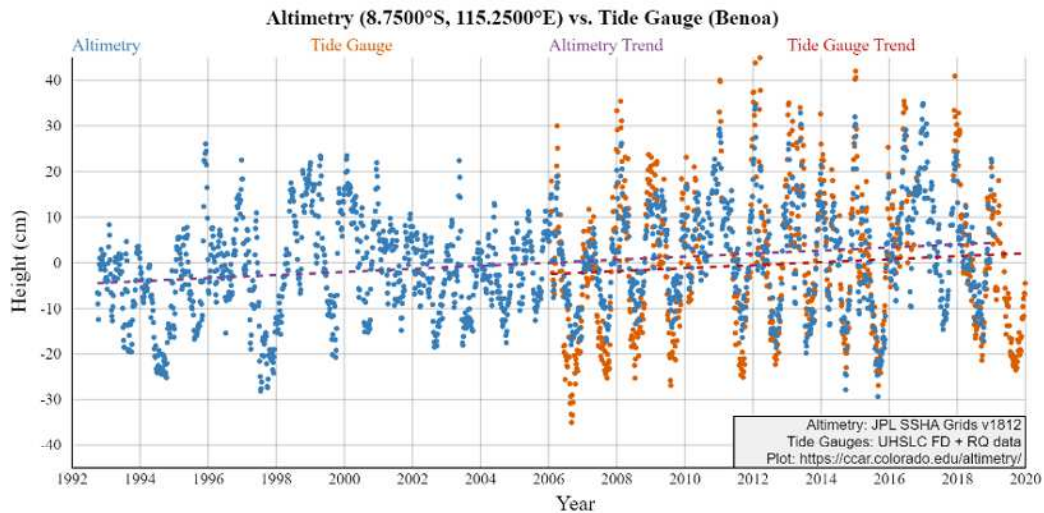


Figure 4-4. Sea level data from altimetry and tide gauge.

Relative sea level rise is a combination of eustatic (global), regional, and local changes in sea level. Relative sea-level change data is a historical record. Figure 4-4 shows the sea level height in Bali for 27 years. Trend of sea level height was retrieved from satellite altimetry and tide gauge. The picture showed that the sea level retrieved from altimetry (satellite observation) shows a clear upward trend, compared with the tide gauge with 0.34 cm/yr and 0.33 cm/yr, respectively.

The satellite trends reflect changes in the sea surface height only, with most of the spatial variation resulting from the influence of winds blowing over the ocean. The tide gauge trends are relative to a fixed point on land and reflect changes in water level plus local vertical land motion. The land near a tide gauge can move up and down for various reasons, such as earthquakes or ground-water withdrawal.

4.3.2. Sea Levels Prediction

Figure 4-5 shows the Highest High-Water Level (HHWL) estimation subjected to the sea-level rise over the study period. It was found that the sea level along the Bali Province coastline is projected to rise.

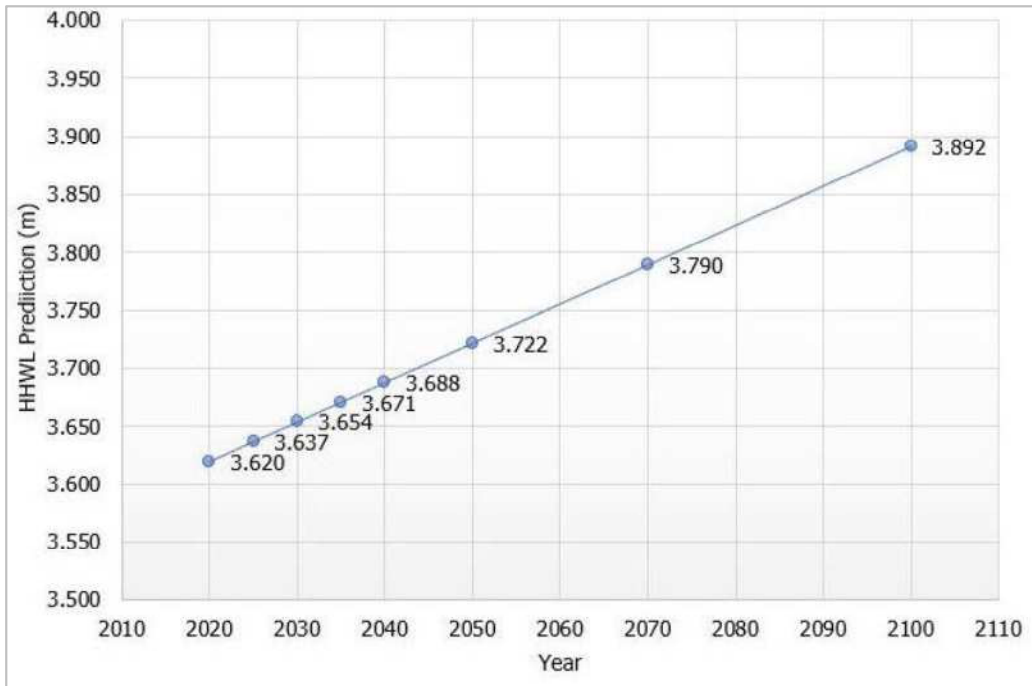


Figure 4-5. Sea level rise prediction based on HHWL.

4.3.3. Flood Risk Map

Coastal flooding is indicated when the coastal areas are inundated, especially in dry and low-lying areas that are submerged by seawater. It was caused by a combination of sea level, tides, and storms that surged up to the height of the ocean and spread over adjacent land. The range of coastal flooding is determined by the elevation of floodwater that penetrates the inland, which is influenced by the topography of the coastal land subjected to flooding (Bell et al., 2017; Doornkamp, 1998).

Inundation models were generated using the digital elevation model (DEM) and the assumption that during the study timeframe the rate of sea level rise was constant at 0.34 cm/year, and the influence of other factors such as earthquakes and land subsidence was not taken into account due to the limited amount of data. Given this context, it is important to note that the absence of these factors simplifies the analysis. Four periods of coastal flooding scenarios that are made, are as follows: 5 years (2025), 10 years (2030), 50 years (2070), and 80 years (2100) from the initial year (2020). Figure 4-6 to Figure 4-9 shows the land projected to be below the annual flood level over the study period.



Figure 4-6. Land projected to be below annual flood level in 2025.



Figure 4-7. Land projected to be below annual flood level in 2030.

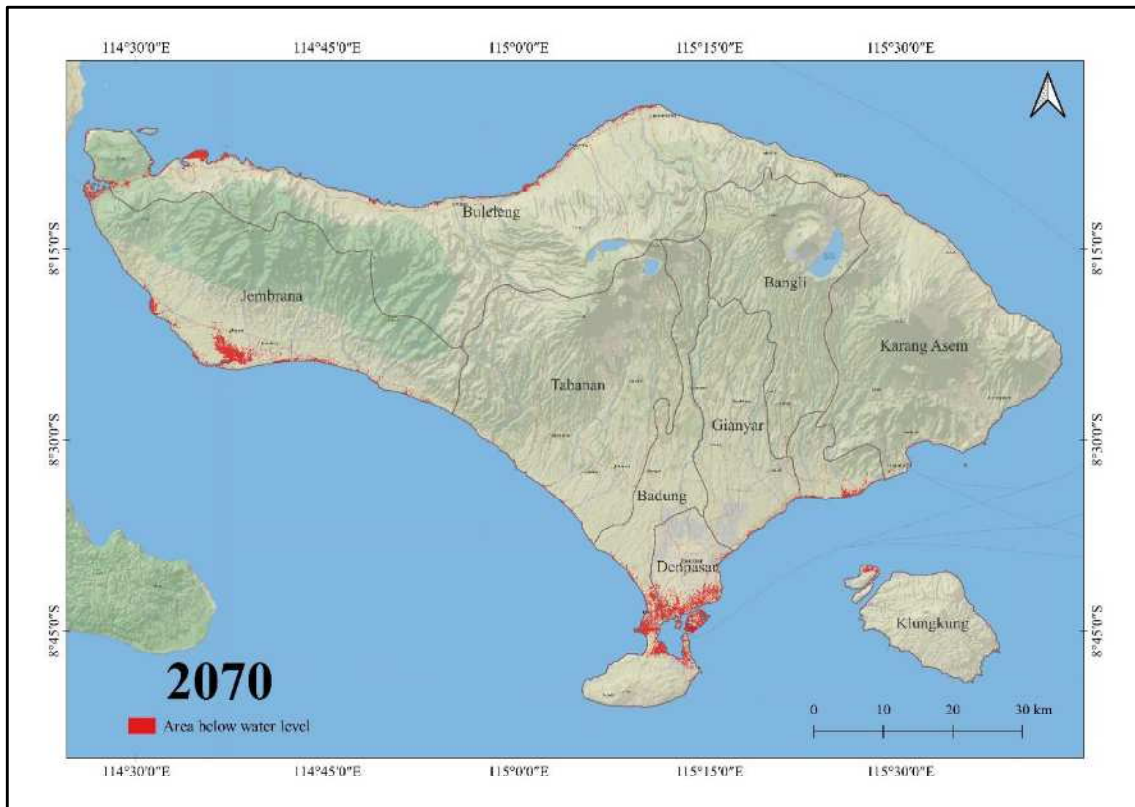


Figure 4-8. Land projected to be below annual flood level in 2070.

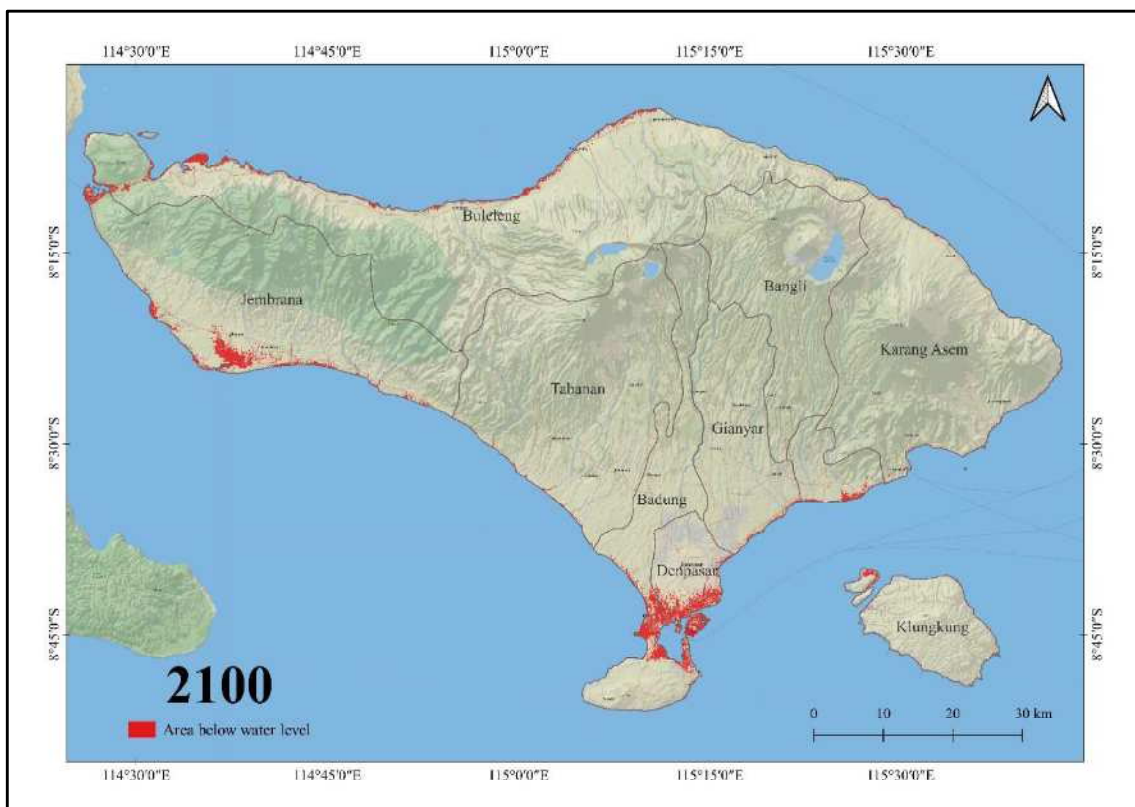


Figure 4-9. Land projected to be below annual flood level in 2100.

The study presents an assessment of the influence of sea level rise on coastal flooding. According to the developed coastal flooding scenarios shown in Figure 4-6 to Figure 4-9, it is anticipated that most of the southern coast of Bali Province is expected to be submerged by 2025, 2030, 2080, and 2100. The prediction of the inundation area in each scenario is shown in Table 4-4.

Table 4-4. The prediction of inundation area.

Regency	Area below water level (ha)			
	2025	2030	2070	2100
Denpasar	1389.75	1404.69	1484.03	1527.89
Badung	1279.23	1287.98	1343.32	1403.20
Tabanan	129.38	131.32	134.85	137.46
Jembrana	1636.10	1639.63	1660.75	1676.59
Buleleng	1308.11	1315.34	1376.16	1424.30
Karangasem	399.74	400.30	406.19	410.65
Klungkung	432.05	433.25	449.31	461.65
Gianyar	123.23	123.95	129.90	134.71
Total	6697.58	6736.46	6984.51	7176.46

Based on Table 4-4 and Figure 4-6 to Figure 4-9, the flooding area increases over time. In the 5-year scenario, by 2025, sea level will reach 363.7 cm, and the inundation area in Bali Province will reach 6697.58 ha. In the 10-year scenario, by 2030, the inundation area will reach 6736.45 ha when the sea level rise reaches 365.4 cm. In the 50-year scenario, by 2070, the sea level will reach 379.0 cm, resulting in 6984.51 ha of land being inundated. And in the 80-year scenario, by 2100, sea level will reach 389.2 cm, and the inundation area in Bali Province will reach up to 7176.46 ha. Based on the scenarios, in the next five to 80 years, all coastal areas in Bali Province with varying degrees of exposure experience coastal flooding, with the exception of Bangli (a non-coastal regency). Coastal flooding highly occurred in the central part of Bali Province, which consists of low-lying areas mainly in Badung, Buleleng, Denpasar, and Jembrana regencies. The length of the coast and topography of the land affect the largest inundation area in Jembrana and Denpasar regencies. Coastal flooding can be exacerbated by numerous variables that are not considered in this approach, such as rainfall, river discharge, and wave impacts such as coastal erosion.

4.3.4. Flood Loss Estimation

Coastal flooding can transform coastal and low-lying areas into submerged areas, which causes an alteration in land use/land cover (LULC). Moreover, flooding can result in economic losses due to damage to infrastructure and property. Flood loss estimation was calculated based

on increased flooding elevation in four scenarios with LULC data in 2020. Recognizing that urban expansion and change in LULC were not considered in this approach. Figure 4-10 shows the land use projected below water level due to coastal flooding.

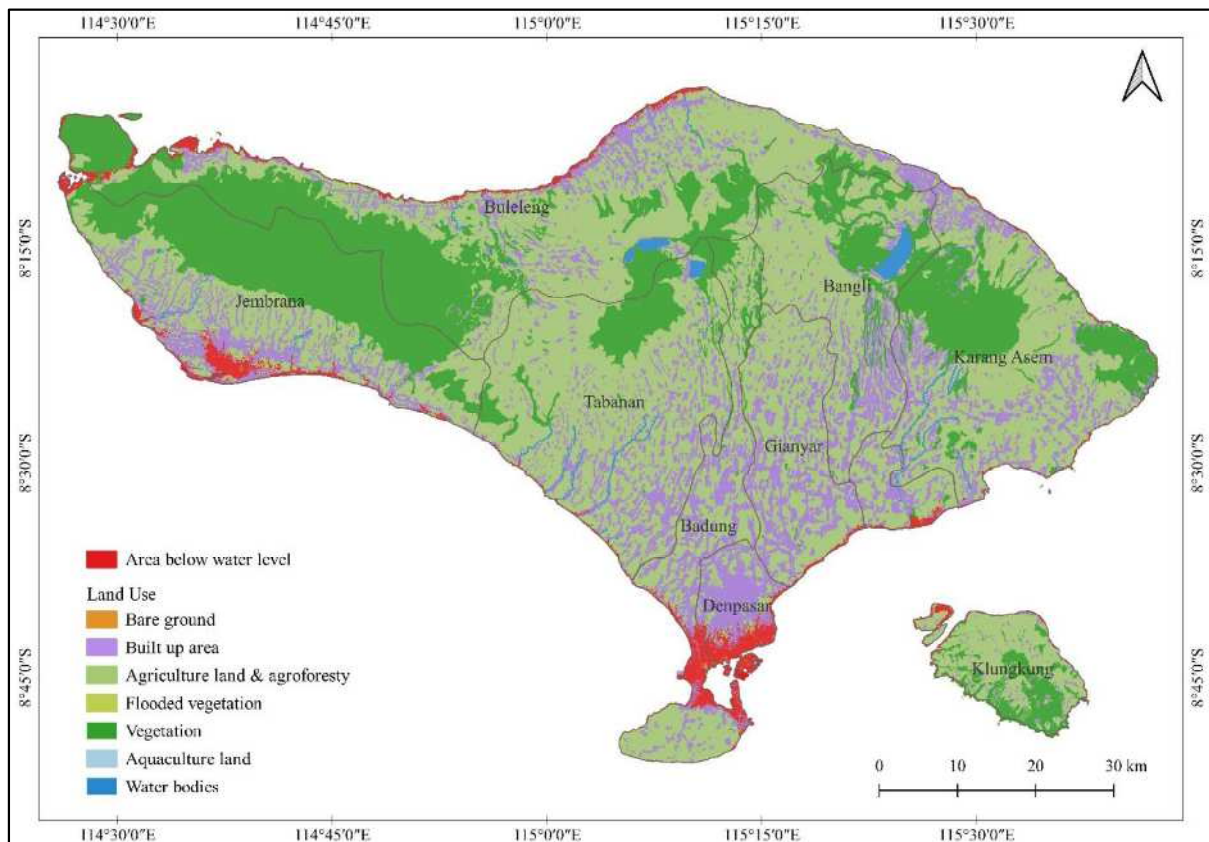


Figure 4-10. Land use projected to be below water level.

Figure 4-11 the estimated damages to LULC under rising sea levels in four scenarios by 2025 to 2100. An increasing trend of rising sea levels results in larger damaged areas with economic value. It is estimated that 3029.75 ha of agriculture land and agroforestry land, 1177.49 ha of built-up area, 1129.39 ha of flooded vegetation, 773.9 ha of aquaculture land, 393.63 ha of bare ground, 362 ha of water bodies, and 305.11 ha of vegetation will be lost to coastal flooding by 2100. Based on Figure 4-11, agriculture land and agroforestry, flooded vegetation, aquaculture land, and built-up areas are among the most impacted areas by the flooding. The increasing trend of sea levels and inundation of these type of land use can be associated with loss of productive land resulting in wider potential damaged to the economic. Given that Bali Island is the major tourist destination in Asia that relies on coastal resources, coastal flooding will have an impact on considerable economic losses, particularly in the tourism and service provision sectors. Coastal flooding is increasingly destroying the LULC of coastal areas. The result shows that coastal flooding will impact quite significant economic losses. The amount of economic loss is based on the economic value of land use.

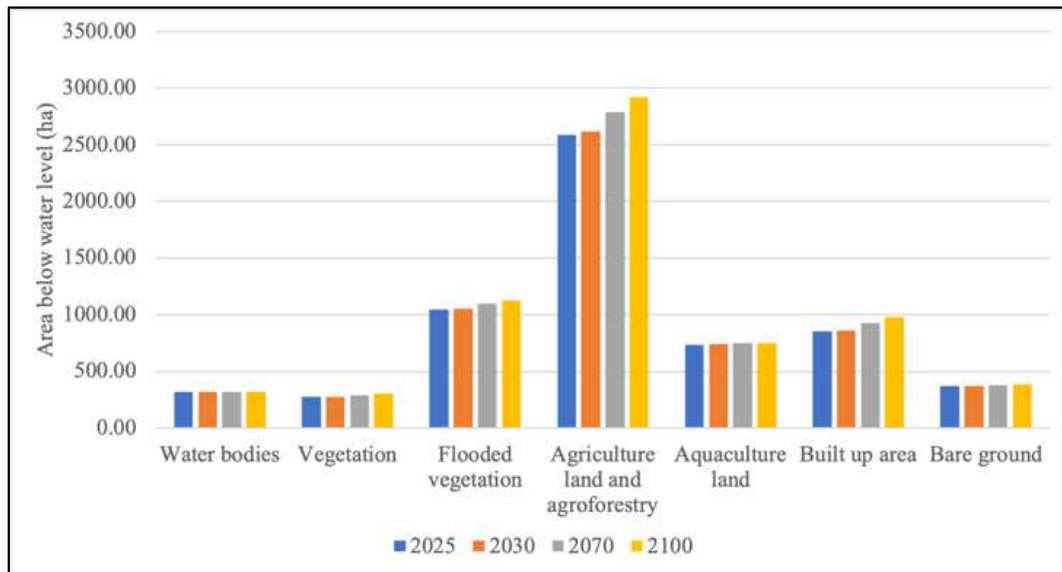


Figure 4-11. The extent of land damage due to inundation.

4.4. Discussion

In this study, satellite altimetry and tide gauge measurements from Port Bena, Bali, were used to determine the sea level condition of Bali Province. The examination of tidal constituents indicates that the Bali Islands have a mixed semi-diurnal type of tide, which is defined by different sizes of two highs and two lows within a day. This result is in accordance with previous studies (A Widiawan and Nurdjaman, 2018; Berlianty and Yanagi, 2015b; Hastuti et al., 2022a; Ray and Dwi Susanto, 2019) that area bordering the Indian Ocean as well as the Arafura Sea includes the coastal areas on the west coast of Sumatra and the south of Java and Bali have a mix semi-diurnal tidal type which is characterized by the strong influence of the moon's gravitational forces.

Based on satellite altimetry and tide gauge observations in Bena, Bali, sea levels have shown an increasing trend over the last 27 years. The satellite trend only reflects changes in sea surface height, with most of the spatial variation resulting from the influence of winds blowing over the ocean. While the tide gauge trend is relative to a fixed point on land and reflects changes in water level coupled with local vertical land motion. The land near a tide gauge can move up and down for a variety of reasons, such as earthquakes or groundwater withdrawal. According to Prabowo, (Prabowo, 2016), Indonesia and Bali Island are susceptible to earthquakes, due to their position within the global ring of fire. In addition, several studies revealed that there is land subsidence in various South Bali locations, (Dwiputra et al., 2020; Elvansha et al., 2022; Triana and Wahyudi, 2020b; Yastika et al., 2020). Differences in sea level height from satellite altimetry data and tide gauges can occur due to this vertical movement. However, in this study, both satellite altimetry and tide gauges show a close value. Moreover, the rate of increase on the island of Bali corresponds to the current global average rate of sea level rise following the IPCC, (Cazenave et al., 2014b; IPCC, 2019).

Using the current rising rate, it is projected that the sea level can reach up to 389.2 cm by 2100. Rising sea levels can change tidal dynamics and have the tendency to increase the Highest High-Water Level (HHWL) in potential flooding and extreme events. Rising sea levels

will significantly change future coastal flooding by causing rising tide levels and reaching farther inland (IPCC, 2018). Differences in sea level height from altimetry data and tide gauges can occur due to vertical movement due to seismic activity in Indonesia (Triana and Wahyudi, 2020a). According to altimetry data, the rate of increase on the island of Bali corresponds to the current global average rate of sea level rise (Cazenave and Cozannet, 2014; Oppenheimer et al., 2019). The rise of sea level along the Bali coastline may not be uniform, it can be influenced by various factors such as local topography, coastal geomorphology, tidal patterns, and oceanographic conditions. Moreover, human-induced climate change conditions have forced a new balance in sea levels. Although it was not taken into consideration in this analysis, land subsidence may have caused greater flooding than anticipated.

The impacts of sea level rise on the coastal area of Bali were simulated based on the current rising rate in four different scenarios in 5 years (2025), 10 years (2030), 50 years (2070), and 80 years (2100) from the initial situation (2020). These maps aim to provide a visual projection of the area that will be inundated in the scenarios. The trend of rising sea levels drives the extent of coastal flooding even greater in the future. Based on the simulation results (Table 4-4), the coastal areas of Jembrana, Denpasar, and Buleleng regencies are among the most vulnerable to coastal inundation due to sea level rise in the region. More specifically in the central coast of the Bali Islands. Flood risk maps are used for coastal area planning efforts and adapting to climate change and sea level rise. This approach enables the quick mapping of any scenario while accounting for the concerns related to long-term projected sea level rise.

SDGs 11 and 13 shed lights on how coastal towns and cities are affected by climate-related risks, such as increasing sea levels. These studies aid in the mitigation and adaptation to the effects of climate change by addressing vulnerability, finding adaptation strategies, and encouraging climate-resilient development. In order to build more resilient and sustainable cities and communities, it is important to understand the causes and effects of coastal flooding. This knowledge may be applied to risk management techniques, infrastructure development, and urban planning.

4.5. Conclusion

This study analyzed the impacts of climate change, particularly sea level rise, on the coastal areas of Bali Province, Indonesia. The impacts of sea level rise on coastal areas of Bali Province were studied in two stages: mapping the potential flood area and analyzing the impact of damage due to coastal inundation. The potential inundation area was projected using the current rising rate and the Digital Elevation Model (DEM). While land use/land cover (LULC) data was utilized to simulate potential impacts in four different scenarios.

This study highlights the imminent threat of sea level rise to Bali Province, Indonesia, a region heavily reliant on coastal resource and vulnerable to coastal inundation. By 2100, projections indicate substantial land loss with significant impact on Jembrana, Denpasar, Buleleng, and Badung. Our approach enables the quick mapping of any scenario and reflects threats from permanent future sea-level rise. However, the maps are not based on physical storm and flood simulations and do not take into account factors such as earthquakes, land subsidence, and future changes in the frequency or intensity of storms, inland flooding, or contributions from rainfall or rivers. Information of climate change and sea level rise impacts

is important for coastal flooding mitigation in archipelagic nations. These findings emphasize the urgency of proactive adaptation policies, including coastal management plans, infrastructure development, and community-based resilience programs. Immediate action is crucial to mitigate the consequences of rising sea levels, protect livelihoods, and ensure the sustainable future of the Bali Islands.

CHAPTER 5. COASTAL VULNERABILITY IN BALI PROVINCE FROM PHYSICAL PARAMETERS

5.1. Overview

As a natural coastal defense system, beaches are essential in reducing coastal erosion risks. Thus, their retreat and eventual disappearance increase their vulnerability to hazardous events. In addition, beach narrowing threatens beach environmental services critical to tourist destinations' economies since recreational activities depend on the beach backshore (Anfuso et al., 2014; Jiménez et al., 2007; Valdemoro and Jiménez, 2006). Considering the threat of sea-level rise in coastal areas and on small islands, it is necessary to conduct a study to determine the degree of vulnerability experienced by a coast since measuring vulnerability is a fundamental phase in achieving effective risk reduction (Birkman, 2006). Therefore, this study aims to quantitatively assess the vulnerability of the coastal zones of Bali Province to the actual rate of SLR by developing a Coastal Vulnerability Index (CVI), considering the geological and physical characteristics of coastal processes.

The most common and straightforward method for assessing coastal vulnerability concerning sea-level rise is based on calculating an index aggregating a set of parameters representing several spatial entities (geographic data) that influence coastal vulnerability. The Coastal Vulnerability Index (CVI) was introduced by Gornitz (1991) and has been adopted and/or applied to assess coastal vulnerability globally (Bagdanavičiute et al., 2015; Boruff et al., 2005; Diez et al., 2007; Hammar-Klose and Thieler, 2001; Kumar and Kunte, 2012; Lien, 2019; López Royo et al., 2016; Özyurt and Ergin, 2010; Pendleton et al., 2005; Rao et al., 2009; Shaw et al., 1998; Zhu et al., 2018). It uses a ranking system; therefore, it is easy to identify the degree of vulnerability. The model developed by Gornitz (1991) is composed of seven variables to determine physical vulnerability in the USA to sea level rise impacts, consisting of relief (elevation), rock type (geology), landform (geomorphology), vertical movement (relative sea-level change), shoreline displacement, tidal range, and wave height.

A significant focus of CVI studies is addressing geophysical vulnerabilities based on remotely sensed data processed using the GIS methodology. The combination of remote sensing and GIS technology has provided valuable data for analyzing a given scenario (Jana and Hegde, 2016) and can help identify disaster-prone regions (Lawal et al., 2011).

5.2. Data Collection and Methods

The parameters used are dynamic and have varying resolutions from different sources. Hence, each parameter was measured in a grid cell known as a shoreline grid. This shoreline grid was 1 km × 1 km (Figure 5-1). Thus, 681 shoreline grids with an identification number were created to assign the vulnerability scale for each specific parameter. We assumed that this size would be sufficient for uniform data scaling. As a result, specific data had to be upscaled or downscaled. This grid cell is widely used for coastal vulnerability assessment (Bagdanavičiute et al., 2015; Gornitz et al., 1997; Husnayaen et al., 2018; Islam et al., 2015;

Koroglu et al., 2019). This study considered six parameters for developing the CVI: geomorphology, shoreline change rate, elevation, sea level change rate, tidal range, and significant wave height. The present study adopts an index-based methodology applying the CVI.



Figure 5-1. The study area with grid cells along the shoreline.

CVI represents a combined result of the parameters influencing coastal vulnerability in the coastal area. The data were compiled from various sources to build a parameters database initially. The database is based on that used by Thieler and Hammar-Klose (2001, 2000, 1999), Rao et al. (2009), and Pendleton et al. (2010) and loosely follows an earlier database developed by Gornitz (1991). Table 5-1 provides information on the data source and period for each parameter used in this study.

Table 5-1. Sources and period of the different usage parameters in the compiling of CVI

Parameter	Data Source	Resolution	Period
Geomorphology	Land use data and geology map by BIG https://portal.ina-sdi.or.id/downloadaoi/ (accessed on 20 December 2020)	Scale 1:25 k	2005
Shoreline change rate (m/yr)	Sentinel—2A imagery https://earthexplorer.usgs.gov/ (accessed on 15 July 2020)	10 m	2015 and 2019
Elevation (m)	DEM imagery by BIG tides.big.go.id/DEMNAS/ (accessed 23 July 2020)	0.27 arcsecond ~8.1 m	-
Sea level change rate (mm/yr)	Tide gauge and satellite data https://ccar.colorado.edu/altimetry/index.html (accessed on 13 June 2020)	1/6th deg	1992–2019
Tidal range (m)	Tide gauge data https://ccar.colorado.edu/altimetry/index.html (accessed on 2 August 2019)	-	1998–2019
Significant wave height (m)	Marine Copernicus data https://marine.copernicus.eu (accessed on 29 September 2020)	0.2 deg ~22.2 km	1993–2019

The data values of parameters were assigned a vulnerability ranking based on value ranges contributing to coastal vulnerability. In contrast, the non-numerical geomorphology parameter was ranked qualitatively according to the relative resistance of a given landform to erosion. Each parameter input was assigned an appropriate risk level (Table 5-2) based on its ability to cause very low, low, moderate, high, and very high damage, respectively, for a particular area of the coastline) (Gornitz, 1991; Pendleton et al., 2010; Rao et al., 2009). Later, the key parameters were integrated into a single index and categorized based on the relative intensity of risk to the coast. A flow chart of the methodology to obtain the CVI map of Bali Province is provided in Figure 5-2.

Table 5-2. The risk rating for different parameters.

Parameters	Very Low 1	Low 2	Moderate 3	High 4	Very High 5
Geomorphology ^{1,2}	Rocky, Cliff coast, Fjords	Medium cliffs, Intended coasts	Low cliffs, Glacial drift, Alluvial plains	Cobble beaches, Estuary, Lagoon	Barrier beaches, Sand beaches, Saltmarsh, Mudflats, Deltas, Mangroves, Coral reefs
Shoreline change rate ³ (m/yr)	≥2.1 Accretion	1.0 to 2.0 Accretion	-1.0 to 1.0 Stable	-1.1 to -2.0 Erosion	≤-2.0 Erosion
Elevation ³ (m)	≥30.1	20.1–30.0	10.1–20.0	5.1–10.0	0.0–5.0
Sea level change rate ³ (mm/yr)	≤-1.1 Land rising	-1.0 to 0.99 Land rising	1.0 to 2.0 within range of eustatic rise	2.1 to 4.0 Land sinking	≥4.1 Land sinking
Tidal range ^{2,3} (m)	≤0.99	1.0–1.9	2.0–4.0	4.1–6.0	≥6.1
Significant wave height ^{1,2} (m)	<0.55	0.55–0.85	0.85–1.05	1.05–1.25	>1.25

Source: ¹Pendleton et al., 2010; ²Rao et al., 2009; ³Gornitz, 1991

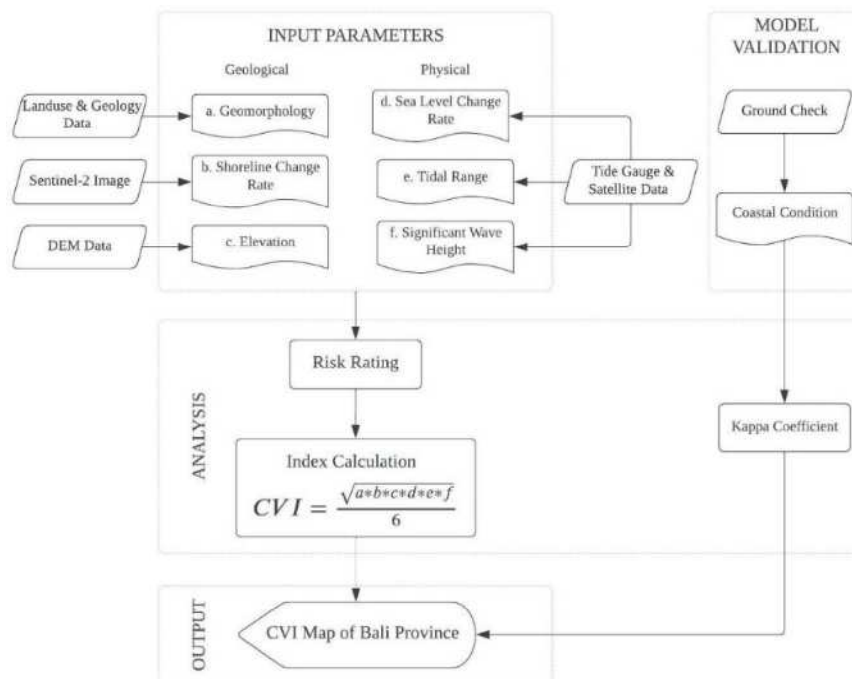


Figure 5-2. Flow chart outlining the process to obtain a CVI map.

5.3. Coastal Vulnerability Index (CVI) Analysis

The CVI analysis was carried out using the software package QGIS version 3.10. This free and open-source GIS application allows creating, visualizing, processing, and analyzing geospatial data. Once each section of the coastline has been assigned a risk value for each parameter, the key parameters are integrated into a single index through a mathematical formula by CVI. The CVI is calculated as the square root of the product of the ranked parameters divided by the total number of parameters (Gornitz, 1991) and represented as shown in Eq. (5.1).

$$CVI = \sqrt{\frac{(a*b*c*d*e*f)}{6}} \quad (5.1)$$

where a = risk rating assigned to coastal geomorphology; b = risk rating assigned to shoreline change rate; c = risk rating assigned to coastal elevation; d = risk rating assigned to sea-level change rate; e = risk rating assigned to tidal range; f = risk rating assigned to significant wave height.

The range value of CVI can be classified into four equal parts (Diez et al., 2007; Gornitz et al., 1991), as quartiles (Abuodha and Woodroffe, 2006; Pendleton et al., 2004) or percentiles range (Kunte et al., 2014; Shaw et al., 1998; Thieler, 2000). This study used quantile classification to classify the CVI range into four risk levels. It divides an equal-sized group of CVI range values into quarters. Therefore, the CVI scores in the lowest range were assigned low vulnerability, followed by moderate vulnerability, high vulnerability, and very high vulnerability for the highest range of CVI values. As a relative quantitative method, this method cannot directly express specific physical processes and effects. Still, it can be a diagnostic tool to determine which regions are most vulnerable to sea-level rise.

5.4. Field Survey

The field survey was designed as a model validation to integrate and apply evidence-based information from the assessment to identify and define the current condition of the study area. The fieldwork was conducted from November 23 – 27, 2020. Before the field survey, the sampling location should be prepared for effective sampling and inspection. The Fitzpatrick-Lins equation (1981) has been applied to decide how many site locations to be inspected.

$$N = \frac{Z^2 pq}{E^2} \quad (5.2)$$

Where: N = number of samples; Z = level of confidence according to the standard normal distribution (level confidence of 80%, $Z = 2$; level confidence of 95%, $Z = 1.96$; level confidence of 99%, $Z = 2.575$); p = estimated proportion of the population that presents the characteristic (when unknown $p = 50$); $q = 100-p$; E = allowable error.

The survey design used to take a sample of beach information is purposive sampling based on the existing vulnerability class map (Figure 5-3). The purposive sampling technique is a type of non-probability sampling that is most effective when needed to study a certain characteristic with knowledgeable expert within. Purposive sampling may also be used with both qualitative and quantitative research techniques.

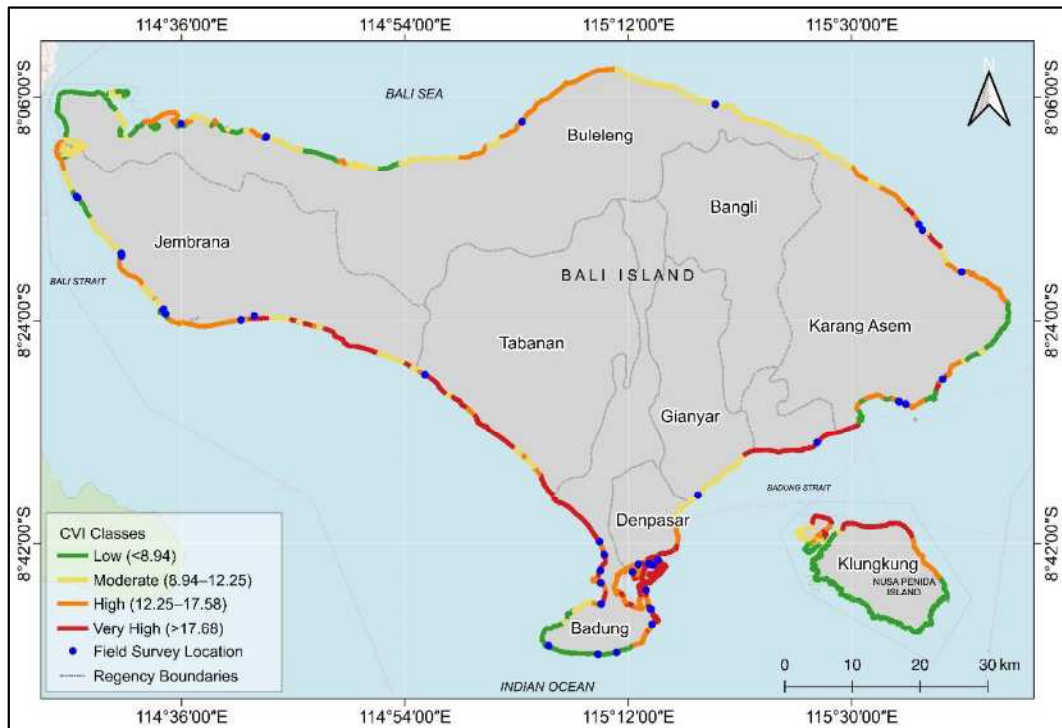


Figure 5-3. Sampling locations for model validation.

To determine the vulnerability class in fieldwork, data and information were collected by visual observation, which considers accessibility and predominant coastal conditions based on the aerial photographs (Google Earth), which can represent an area within a 1 km grid. Each sampling location will have a database containing all information related to physical aspects (land use and/or geomorphology, substrate, elevation, and coastline condition). Simple tabulation was used for displaying numerical data by logically using rows and columns to provide visual relationships and connections and transform raw data into information. Physical data (i.e., location, elevation, photos) were gathered using LocusMap, a multi-functional mobile map, and GPS application, adding advanced online and offline GPS capabilities to Android devices. This application allows users to create, plan, edit, record, save, or share trips and collect geospatial data efficiently and effectively. The additional data that might be collected is an interview with the local community.

5.5. Result and Discussion

As a result of the CVI determination, it is possible to classify the physical vulnerability of the Bali Province coastal zone based on six parameters. Below is a more detailed description of each parameter's coastal vulnerability rank.

5.5.1. Geomorphology

The geomorphology of Bali Province varies from very low to very high vulnerability (Figure 5-4). The classification based on geomorphological characteristics indicates that 152.34 km (24%) of the coastline is very highly vulnerable, another 24% (155.28 km) is highly vulnerable, 228.09 km (36%) is moderately vulnerable, 25.68 km (4%) is at a low level of

vulnerability, and 77.87 km (12%) has a very low vulnerability rank. The most dominant geomorphology of Bali Province is alluvial plains and sandy beaches.

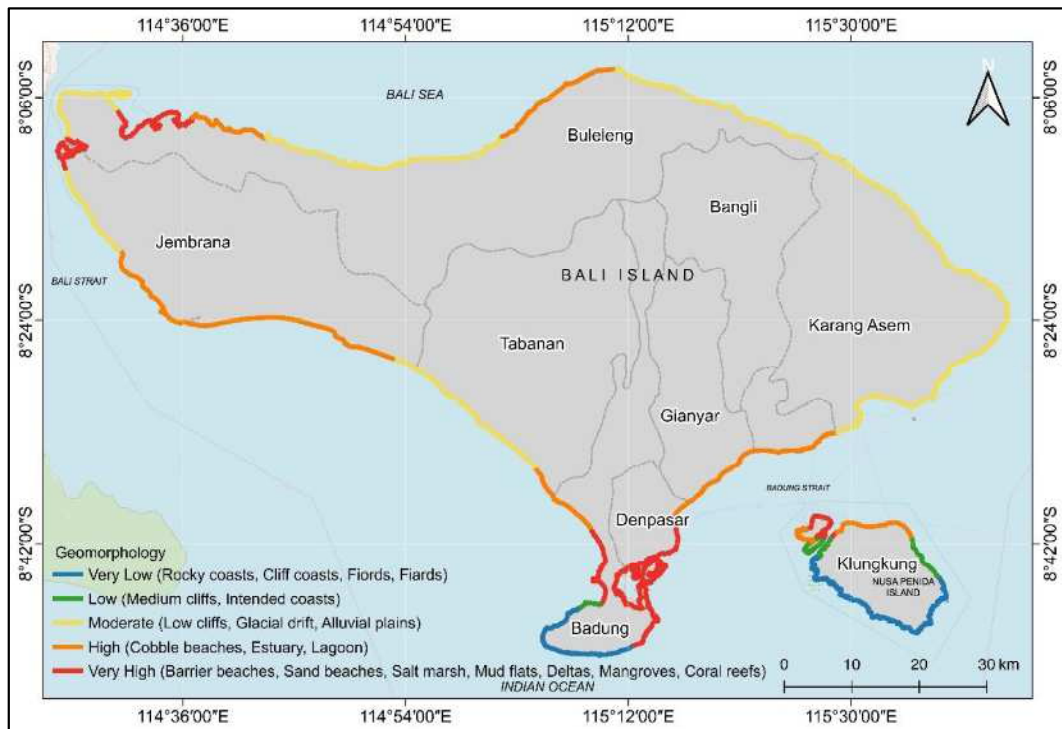


Figure 5-4. The vulnerability rank of geomorphology.

The coastline of Bali Province is segregated into three distinct types: a rocky and cliff coast in the southern part of Bali Island and Nusa Penida Island; a vegetation coast in the center and west of Bali Island and northern Lembongan Island; and a sandy coast for the remainder, which is located in the most coastal area of Bali Province. Coastal areas with rocky and cliff shorelines are highly resistant to erosion (Rao et al., 2009), as is the case on the southern coast, indicated with blue color, and are less vulnerable and classified with a very low rank. Cliff coastlines typically occur along mountainous and hilly coasts, where the offshore slope is steep, and little sediment is available for coastal progradation (Short, 1984).

Sandy beaches, mangroves, and wetlands are found in areas with high and very high vulnerability. Coastal vegetated wetlands and mangrove communities are sensitive to climate change and long-term sea-level change, as their location is intimately linked to sea level. These areas are the least resistant and are, therefore, highly vulnerable to the effects of erosion and sea-level rise (Kumar et al., 2010; Rao et al., 2009).

5.5.2. Coastline Change

According to the results of this analysis, each regency has experienced both erosion and accretion (Figure 5-5). Over 630 km of coastline was evaluated, with 163.56 km (26%) of coastline having a very high-risk level of vulnerability. In comparison, 136.74 km (21%) is highly vulnerable, 56.62 km (9%) is moderately vulnerable, 100.82 km (16%) is at a low level of vulnerability, and 181.50 km (28%) has very low vulnerability. The Klungkung, Badung, Jembrana, Buleleng, and Karangasem Regencies observed the most significant erosion changes.

The study revealed that about 300 km of coastline in Bali Province experienced erosion at various rates due to high waves, coastal sediment mining, beach arching infrastructure construction, and inappropriate beach structures (Putra et al., 2017). Coastlines subjected to erosion are considered more vulnerable because of the loss of coastal habitats, infrastructure, and land.

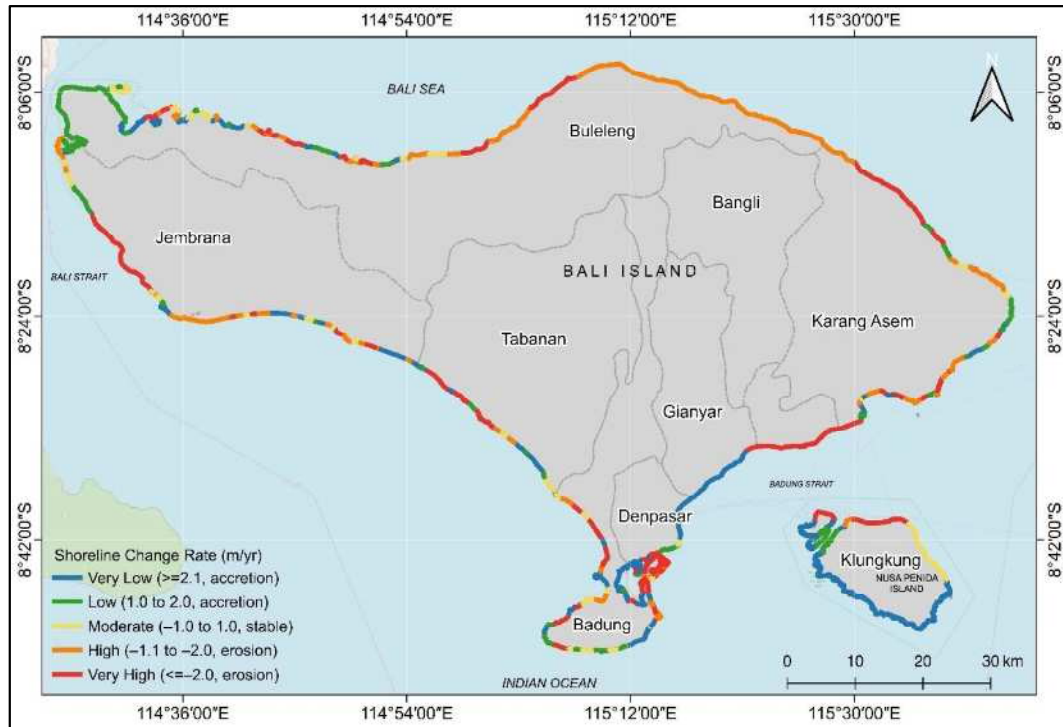


Figure 5-5. The vulnerability rank of shoreline changes rate.

The shoreline changes between 2015 and 2019 are significant due to sediment transport, erosion, accretion, and the impact of reclamation. The impact of reclamation can be noted in Benoa Bay. Many land-reclamation projects are also found in coastal cities that are short of space for expansion, particularly for port activities, such as the I Gusti Ngurah Rai International Airport expansion. The land reclaimed will be used to extend the runway and additional aprons and terminals. Land expansion also took place at Benoa Harbour and Serangan Island. Land reclamation causes significant negative impacts on coastal habitats and the ecosystem services they provide (Wang et al., 2014, 2010). Changes in wave regimes may affect the stability of the sandy shoreline. Large-scale reclamation can affect the wave regime (wave reflection and diffraction) and changes in current patterns, causing coastal erosion in the coastal area and its surroundings, as happened in Serangan Island (Government of Bali Province, 2015).

The most significant factor causing the coastal erosion along most of the coastline in Bali Province is large waves and storms, which result in the occurrence of high sand piles as well as damage to coastal infrastructure. In the eastern part of Bali, strong currents and waves on the northeast coast of Bali cause significant coastal erosion. The waves are influenced by distance and wind in the fetch. The fetch is the area in which the wind generates ocean waves. The coastal fetch in Buleleng Regency predominantly comes from the northeast and the west. The waves occurring from the east and west, depending on the wind season, occurring on

Buleleng's coast cause the movement of alongshore current processes. These processes allow the water to transport sediment along the coast.

Shoreline changes are greatly influenced by processes occurring in the surrounding beach area (nearshore processes), where the beach constantly adapts to various conditions (Muñoz-Pérez et al., 2001). This complex process is influenced by three factors: the combination of waves and currents, sediment transport, and beach configuration, which mutually affect each other. The changes in these factors vary spatially and temporally, lasting a long time.

5.5.3. Elevation

Coastal elevation vulnerability rank based on the spatial distribution of coastal elevation is shown in Figure 5-6, indicating that a length of 374.14 km (59%) of the 640 km of coast of Bali Province has very high vulnerability, indicated with red color, with an elevation of less than 5 m. Meanwhile, 136.74 km (21%) is highly vulnerable, with a range of elevation between 5 and 10 m. The elevation within 1 m of the shoreline faces the highest probability of permanent inundation. In comparison, the coastal strip within 5 m above the normal tides of the present shoreline is also at high risk from severe storm surges.

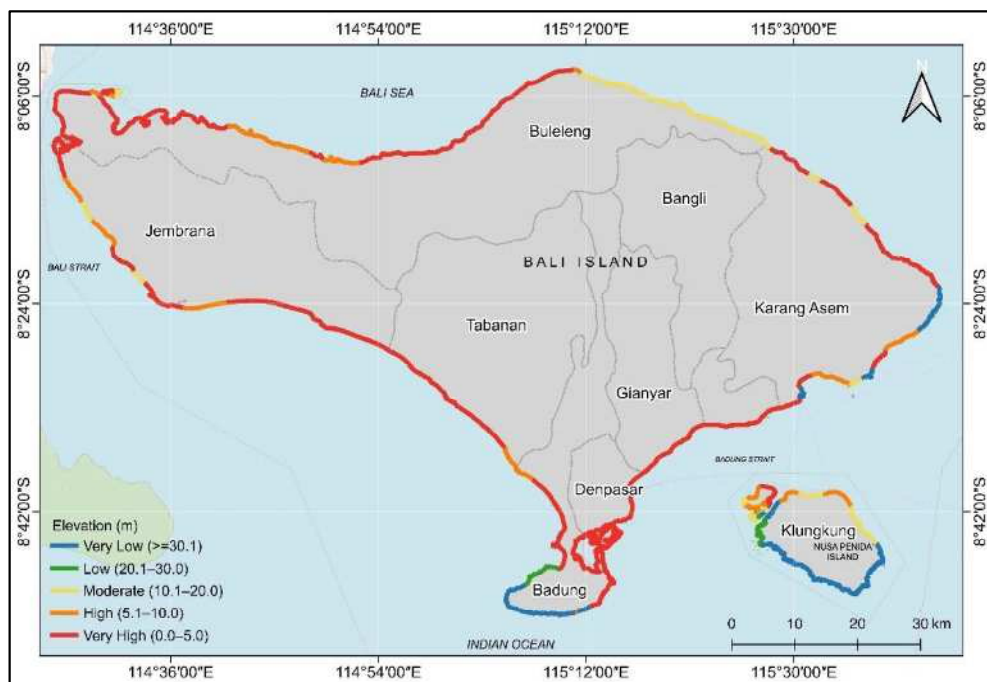


Figure 5-6. The vulnerability rank of coastal elevation.

Following the analysis results in Figure 5-6, the southern part of the Bali Province area, known to possess high cliffs, has the highest coastal elevation, at more than 30 m, and is classified as having very low vulnerability. On the other hand, most of the coastline in Bali Province has the lowest elevation and is classified as having very high vulnerability.

Using geomorphology and elevation as indicators of sea level vulnerability, the impacts of shoreline change and flood hazards are likely to have a significant effect (Rogers and Woodroffe, 2016). Gornitz (1991) stated that the hazard decreases progressively with higher average elevation. Of the coastline, 85.74 km (13% of coastline) comprises a very low

vulnerability zone, indicated with blue color, corresponding to the cliff coast, which has an elevation of more than 30 m and is considered to be resistant to inundation from the sea-level rise or storm surge. The area with low vulnerability, indicated with green color, is also a coastal zone with a moderate cliff coast. Of the coastline, 19.62 km (3%) has low vulnerability, and 56.62 km (9%) has moderate vulnerability.

5.5.4. Sea Level

Based on the range value of the sea-level change rate of Bali Province and the scoring table, Bali's coastline is subjected to very high relative sea-level rise rates. It can be considered a highly vulnerable area due to the potential inundation of coastal land (Figure 5-7). The range value of mean sea-level variation in Bali Province for May 1992–June 2019 is 4.5 to 5.2 mm/yr, higher than the global average.



Figure 5-7. The vulnerability rank of sea level change rate.

Sea-level rise is a relatively weak amplitude signal, with changes in the range of mm to cm over decades. For this reason, tide gauge datum stability is one of the vital observation considerations. The rate of sea-level rise at any given location also varies. According to Unnikrisnan and Shankar (2007), sea-level changes can be due to two phenomena—one is global, while the other is a regional contribution from land and ocean processes. The relative sea level change variable naturally includes land subsidence and tectonic motion (Cooper et al., 2008). Higher sea levels mean deadly and destructive storm surges, which also means more frequent nuisance flooding and accelerated coastal erosion as sea level rises (Bird, 1996; Enríquez et al., 2016; Feagin et al., 2005).

5.5.5. Tidal Range

Based on the tide data obtained from the four permanent tide stations, the mean tidal range in Bali Province is between 2.133 and 3.265 m. The mean tidal range in Celukan Bawang, Singaraja (northern part) is 2.133 m while in Port of Benoa, Denpasar (southern part) is 3.189 m. The highest mean tidal range is in Pengambangan, Jembrana (western part), at 3.265 m. The tidal range on Bali's coast is classified as mesotidal. Remarkably, it is claimed that vulnerability evaluations for the tidal range rank at a moderate vulnerability level, indicated by the yellow color (Figure 5-8). The CVI incorporated the tidal range as an indicator of the zone impact, with micro-tidal coastlines ranked less vulnerable than macro-tidal coastlines.



Figure 5-8. The vulnerability rank of tidal range.

Based on the measured mean tide level, it was found that the tide cycle on Bali's coast is mixed semi-diurnal. A mixed semidiurnal tide cycle has two high and low tides of different sizes every lunar day, with a maximum range of approximately 2.24 m. As an archipelagic country, Indonesia can be regarded as an example of tidal complexity. Wyrki (1961) constructed an overview of the tidal pattern occurring in Indonesian seas (Southeast Asian water), generally a mixed type that tends to be semidiurnal, influenced by the Indian Ocean. In most of the Java Sea, the tidal cycle type is mixed (predominantly diurnal). Meanwhile, the semidiurnal type generally occurs in the Malacca Strait, and the diurnal type occurs only in a few places. The tides throughout the eastern archipelago, as well as in the adjoining Pacific, are mixed and predominantly semi-diurnal.

5.5.6. Significant Wave Height

The present study revealed that the mean significant wave height (SWH) ranges between 0.55 and 1.86 m. Most of the northern coast is in the very low vulnerability rank, while the

southern coast is in the very high vulnerability rank (Figure 5-9). This is because the northern coast is a closed ocean (Bali Sea), in contrast with the southern coast, which directly faces the open ocean. The largest waves occur where there are large expanses of open ocean (Indian Ocean) that can be affected by wind. Moreover, the waters of southern Bali are close to existing passages of the Indonesian Throughflow (ITF) into the Indian Ocean. The waves are primarily caused by the wind blowing over the sea's surface and transferring energy from the air to the water, forming waves (S. Chen et al., 2019; Ubong et al., 2017). Wave heights depend on the characteristics of the wind that produces them.

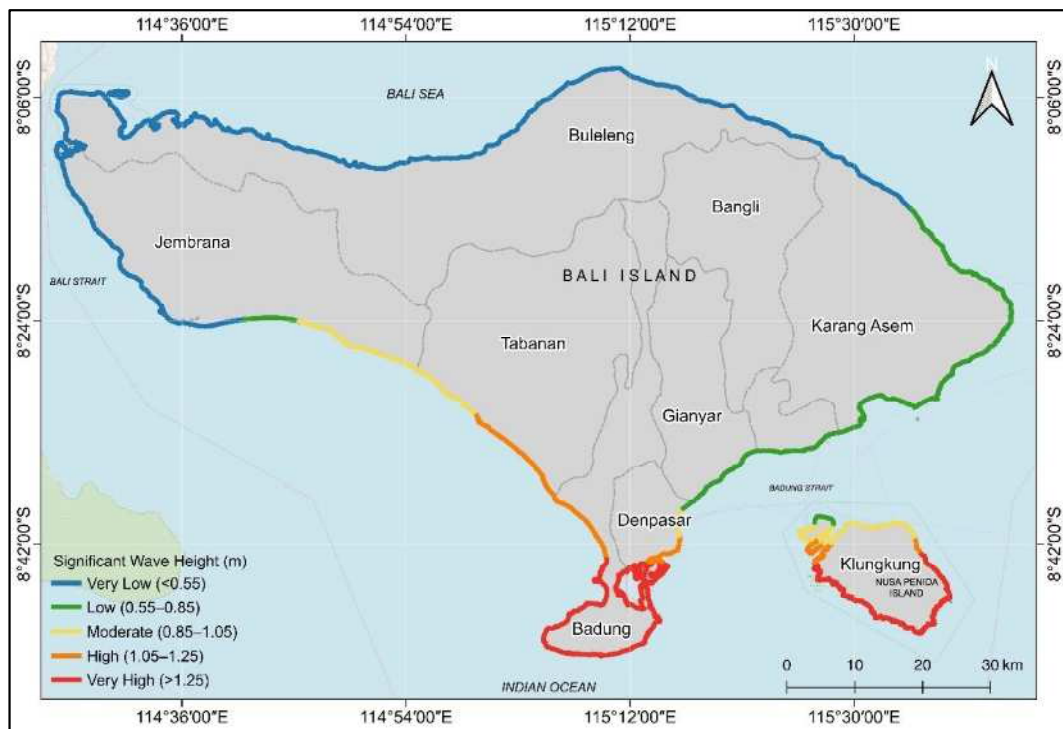


Figure 5-9. The vulnerability rank of significant wave height.

The significant wave height can be used instead of the wave energy, indicating waves' influence on coastal erosion. Stronger wave energy corresponds to more intense and accelerated coastal erosion (Leonardi et al., 2016; Zhu et al., 2018). Hence, the distribution of wave energy along coastlines is an important control of spatial variability of coastal erosion (Murray and Ashton, 2013; Sallenger Jr. et al., 2002).

5.5.7. Coastal Vulnerability Index of Bali Province

Over 640 km of shoreline is evaluated and ranked along the Bali Province. The classes of CVI values are divided into “low vulnerability” (green), “moderate vulnerability” (yellow), “high vulnerability” (orange), and “very high vulnerability” (red) categories based on the quartile ranges and visual inspection of the data. The calculated CVI values range from 8.94 to 12.25 are considered moderate vulnerability. High vulnerability corresponds to values between 12.25 and 17.68. CVI values above 17.68 are classified as very high vulnerability. About 138 km (22%) of the mapped shoreline is classified as very high vulnerability, and 164 km (26%) of the shoreline is highly vulnerable. The remaining shoreline, 168 km (26%) and 169 km (26%) are in the moderate and low vulnerability categories, respectively. Figure 5-10 shows a

histogram of the percentage of Bali Province shoreline in each vulnerability category based on CVI analysis.

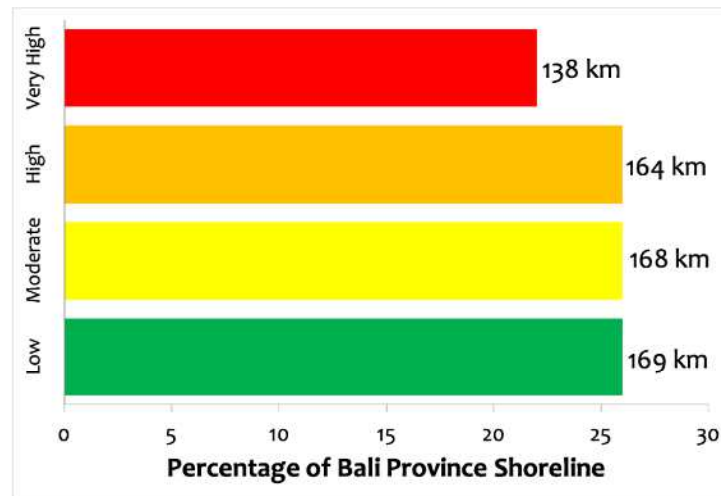


Figure 5-10. The shoreline length of vulnerability categories as determined by CVI.

Figure 5-10 shows the overall ranking category distribution for the classes' CVI values and Bali Province's CVI map. Regions with low vulnerability are formed by variations in geomorphological parameters, with cliff coasts and elevations more than 30 m. The rate of shoreline change between accretion and erosion is in the range of -1 to 1 m/yr and is categorized as stable due to the balanced condition of accretion and erosion. Regions with low vulnerability spread and dominate along the coastal regions in the southern of Bali Island (Badung Regency, 22.35 km), West Bali National Park (Buleleng Regency, 50.31 km), the southern part of Nusa Penida (Klungkung Regency, 65.25 km), Jembrana (9.13 km), and Karangasem (21.60 km). These regions are relatively safe from sea-level rise threats despite their mean significant wave heights indicating very high vulnerability.

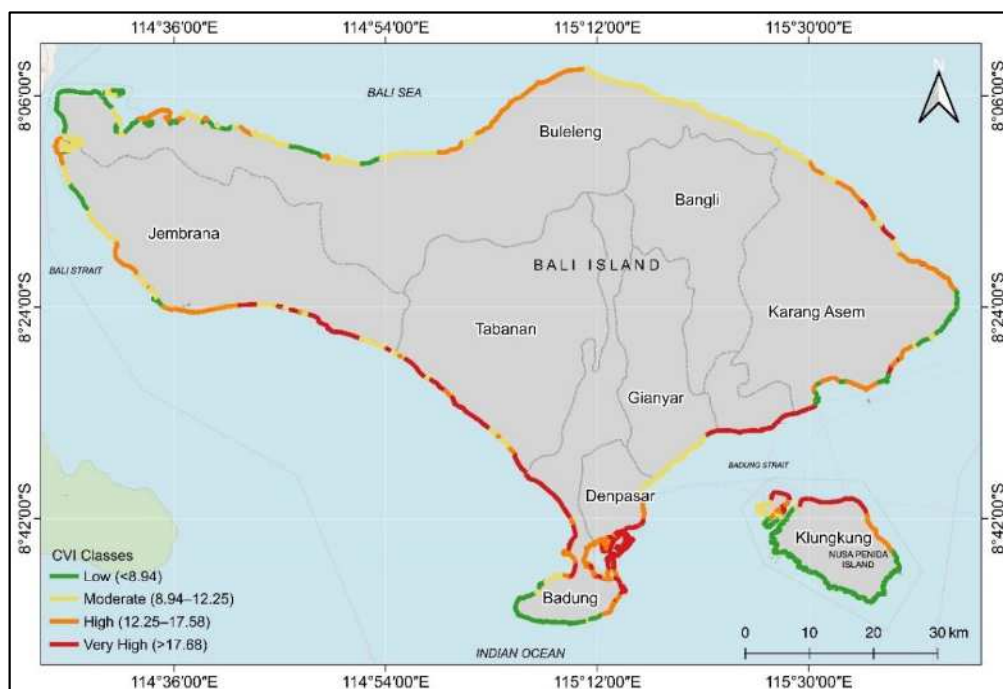


Figure 5-11. The coastal vulnerability index (CVI) map of Bali Province.

Regions with moderately vulnerable zones are formed by variations in the geomorphological parameters with alluvial plains and low cliffs, followed by an elevation of 10–20 m. The rate of shoreline change due to accretion and erosion is in the range of -1.1 to -2 m/yr and is the most dominant factor. Regions with moderate vulnerability are located in the eastern part of Buleleng (74.49 km), Jembrana (38.21 km), Karangasem (13.50 km), Klungkung (11.57 km), Gianyar (11.33 km), Tabanan (7.05 km), Badung (5.94 km), and Denpasar City (1.11 km). Regions with moderate vulnerability can also be categorized as safe regions; however, if they are not managed appropriately, they could become high or very high-vulnerability regions.

Regions with high vulnerability are formed from variations in geomorphological parameters, including estuaries, sandy beaches, and mangroves, with elevation heights of less than 5 m. The rate of shoreline change is in the range of -1.1 to -2 m/yr in some locations at Buleleng Regency and Perancak estuary (Jembrana Regency), as well as more than -2 m/yr in some locations at Jembrana Regency and Karangasem Regency. Regions with high vulnerability are scattered throughout moderate vulnerability regions and are present in the Buleleng (40.56 km), Karangasem (36.57 km), Jembrana (27.75 km), Denpasar (12.96 km), Klungkung (12.77 km), and Tabanan Regency (5.82 km). Regions with high vulnerability require attention to protect them from potential damage or the degradation of coastal areas.

Regions with very high vulnerability zones are formed from variations in geomorphology parameters, including sandy beaches, mangroves, and coastal buildings, and have elevations of less than 5 m in height. The shoreline change rate is more than -2 m/yr, meaning that such regions experience coastal erosion. Regions with very high vulnerability are found at Klungkung (32.07 km), Badung (30.49 km), Denpasar (30.07 km), Tabanan (19.99 km), Jembrana (15.29 km), Karangasem (11.76 km), and Gianyar Regency (1.95 km). Regions with very high vulnerability also require more attention, similar to high vulnerability regions, to avoid the damage and degradation of coastal areas.

The present study attempts to categorize Bali Province's coast according to its coastal vulnerabilities. The most important parameters for the study area are geomorphology, shoreline change rates, elevation, and significant wave height since the other variables are constant (classified into the same class). The CVI method is commonly used to assess the effects of sea-level rise on coastal areas. The CVI method is simple, as it uses a ranking system; therefore, it is easy to identify regions with high vulnerability. It is accessible for policy and decision-makers to make decisions regarding proper management programs for coastal regions with high vulnerability to prevent the effects of sea-level rise (Gornitz et al., 1997; Gutierrez et al., 2009; Kasim and Siregar, 2012). However, the CVI method has several disadvantages; it is only based on geological and physical parameters. It does not consider the effects of social/human activities on ecological and physical changes, and a limited number of parameters are used as input for assessing vulnerability. Therefore, further studies in this area need to include the socio-economic aspect, local factors at a detailed scale, etc., as additional inputs to produce better and more accurate results concerning coastal vulnerability assessment.

This study proves that the quality of the results is highly dependent on data quality. Access to reliable data was one of the most challenging factors throughout this study since the

available free data have low positional accuracy and detail due to the scale of the products made available to the public through the website. In these circumstances, it is necessary to compare the primary data from the local related institution to make a high-accuracy vulnerability map.

Despite these limitations, the grid cells were used for detailed assessment and validated on 35 points. The fieldwork performed as part of the model validation was conducted along Bali Island beach. However, some areas were prohibited from being accessed due to being private areas or subject to ongoing construction, and some areas were difficult to visit due to no access roads leading to the beach area. Nevertheless, representative locations were selected and visited for ground check and validation. By following Eq. (2.2), the agreement between fieldwork and CVI was calculated to be 0.80, indicating good agreement.

The methodological approach is simple, robust, and easy to implement for nationwide mapping since it is based on well-defined criteria through an index-normalized formulation, and additional parameters can be included with the determination of different weights. Although further improvements in the methodology are required to be able to assess coastal risk for sea-level rise mitigation and adaptation measures, the present results are an essential contribution to the identification of coastal vulnerability, constituting an additional instrument for decision-makers with responsibilities of management and planning of areas exposed to the sea-level rise.

Despite the coastal vulnerability assessment at the national level using CVI having already been calculated in Indonesia, the method for acquiring CVI was different from that used in the current study. The national assessment did not calculate the shoreline change rate based on satellite data or regional changes to the coastline. The risk level of coastal erosion/accretion (shoreline change) was determined based on the results of proxies of coastal geomorphology, coastal slope, and significant wave height. Moreover, the scale values of the shoreline changes were principally determined by weighting the scale values of those parameter proxies. A slight coastal slope, a high level of vulnerability in geomorphology, and high ocean waves mark coastal areas with very high levels of vulnerability. The current study used updated and high-resolution satellite imagery data to obtain the shoreline change and analyzed grid cells to acquire the precise index score. It is essential to highlight that for index-based methodologies such as CVI, the availability of reliable and up-to-date databases is crucial (Ružić et al., 2019).

5.6. Conclusion

CVI can perform the coastal vulnerability assessment with remote sensing, and GIS approaches to measure the risk level of coastal areas in Bali Province efficiently and appropriately, in consideration of dynamic processes and both geological and physical parameters. Using a 1 km grid cell and recent data, this study provides an up-to-date coastal vulnerability map of Bali Province that is more precise than previous studies. Although the similar parameters were used in previous study and present study, but the way to acquire is different. This difference implies the different result analysis and display on the CVI map in Bali Province. The detailed and updated coastal vulnerability map of Bali Province can be used

by coastal scientists, local authorities, and district councils to improve and design new coastal management procedures to protect the shoreline.

This study indicated that geomorphology, shoreline change rate, coastal elevation, and significant wave height are the most contributing parameters determining coastal vulnerability since the sea level change rate and tidal range were given the same risk level along the coast. The most contributing parameter could be further improved using weighted determination.

CHAPTER 6. ACCURACY ASSESSMENT OF COASTLINE EXTRACTION

6.1. Overview

Monitoring and documenting a specific region over a defined timeframe are crucial for assessing changes along the coastline (Dellepiane et al., 2004). Access to coastline alteration trends and rates data is fundamental for effective coastal zone management planning (Dewi and Bijker, 2020). Remote sensing technology is generally cost-effective for acquiring spatial data, enabling the detecting of Earth's features without direct physical contact (Janga et al., 2023; Lambin, 2001). Additionally, it offers access to historical image archives captured at different times (multi-temporal) (Chen et al., 2022). The widespread use of Near-infrared bands (NIR) has proven valuable in distinguishing between water bodies and land, particularly for coastline delineation (Mondejar and Tongco, 2019). Moreover, DeWitt (A. A. Alesheikh et al., 2007) has emphasized that the water's absorption of infrared wavelengths and the strong reflectance of vegetation and soil in these images make them ideal for mapping the spatial distribution of land and water.

The coastal zone requires regular and precise monitoring as an essential component in maintaining sustainable coastal resource management since it is one of the planet's most dynamic and constantly changing environments (Melet et al., 2020). This important monitoring effort depends on using advanced remote sensing technologies to accurately assess and comprehend the fluctuations and transformations within this highly dynamic coastal region (Zhao et al., 2022). The complex procedure known as coastline extraction, which allows the accurate identification and characterization of coastal features and their changes over time, is an essential aspect of this technical approach (An Overview et al., 2023; Domazetović et al., 2021).

Coastline extraction with conventional methods is difficult, costly, time-consuming, and sometimes impossible for the entire coastal system. In this context, coastlines can be detected quickly and accurately by integrating remote sensing and GIS technologies. Automatic shoreline extraction indexes also make this detection much easier. However, it is known that different land cover types adjacent to the shoreline directly affect the performance of the indexes used in the shoreline extraction. This study applies remote sensing techniques to detect and analyze the spatial changes and quantify the coastline change in a particular location in Bali Province. This study also proves that the remote sensing approach can easily detect coastline change at larger spatial and long-term temporal scales using satellite images.

Furthermore, this study aims to perform a comparison of five well-known methods that are widely employed for the automatic extraction of coastlines. These methods include the Normalized Difference Vegetation Index (NDVI), Normalized Difference Water Index (NDWI), Modified Normalized Difference Water Index (MNDWI), Water Ratio Index (WRI), and Automated Water Extraction Index (AWEI). The study assesses the effectiveness of these approaches specifically in the context of automatically outlining the complex sandy beach coastline. To do this, the study employed high-resolution imagery obtained from the Sentinel-2 satellite, focusing on the sandy coastal area of Bali, Indonesia, as the study area. To improve the accuracy and precision of the coastline extraction process, the Otsu algorithm is also employed as a key tool for choosing the best threshold value for image processing.

6.2. Data Collection and Method

Bali Province is central to the Indonesian archipelago and is renowned as a prime tropical destination for domestic and international tourists (Antara and Sumarniasih, 2017; Sutawa, 2012). As of the 2020 census, the population of Bali Province was estimated to be around 4,317,404 (Amboro et al., 2022; Badan Pusat Statistik - Statistics of Bali Province., 2022). The majority of this population heavily relies on coastal and marine resources for their livelihoods, and consequently, many essential public facilities and services have been established in coastal areas (Furqan and Winandi, 2018). However, this region has faced challenges such as rapid coastal erosion and land subsidence, attributed mainly to the excessive exploitation of coastal resources (Mujiburrahman et al., 2020; Rajendra, 2020a).

The applied indices were compared at Karang Dadi Beach, situated in the Klungkung Regency of Bali Province, Indonesia. The study area covers a 3.5 km coastline and has sandy beaches. Karang Dadi Beach is approximately 35.5 km from Denpasar, the provincial capital of Bali. Given the characteristics of the beaches and the challenges presented by the area's rapid coastal erosion, this area was selected as a study area. The location of the study area is shown in Figure 6-1.

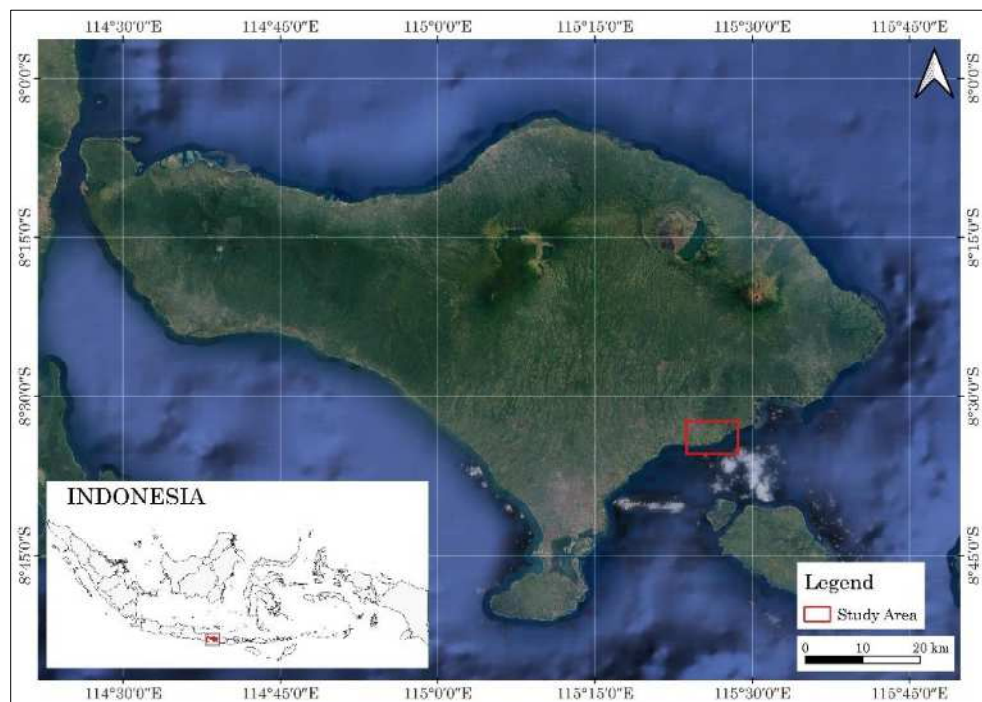


Figure 6-1. The location of the study area is Southeast of Bali Island, Indonesia.

To determine the coastline position, the present study employed Sentinel-2 image data with acquisition data on March 13, 2023. In addition, for comparison, PlanetScope ortho-tile imagery with acquisition data on June 13, 2021, and field survey data conducted on March 13, 2023, was used. The image was subjected to orthorectification using the WGS84 datum and UTM Zone 51 South projection.

Five indices were used to delineate the sandy coast in the study area: Normalized Difference Vegetation Index (NDVI), Normalized Difference Water Index (NDWI), Modified

Normalized Difference Water Index (MNDWI), Water Ratio Index (WRI), and Automated Water Extraction Index (AWEI) (Selim et al., 2022).

The Normalized Difference Vegetation Index (NDVI) is a technique employed to assess vegetation's density and health status. It is also applicable to coastal vegetation and coastline delineation (Akbar et al., 2020; Guha, 2016; Tran et al., 2022). The NDVI is defined by Eq. (6.1).

$$NDVI = \frac{NIR-Red}{NIR+Red} \quad (6.1)$$

The Normalized Difference Water Index (NDWI) method was developed by McFeeters (McFeeters, 1996) and is widely employed for water body extraction. This method uses green and near-infrared bands to differentiate between water and non-water pixels (Laonamsai et al., 2023; Wicaksono and Wicaksono, 2019). As a result of this process, water features yield positive values, while vegetation and soil features produce zero or negative values. The NDWI is defined by Eq. (6.2).

$$NDWI = \frac{Green-NIR}{Green+NIR} \quad (6.2)$$

The Modified Normalized Difference Water Index (MNDWI) is a variation of the NDWI method, initially formulated by Xu (2007). Using green and short-wave infrared bands, MNDWI effectively distinguishes between water bodies and land features. This process yields a greyscale image with values from -1 to 1 (Laonamsai et al., 2023; Wicaksono and Wicaksono, 2019). The MNDWI is defined by Eq. (6.3).

$$MNDWI = \frac{Green-SWIR}{Green+SWIR} \quad (6.3)$$

The Water Ratio Index (WRI) is derived from water's primary spectral reflection characteristics in the green and red bands, incorporating data from four spectral reflectance bands (Laonamsai et al., 2023). The WRI is defined by Eq. (6.4).

$$WRI = \frac{Green+NIR}{NIR+SWIR} \quad (6.4)$$

The Automated Water Extraction Index (AWEI) enhances the identification of coastlines by heightening the distinction between water and other surfaces, thus optimizing the differentiation between water and non-water pixels (Laonamsai et al., 2023; Wicaksono and Wicaksono, 2019). The AWEI is defined by Eq. (6.5).

$$AWEI = BLUE + 2.5 * GREEN - 1.5 * (NIR + SWIR1) - 0.25 * SWIR2 \quad (6.5)$$

The process of coastline extraction can be separated into two main phases: image pre-processing and image analysis. Both phases were executed using the *Google Earth Engine* (GEE) platform, while image visualization was carried out with an open-source GIS program such as QGIS 3.28 LTR (QGIS Development Team, 2022). The visualization of the present study's workflow is shown in Figure 6-2.

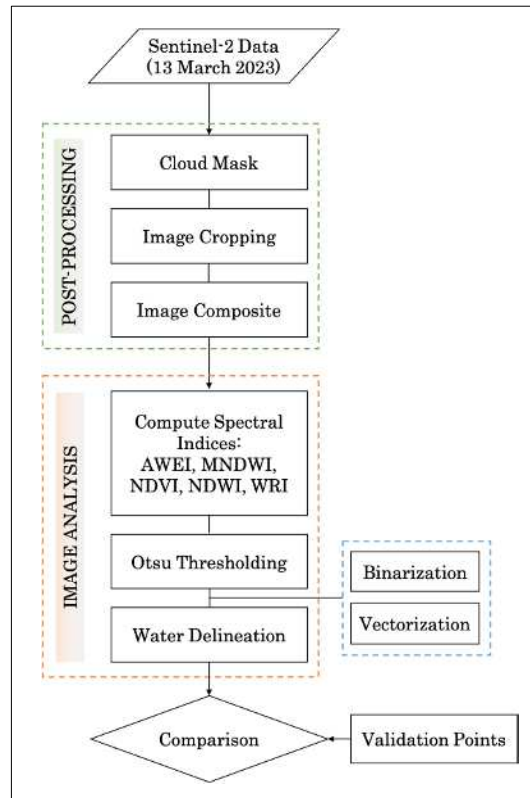


Figure 6-2. Flowchart of coastline extraction indices comparison.

The coastline changes analysis study using the MNDWI index was conducted in two different locations. First is located along the coast in Jembrana Regency (Figure 6-3), the western part of Bali Province, and astronomically located at $08^{\circ}09'58''$ - $08^{\circ}28'02''$ S and $114^{\circ}26'28''$ - $115^{\circ}51'28''$ E, consists of 24 villages in 5 sub-districts. The second study location is located along the coast in Gianyar ($08^{\circ}18'48''$ - $08^{\circ}38'58''$ S and $115^{\circ}13'29''$ - $115^{\circ}22'23''$ E) and Klungkung ($08^{\circ}27'37''$ - $08^{\circ}49'00''$ S and $115^{\circ}21'28''$ - $115^{\circ}37'28''$ E) Regency, Bali Province (Figure 6-4). Both study location is characterized by a low-lying landscape with an elevation of less than 10 m above sea level, sandy beach, and mesotidal.

The coastal change monitoring is carried out by comparing the Sentinel-2 image (downloaded from <https://earthexplorer.usgs.gov>) with the acquisition date of 26 April 2019 to describe the current condition and 12 January 2016 as an initial condition (for Jembrana Regency) and date of 28 April 2019 to describe the current condition and 8 February 2016 as an initial condition (for Gianyar and Klungkung Regency). The study was only conducted from 2016 to 2019 because the Sentinel-2 imagery data with the high spatial resolution was just launched in June 2015. Sentinel-2 Level-1C product has radiometric and geometric corrections, including ortho-rectification and spatial registration with sub-pixel accuracy. It provides the Top of Atmosphere (TOA) reflectance in the UTM/WGS84 projection. Images acquired in 2016 and 2019 were downloaded and projected in UTM Zone 50S.

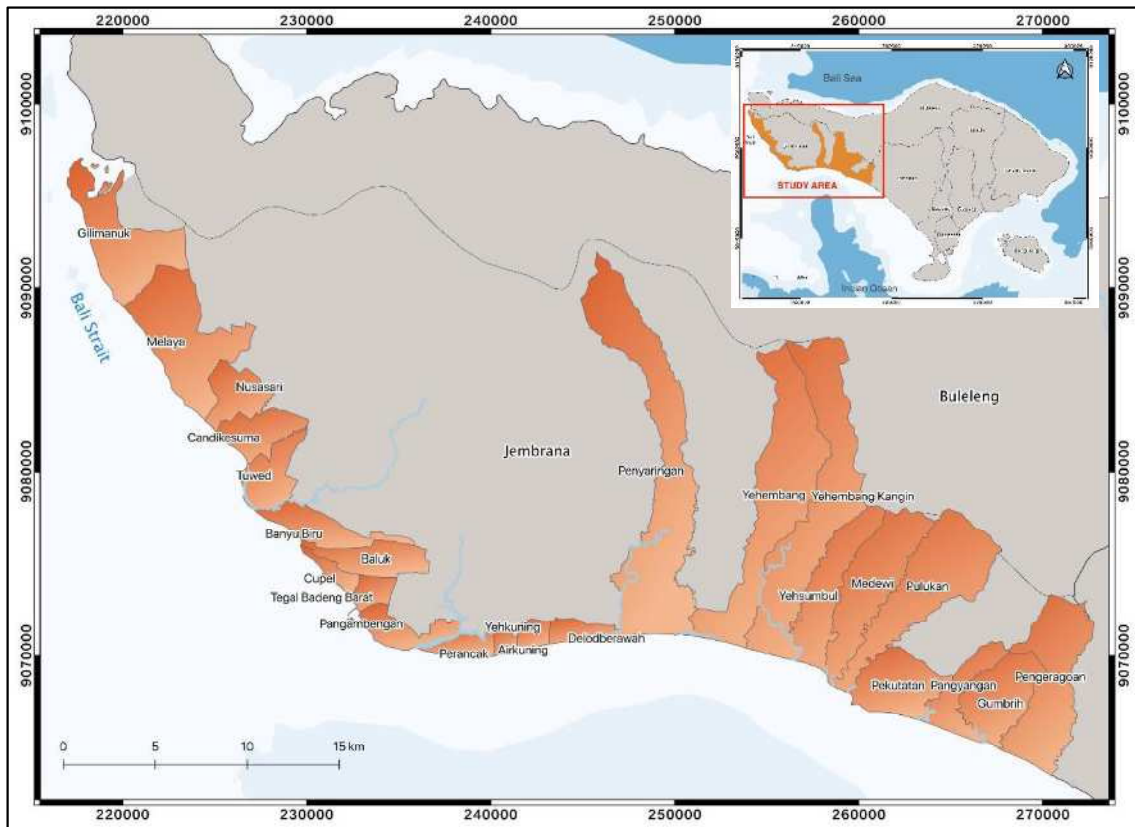


Figure 6-3. Study area in Jembrana Regency.

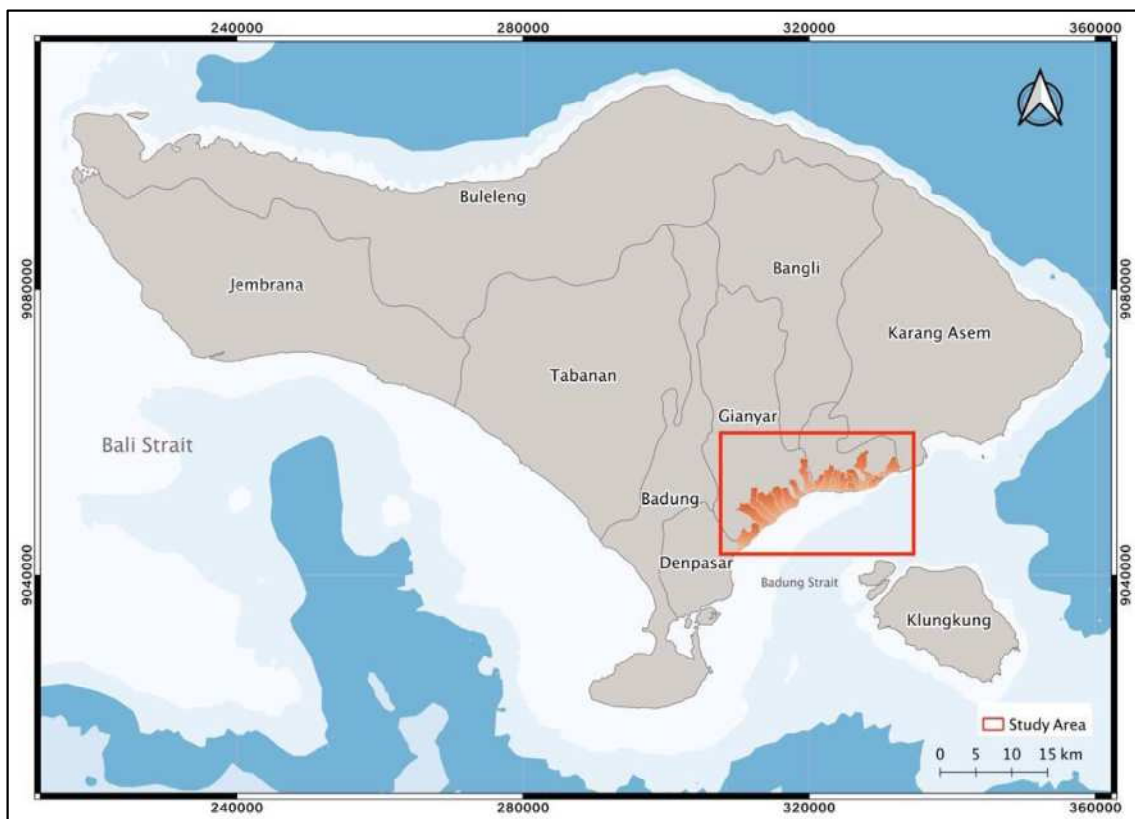


Figure 6-4. Study area in Gianyar and Klungkung Regency.

Considering the data set from multitemporal images used in this study, it was not expected to obtain images with similar conditions. Based on the equiangular triangle theory, the water lines were shifted to the tidal datum-based coastline position.

The first step in tidal correction is to determine the tide height between the image acquisition date and the tide prediction date. The necessity for tidal correction considering the magnitude of the effect of sea level height variations during highs and lows affected by coastal slope and the spatial resolution of the image. The water lines were shifted to the tidal datum-based shoreline position based on the equiangular triangle theory. Sectional calculations were used to conduct the shifting process and determine the bottom slope (Dwi Artama et al., 2019). Beach slope is calculated using the following equation:

$$\tan \beta = \frac{d}{m} \quad (6.6)$$

$\tan \beta$ = coastal slope ($^{\circ}$); d = water depth (m); m = distance from the shoreline to the d (m)

The sectional coastal slope was obtained from river basin management organizations (RBOs), called either Balai Wilayah Sungai Bali-Penida (BWS-BP) shown in Figure 6-5.

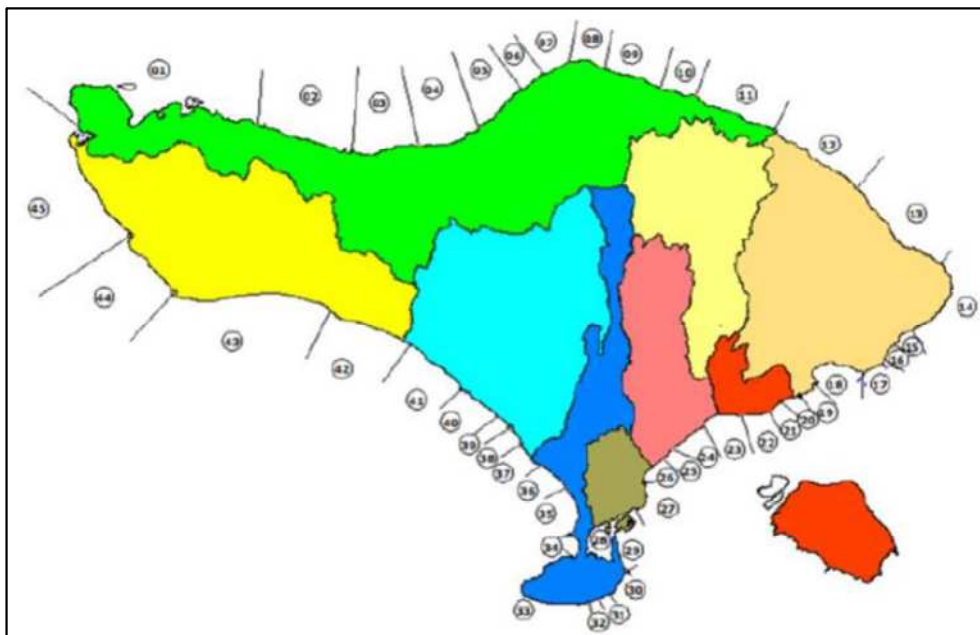


Figure 6-5. Section division for coastal slope values in Bali Province.

The shift distance of the water line correction is calculated using the equation below.

$$x = \frac{\eta}{\beta} \quad (6.7)$$

x = coastline shift distance (m); η = water level at the time of image acquisition (m); β = coastal slope ($^{\circ}$)

6.3. Result and Discussion

In the present study, a 3.5 km length coastline was automatically delineated and mapped on Sentinel-2 images by performing five widely employed indices for coastline extraction

(NDVI, NDWI, MNDWI, WRI, and AWEI). Karang Dadi beach is characterized by sandy beaches with varying widths or distances to various land cover/land use and coastal vegetation. In general, these varying beach characteristics distinguish the results of the performance of the applied coastline extraction indices.

In the present study, high-resolution satellite images from PlanetScope were employed for coastline mapping, and the resulting coastlines were utilized as the baseline (reference) for calculating coastline length. The coastline length determined through on-screen digitization was measured at 2,985 m, covering an area of 652,867 m².

6.3.1. Normalized Difference Vegetation Index (NDVI)

The study obtained a shoreline of 4,983 m with a difference of 1,998 m from the reference coastline by using the NDVI index to detect coastlines in the study area. The results revealed that NDVI performed exceptionally better in identifying coastal vegetation. Based on visual interpretation, the index provides a precise coastline where the coast is adjacent to vegetated coasts. According to Esendağlı et al. (2022), the NDVI can identify objects according to their moisture content and has demonstrated its superior performance in vegetated coastal areas. As a result, NDVI had limitations in detecting sand dunes and rocky shores within the study area. The result of NDVI is shown in Figure 6-6.



Figure 6-6. Result of coastline extraction using Normalized Difference Vegetation Index (NDVI)

6.3.2. Normalized Difference Water Index (NDWI)

The study obtained a coastline of 4,409 m with a difference of 1,424 m from the reference coastline by using the NDWI index to detect coastlines in the study area. According to data based on visual interpretation, NDWI outperformed NDVI in identifying coastline. Due to its coverage of the study area's rocky coasts and sand dunes, the index produces higher results for sandy beaches. According to a study by Wicaksono and Wicakson (2019) the NDWI also

showed the best performance in identifying artificial coasts. The result of NDWI is shown in Figure 6-7.



Figure 6-7. Result of coastline extraction using Normalized Difference Water Index (NDWI).

6.3.3. Modified Normalized Difference Water Index (MNDWI)

The coastline length obtained in this study, which used the MNDWI index to detect coastlines in the study region, was 4,169 m, a difference from the reference coastline of 1.184 m. The results of visual interpretation showed that MNDWI outperformed NDWI and NDVI in locating the shoreline. NDWI and MNDWI results were found to be closely related. The MNDWI index is sensitive to sediment shadow, which is advantageous for shoreline extraction, according to Li et al. (Li et al., 2021). With an accuracy rate of 99.85 percent, MNDWI was often used to map water bodies and was thought to be the most excellent tool to differentiate between water and land features (Xu, 2007). The result of MNDWI is shown in Figure 6-8.



Figure 6-8. Result of coastline extraction using Modified Normalized Difference Water Index (MNDWI).

6.3.4. Water Ratio Index (WRI)

The WRI index was used in this study's shoreline detection in the study area, where the coastline measured 6,649 meters, which was longer than the reference coastline of 3.664 meters. Based on visual interpretation, the findings showed that WRI performed poorly in the research area when recognizing shorelines compared to NDWI and NDVI. The result of WRI is shown in Figure 6-9.



Figure 6-9. Result of coastline extraction using Water Ratio Index (WRI).

6.3.5. Automated Water Extraction Index (AWEI)

This study used the AWEI index for shoreline detection in the study area with a coastline length of 4.210 m, resulting in a deviation from the reference coastline of 1,225 m. Based on visual interpretation, AWEI performed better than the WRI index and close to the MNDWI results. This result demonstrated continuity along the study area's coast. According to a study by Selim et al. (Selim et al., 2022), the unique property of absorbing more MIR light (SWIR-2) than NIR light gives AWEI-positive results. The result of AWEI is shown in Figure 6-10.



Figure 6-10. Result of coastline extraction using Automated Water Extraction Index (AWEI).

The results of all employed indices are shown in Figure 6-11. The comparison of the applied five coastline extraction indices is shown in Table 6-1.



Figure 6-11. Comparison of all coastline extraction indices.

Table 6-1. Comparison of all applied indices to PlanetScope baseline (references).

Index	Length (m)	Area (m ²)	Difference		The average distance from the validated point (m)
			Length (m)	Area (m ²)	
NDVI	4,983	698,905	-1,998	-46,038	21.270
NDWI	4,409	687,548	-1,424	-34,681	28.517
MNDWI	4,169	646,383	-1,184	6,484	12.901
WRI	6,649	574,953	-3,664	77,914	35.200
AWEI	4,210	635,283	-1,225	17,584	15.763
<i>Baseline</i>	<i>2,985</i>	<i>652,867</i>			

Table 6-1 shows that MNDWI, followed by AWEI, NDWI, and NDVI indices, performed close results to the reference coastline from on-screen digitizing the data of PlanetScope satellite imagery. In contrast, WRI was the result that achieved the furthest from the reference. The manual on-screen digitization techniques are time-consuming and labor-intensive, yet they produce high-quality results. The application of these indices made it possible to detect coastlines faster than using Sentinel-2 satellite imagery. Several studies approved that MNDWI provides higher accuracy than NDWI and other coastline extraction indices (Wicaksono and Wicaksono, 2019).

The results of our study highlight the effectiveness of the Modified Normalized Difference Water Index (MNDWI) in accentuating water bodies, demonstrating its superior performance in this crucial aspect of coastline analysis. The Normalized Difference Vegetation Index (NDVI) similarly shows an exceptional capacity for identifying and characterizing coastal vegetation, reflecting a high level of proficiency in this regard. A thoughtfully chosen threshold is essential for precise application. These results contribute to advancing our

understanding of coastline extraction techniques and highlight the great potential of enhancing the effectiveness of coastline monitoring by combining Sentinel-2 satellite images with the robust Google Earth Engine (GEE) platform.

The use of spectral water indicators in this work also provides strong scientific support for the accuracy and dependability of shoreline extraction. As a result, remote sensing is proven to be a useful technique for managing coastal resources, and its crucial role in guaranteeing the sustainability of coastal ecosystems and resources in places like Bali, Indonesia, and elsewhere is highlighted. The implications of these findings extend beyond the confines of this study, providing insightful information and prospects for improvements in coastal monitoring and environmental conservation initiatives.

6.3.6. Coastline Change Analysis of Jembrana Regency

Coastline changes occurred in Jembrana Regency based on Sentinel-2 imagery between 2016 and 2019. The expansion (accretion) and reduction (erosion) of the coastal area are available in Table 6-2. Based on Table 6-2, the greatest coastline changes occur in Melaya sub-district, with 62,838 m² of accretion and 220,313 m² of erosion as a consequence of Melaya Sub-district having the longest coastline than other districts (Figure 6-12). Coastline change in Gilimanuk Village experience more abrasion (77,345 m²) than accretion (16,593 m²). The abrasion occurs near the Gilimanuk Port, which is the residential area and natural sandy beach with tropical vegetation such as palm trees. This area also directly facing to the Bali Strait. Similar to Gilimanuk Village, Melaya, Candikesuma, and Tuwed Village are also experiencing more abrasion than accretion.

Table 6-2. Information of coastal area changes (m²) in Jembrana Regency.

Sub-District	Village	Accretion (m ²)	Abrasion/Erosion (m ²)
Melaya	Gilimanuk	16,593	77,345
	Melaya	9,403	56,341
	Nusasari	11,705	9,074
	Candikesuma	23,627	55,698
	Tuwed	1,510	21,855
	<i>Total</i>	<i>62,838</i>	<i>220,313</i>
Negara	Banyu Biru	-	81,652
	Baluk	-	8,085
	Cupel	1,868	44,066
	Tegal Badeng Barat	1,496	3,393
	Pengambengan	40,168	42,628
	<i>Total</i>	<i>43,531</i>	<i>179,824</i>
Jembrana	Perancak	11,789	5,999
	Airkuning	711	3,886
	Yehkuning	31	11,479
	<i>Total</i>	<i>12,531</i>	<i>21,364</i>
Mendoyo	Delodberawah	1,265	22,174
	Penyaringan	16,690	27,854
	Yehembang	9,569	12,730
	Yehembang Kangin	12,399	3,283
	Yehsumbul	5,630	4,855

Sub-District	Village	Accretion (m ²)	Abrasion/Erosion (m ²)
	<i>Total</i>	45,553	70,895
Pekutatan	Medewi	2,559	4,279
	Pulukan	3,847	1,623
	Pekutatan	7,278	11,366
	Pangyangan	14,645	28,631
	Gumbrih	9,292	44,747
	Pengerangoan	24,923	2,999
	<i>Total</i>	62,545	93,646
TOTAL		226,999	586,042

Candikesuma Village has the largest accretion than other villages. This is caused by sediment accumulation at one side of the river mouth. In contrast, the river at Tuwed Village is eroded due to sediment transport from breakwater construction in the Pangambengan fishing port, which resulted in wave direction (Uda et al., 2004). The position of the river mouth in Tuwed Village also shifts with time along the coast in the direction of the net longshore sediment transport along the coast. The river flows landward of the spit, more or less parallel to the coast for some distance. With the growing spit, the river's length becomes longer and longer with time. Furthermore, the river mouth is also a great vulnerable area to coastline changes.

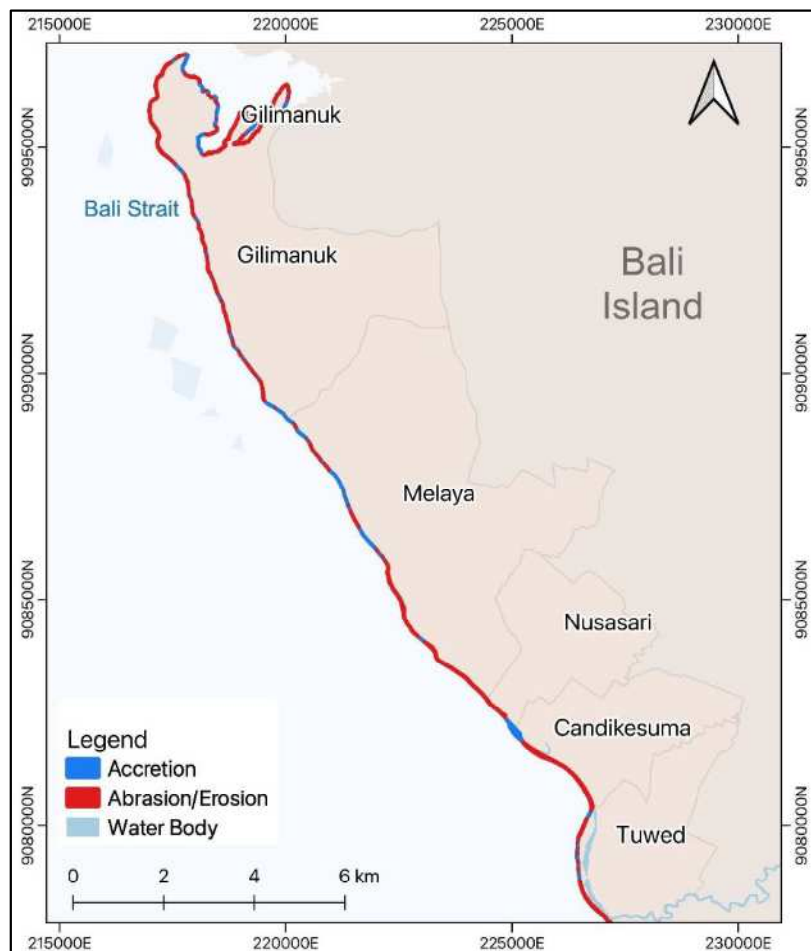


Figure 6-12. Coastline change at Melaya Sub-District.

Similar to the Melaya Sub-district, the coastline in the Negara Sub-district is also changing. Table 6-2 shows that Banyu Biru and Baluk Village are the only villages experiencing coastal erosion, with 81,652 m² and 8,085 m², respectively. Moreover, the coastal erosion that occurred in Banyu Biru Village makes this village with the highest erosion rate among all coastal villages in Jembrana Regency. As shown in Figure 6-13 and area changes in Table 6-2, a fishing port and a breakwater in Pangambengan Village were constructed in 2000, resulting in accretion and erosion along the coastline.

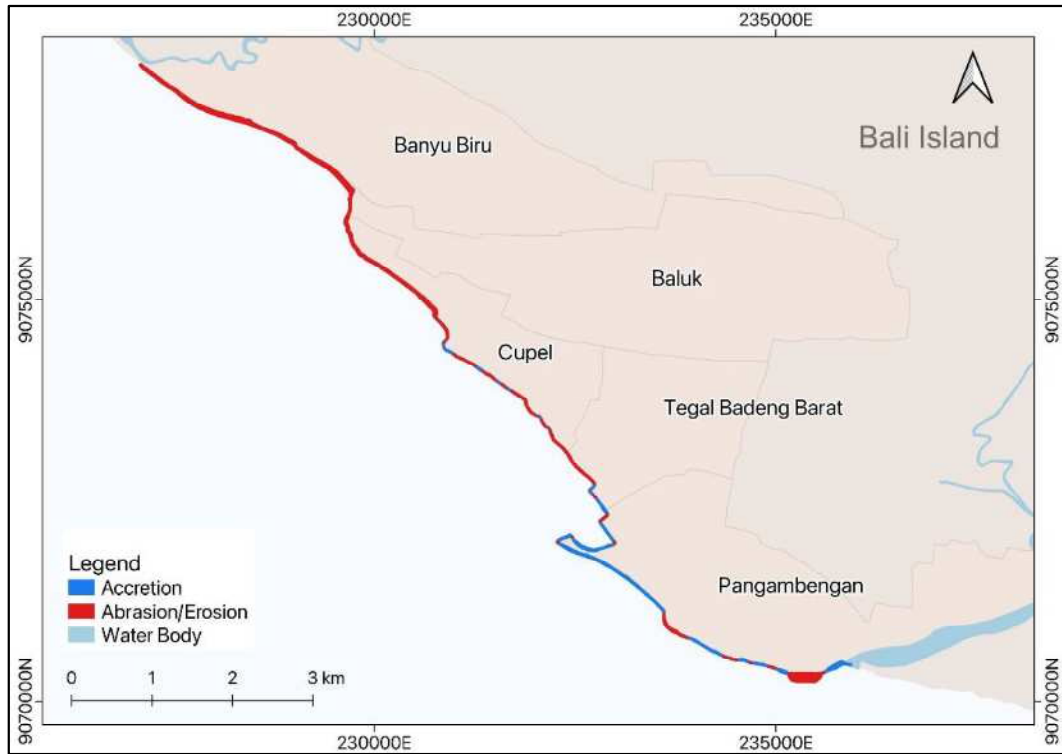


Figure 6-13. Coastline change at Negara Sub-District.

The construction of a breakwater blocked the longshore sediment transport, so a seawall was built to prevent coastal erosion, but this resulted in the further expansion of the eroded area. The accretion occurs in the southern part of the fishing port (up drift side) because predominant waves come from the southeast and longshore sediment transport from the northwest (Uda et al., 2015). Otherwise, the northern part of the fishing port (downdrift side) has been eroded and even elongated to the northward because of the blockage of longshore sediment transport by breakwater (Uda et al., 2004). The updrift breakwater in the fishing port interrupts the longshore sediment transport, and then accretion will occur at the updrift side of the port. Because at the downdrift side of the port is the undisturbed (the original) longshore sediment transport takes place again, while no sediment is passing the breakwaters, large gradients in longshore sediment transport do occur at the downdrift side of the port, resulting the occurrence of erosion at this side (van de Graaff, 2021). The sand deposition also occurs inside the fishing port. Furthermore, the erosion in southern Pangambengan Village which is adjacent to Perancak Village occurs in the river mouth, and this is affected not only from river discharge but also a coastal dynamic.

Jembrana Sub-district consists of 3 villages, with Perancak Village has highest accretion rate of 11,789 m². Considering that the material at times is carried by the river in the Perancak Estuary. As a result, this material, together with a mixture of marine sediments, creates sediment in the coastal area. In addition, there is also mangrove forest in Perancak Village which functions as an erosion barrier. On the other hand, 11,479 m² of coastal area in Yehkuning Village is experiencing coastal erosion. As shown in Figure 6-14, coastline along Yehkuning Village has been eroded within 3 years.

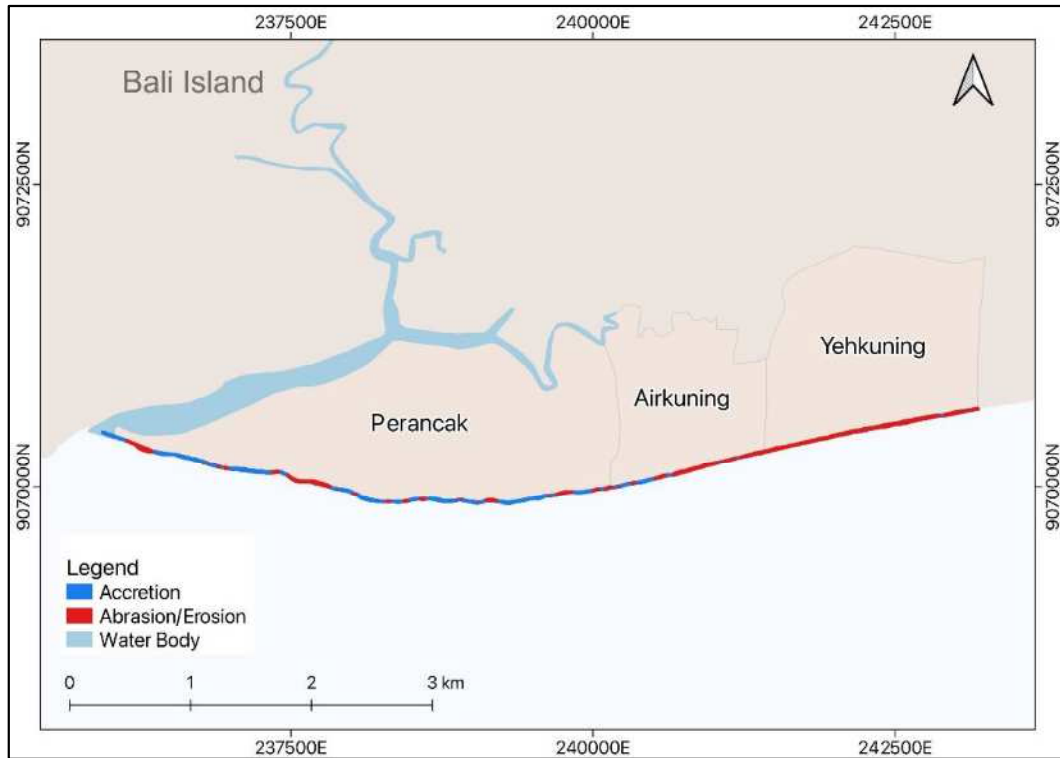


Figure 6-14. Coastline change at Jembrana Sub-District.

The coastal area along Delodberawah Village is used as a tourist spot. Unfortunately, the coastline in this village also eroded. Regarding Istiqomah et al. (2018), erosion in Delodberawah is happening yearly, and the coastline has retreated by 50 m. This condition also occurred in Penyaringan Village where a coastal area reduction of 27,854 m². Figure 6-15 shows the coastline change in Mendoyo Sub-district, and coastal erosion is obviously stretched along Mendoyo Sub-district.

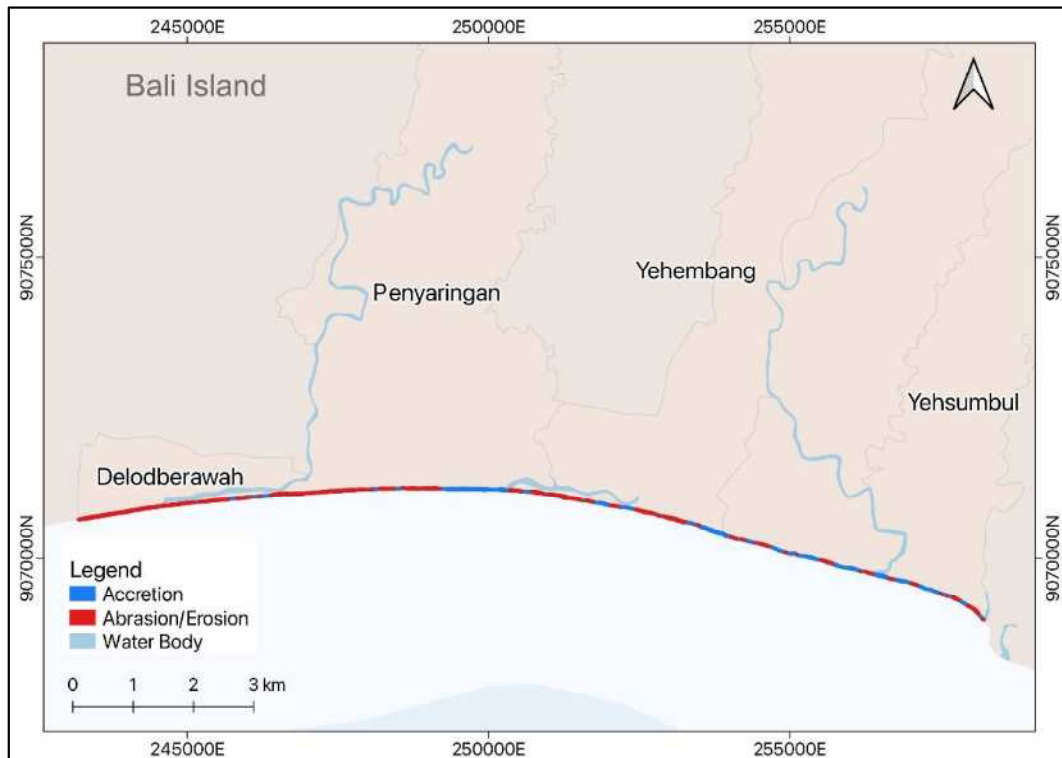


Figure 6-15. Coastline change at Mendoyo Sub-District.

The coastal area of Pekutatan Sub-district is mostly known as a tourism area in Jembrana Regency. The beaches along Pekutatan Sub-district are sandy and rocky beaches. With this condition, beaches along Pekutatan Sub-district tend to escape from severe coastal erosion. Erosion in Pekutatan Sub-district obviously occurs in a location close to the river mouth in Pekutatan, Pangayangan, and Gumbrih Village (Figure 6-16). This sediment loss triggered the erosion. The volume of sand can be maintained if the river from the upstream area flows deposit material to the beach in large volumes. However, the sediment supply from the river is reduced, therefore that the ocean waves will easily erode the land.

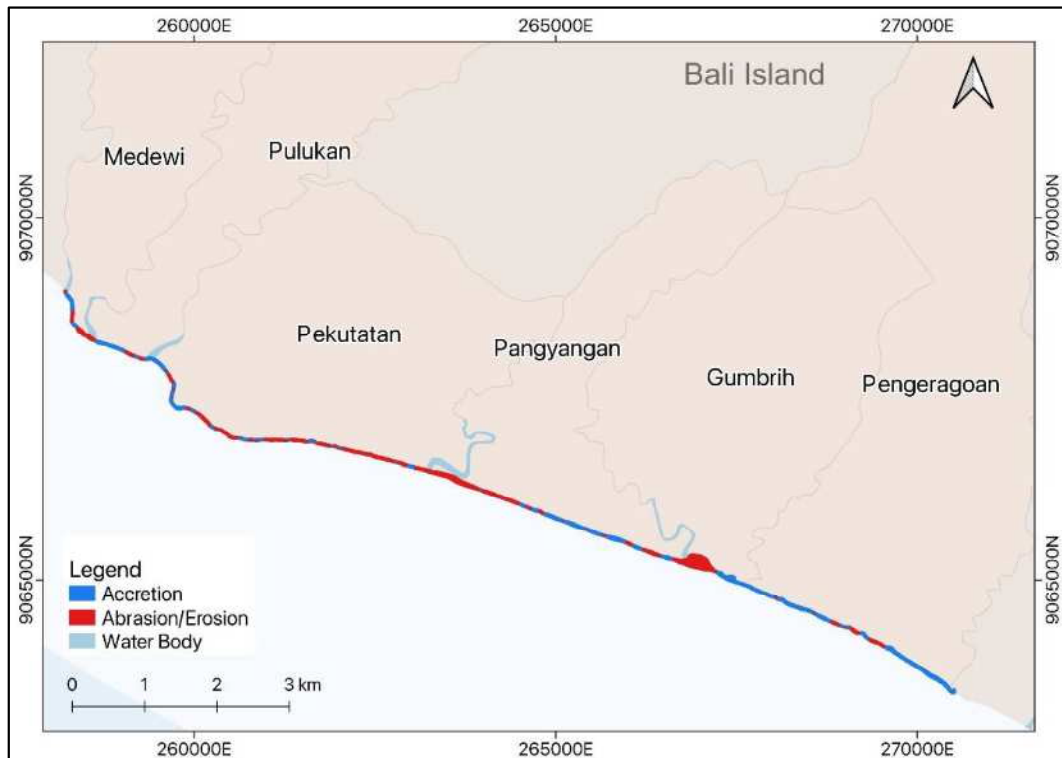


Figure 6-16. Coastline change at Pekutatan Sub-District.

The entire coastal area in Jembrana Regency has changed. Not only the reduction of the coastal area due to erosion and sediment loss but also accretion caused by the expansion of fishing port in Pangambengan Village. The impact of coastal erosion in Jembrana Regency has destroyed the sandy beaches and begun engulfing the surrounding private properties, food stalls, houses, and rice fields. Jembrana Regency is directly adjacent to the Bali Strait and the Indian Ocean, causing fluctuations in wind pressure and wave height. In certain seasons, the wave height can reach 5 meters and have an impact on increasing coastal erosion.

Pekutatan Sub-districts, which are directly facing the Indian Ocean, make this sub-district experience waves that dominantly come from the south. In addition, the Bantenan Cape which is located along the southeast of Java Island, effectively protects the incoming waves from the Indian Ocean, especially for Melaya, Negara, and Jembrana Sub-district, the waves dominantly come from the Bali Strait. These waves' direction is approximately the same as the orientation of the coast in west Bali, implying the dominance of sediment transport along the northwest coast (Uda et al., 2015). During the period 2016 to 2019, the average rate of coastal erosion in Jembrana Regency was 2.18 m/yr. The highest erosion rates of 3.38 m/yr were observed in Melaya Sub-district, while the smallest were 0.61 m/yr in Jembrana Sub-district. The erosion rates of 3.34, 1.69, and 1.88 m/yr were detected on the Negara, Mendoyo and Pekutatan coasts, respectively. In the term of coastal vulnerability, an erosion rate exceeding 2 m/yr is categorized as very high risk (Gornitz, 1991). This mean that immediate attention and better action needs to be given in Jembrana Regency to minimized the damage and protect the coastal resources and communities. Moreover, appropriate methodology is to be adopted to control the erosion for various site conditions. This study was not expected to obtain multi-satellite images with similar conditions. In this case, coastline data needs to be corrected to the tidal level to

eliminate the tide's effect on the coastline's position. The coastline shift calculation in different tidal levels was conducted by using the triangular theory between water levels and beach slopes. According to the tidal correction measurement, no section of the coastline experiences a shift in position due to tidal influences greater than one pixel of Sentinel-2 imagery. The coastline shift position ranges from 0.082 m to 0.770 m. Hence, it was determined that tidal correction could be abandoned in this study since the shift in coastline position by tidal influence was not visible in satellite imagery.

6.3.7. Coastline Change Analysis of Gianyar and Klungkung Regency

From the image analysis results, the coastline in Gianyar and Klungkung Regency changed from 2016 to 2019. Accretion and abrasion are essential factors for the changing of coastline. The total area change is shown in Table 6-3.

Table 6-3. Information on coastal changes in Gianyar and Klungkung Regency.

Regency	Sub-District	Village	Accretion (m ²)	Abrasion/Erosion (m ²)	
Gianyar	Sukawati	Batubulan	18,434	-	
		Ketewel	76,167	-	
		Sukawati	13,019	1,270	
		<i>Total</i>	<i>107,620</i>	<i>1,270</i>	
	Blahbatuh	Saba	7,915	1,461	
		Pering	7,193	243	
		Keramas	10,046	5	
		Medahan	13,330	1,009	
		<i>Total</i>	<i>38,484</i>	<i>2,718</i>	
	Gianyar	Lebih	Tulikup	8,137	1,267
				4,374	3,993
		<i>Total</i>	<i>12,511</i>	<i>5,260</i>	
	<i>TOTAL</i>	<i>158,615</i>	<i>9,248</i>		
Klungkung	Banjarangkan	Negari	887	10,665	
		Takmung	877	23,178	
		<i>Total</i>	<i>1,764</i>	<i>33,843</i>	
	Klungkung	Satra	Tojan	-	4,620
			Gelgel	-	13,324
			Jumpai	6,559	649
			Tangkas	9,266	5,404
				6,280	-
			<i>Total</i>	<i>22,105</i>	<i>23,997</i>
	Dawan	Gunaksa	Kusamba	7,574	17,149
			Kampung Kusamba	410	32,739
				32	829
			Pesinggahan	274	12,443
			<i>Total</i>	<i>8,290</i>	<i>63,160</i>
		<i>TOTAL</i>	<i>32,159</i>	<i>121,000</i>	

Based on the satellite image overlay, the study area experienced the coastline change due to accretion and/or abrasion. The largest coastline changes due to accretion occurred in Ketewel village, while the largest abrasion occurred in Kusamba village (Table 6-3). The coastline along

Gianyar Regency generally experiences accretion (Figure 6-17) with a total area of 158,615 m². Meanwhile, Klungkung Regency mostly experiences abrasion (Figure 6-17) with a total of 121,000 m².

Figures 6-17 show that accretions predominantly occurred in Gianyar Regency for a period of the study. In this regency, the abrasion areas were 9,248 m², smaller than the accretion area.

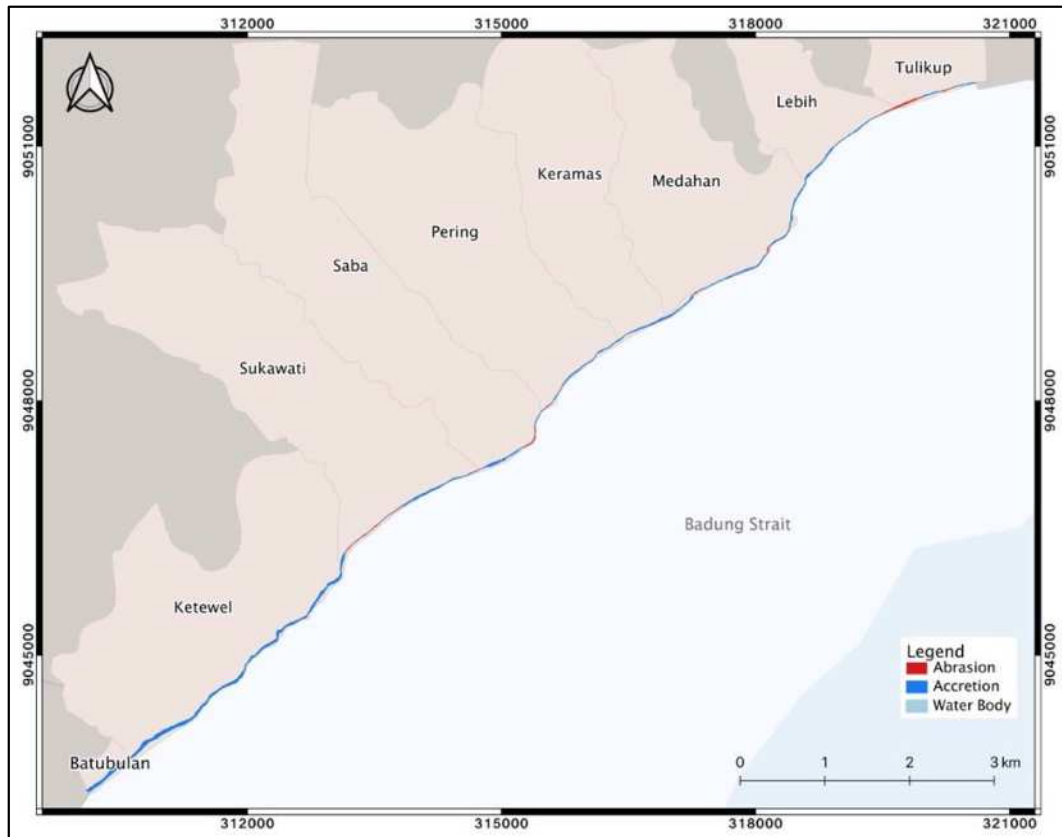


Figure 6-17. Coastline changes of Gianyar Regency.

Figures 6-18 show the coastline change that occurred in Klungkung Regency. The coastal area that experienced abrasion is larger than accretion, with 121,000 m² and 32,159 m², respectively.



Figure 6-18. Coastline changes of Klungkung Regency.

As with abrasion, accretion will occur. The accretion happened in the western part of the Gunaksa Port, while the abrasion occurred in the eastern part of the port (Figure 6-18). The breakwater construction blocked the longshore sediment transport, resulting in an eroded area.

Tide is a natural factor that considers the coastline from satellite images. The map of coastline changes of Gianyar and Klungkung Regency from 2016 to 2019 has been corrected from the tides. The tidal correction is shown in Table 6-4.

Table 6-4. Tidal correction.

Acquisition Date and Time	Section	Coastal Slope (°)	η (m)	x (m)
February 8, 2016 10:31:15 (UTC+8)	20	15	1.16	0.077
	21	16	1.16	0.073
	22	7	1.16	0.166
	23	7	1.16	0.166
	24	10	1.16	0.116
	25	9	1.16	0.129
	26	10	1.16	0.116
	<i>Average</i>			<i>0.121</i>
April 28, 2019 10:40:23 (UTC+8)	20	15	2.00	0.133
	21	16	2.00	0.125
	22	7	2.00	0.286
	23	7	2.00	0.286
	24	10	2.00	0.200
	25	9	2.00	0.222
	26	10	2.00	0.200
	<i>Average</i>			<i>0.207</i>

Table 6-4 presents the required parameter values in tidal correction and the result. According to the tidal correction measurement, no section of the coastline experiences a shift in position due to tidal influences greater than one pixel of Sentinel-2 imagery. The coastline shift position ranges from 0.077 m to 0.286 m. As a result, it was determined that tidal correction was not necessary in this study since the shift in the coastline position by tidal influences was not identified in Sentinel-2 images because the shift distance was less than 10 m. Furthermore, the tidal correction can be ignored because the change in coastline position between before and after tidal correction is not visually significant.

6.4. Conclusion

This study underscores the significance of employing advanced remote sensing technology for continuously monitoring and managing coastal zones, which are inherently dynamic environments. The comparative analysis of five prominent coastline extraction techniques revealed that the Modified Normalized Difference Water Index (MNDWI) is the most effective method for delineating water bodies along sandy beaches. In contrast, the Normalized Difference Vegetation Index (NDVI) displayed a commendable ability to detect coastal vegetation. These findings demonstrate the potential of harnessing high-resolution imagery from the Sentinel-2 satellite and leveraging the Google Earth Engine (GEE) platform for efficient and accurate coastal monitoring. Additionally, stakeholders and policymakers should consider investing in continued remote sensing-based monitoring efforts to ensure the sustainability of coastal ecosystems and resources in regions like Bali, Indonesia. Further research could explore the applicability of these techniques in other coastal areas to broaden their practical utility in coastal resource management worldwide.

Furthermore, integrating satellite imagery into a GIS environment provides an essential and valuable information base. Additionally, this study shows that satellite imagery has the potential to monitor coastline change and coastal volume change over some time. This study did not perform the influences of wind patterns, wave actions, water currents, and other climate variables for coastline change analysis. However, it should be considered for better results and further analysis. This study provides valuable information on coastline changes in this area that can be used to prepare and develop adaptation policies for future mitigation.

CHAPTER 7. CONCLUDING REMARKS AND OUTLOOK

7.1. Conclusion and Main Findings

The main objective of this research is to conduct the Coastal Vulnerability Index (CVI) to assess the degree of vulnerability of coastal zones to the effect of coastal erosion. The following discussion describes the conclusion and main contributions linked with the research-specific objectives presented in the first chapter of this thesis. The CVI has emerged as a useful tool for coastal managers to prioritize areas for further detailed assessment of vulnerability, risk, resilience, and adaptation options. Additionally, this research shows that satellite imagery has the potential to monitor coastline change and coastal volume change over a period of time and provides essential and valuable information.

The geological parameters were the variables that contributed the most to determining coastal vulnerability.

The data analysis found that the most contributed variables that determined the coastal vulnerability were the geological variables (geomorphology, shoreline change rate, coastal elevation) and physical variables (significant wave height). Since the physical variables (sea level change rate and tidal range) were given the same risk level along the coast, the parameter that contributed the most could be further improved with weighted determination. Moreover, the southern part of Bali province is the most vulnerable area compared to the northern part.

7176.46 ha area of Bali Province will be below the water level in 2100.

Based on the simulation results, the coastal areas of Jembrana, Buleleng, and Denpasar regencies are among the most vulnerable to coastal inundation due to rising sea levels in the region, more specifically, on the central coast of Bali Island, which is a low-elevation area.

Rapid erosion, primarily driven by human activities and coastal hydrodynamics, is emerging as a major concern in Bali Province.

From 2016 to 2021, the shoreline in Bali Province decreased from 668.64 km to 662.59 km at an average rate of -1.21 m/yr due to continuous erosion, with the most significant retreat occurring at Klungkung Regency. On the other hand, human-caused shoreline advancement, such as land reclamation, harbor, and airport construction, has resulted in a net land increase of 1.25 km². The protection strategies include structural interventions such as breakwaters and seawalls have been made.

7.2. Contribution of This Research

This research was conducted to comprehensively assess coastal vulnerability, coastal erosion hazards, and risks along the Bali Province coast. Based on the findings on the prevalence of coastal erosion, increased impacts of risk, low adaptive capacity, and the current management measures implemented along the study coast. The local government can adopt the research methodology for assessing coastal vulnerability, coastal erosion, and mapping coastal flooding because it is efficient in implementation and a relatively low-cost method. Moreover, the vulnerability assessment and analysis of coastal erosion can be used as valuable information for local government, local community, and related stakeholders to assess the micro-level vulnerability and design policies related to coastal vulnerability.

7.3. Recommendations

This research recommends monitoring an understanding on how the coast is evolving over time, particularly in response to coastal erosion. The recommended collaborative research between academia, government, and coastal communities is crucial for coastal planning. It will enable up-to-date information on coastal erosion, paving a pathway for more informed coastal management practices. It will also provide more insight and understanding of the impacts of coastal erosion, which will inform adaptation and mitigation measures and increase resilience along the study coast. Furthermore, there is a need to improve coastal erosion and adaptation options awareness in the region, from local communities through to national government levels, to increase understanding and financing of adaptation measures to improve the resilience of the communities to impacts of coastal erosion and other coastal climate change impacts (e.g., flooding).

Technical recommendations for future researches are as follows:

- This research was aimed at utilizing satellite images to obtain the geological and physical parameters that contribute the coastal vulnerability and did not consider other aspects; therefore, further studies in this area need to include the socio-economic aspect, local factor at a detailed scale, etc. as additional inputs to produce a better and more accurate result on coastal vulnerability assessment;
- Future studies will need to assess strategies for incorporating coastal vulnerability assessments with specific mechanisms that can be addressed through coastal restoration and protection;
- A comprehensive analysis of shoreline changes, including a detailed assessment of cost and benefit associated with potential adaptations and mitigation should be undertaken to evaluate the possible actions for coastal protection strategies;
- Advanced imaging techniques also need to be considered. Investigate the use of advanced imaging techniques such as hyperspectral and LiDAR for more accurate shoreline change detection;
- Applied machine learning. Explore the use of machine learning algorithms.

REFERENCES

- Abdelhady, H.U., Troy, C.D., Habib, A., Manish, R., 2022. A Simple, Fully Automated Shoreline Detection Algorithm for High-Resolution Multi-Spectral Imagery. *Remote Sensing* 2022, Vol. 14, Page 557 14, 557. <https://doi.org/10.3390/RS14030557>
- Abuodha, P.A., Woodroffe, C.D., 2006. Assessing vulnerability of coasts to climate change: A review of approaches and their application to the Australian coast, in: Woodroffe, C., Bruce, E., Poutinen, M., Furness, R. (Eds.), *GIS for the Coastal Zone: A Selection of Papers from CoastGIS 2006*. University of Wollongong, Wollongong, Australia, p. 458.
- Akbar, M.R., Arisanto, P.A.A., Sukirno, B.A., Merdeka, P.H., Priadhi, M.M., Zallesa, S., 2020. Mangrove vegetation health index analysis by implementing NDVI (normalized difference vegetation index) classification method on sentinel-2 image data case study: Segara Anakan, Kabupaten Cilacap. *IOP Conf Ser Earth Environ Sci* 584, 012069. <https://doi.org/10.1088/1755-1315/584/1/012069>
- Alesheikh, A A, Ghorbanali, A., Nouri, N., 2007. Coastline change detection using remote sensing. *International Journal of Environmental Science & Technology* 2007 4:1 4, 61–66. <https://doi.org/10.1007/BF03325962>
- Almar, R., Ranasinghe, R., J Bergsma, E.W., Diaz, H., Melet, A., Papa, F., Vousdoukas, M., Athanasiou, P., Dada, O., Pedro Almeida, L., Kestenare, E., 2021. A global analysis of extreme coastal water levels with implications for potential coastal overtopping. *Nat Commun* 12, 1–9. <https://doi.org/10.1038/s41467-021-24008-9>
- Amboro, R.N.T., Saptari, N., Syanthi, N.P.P., 2022. Provinsi Bali dalam Angka 2022 - Bali Province in Figures 2022. Badan Pusat Statistik (BPS) Provinsi Bali.
- Anfuso, G., Williams, A.T., Cabrera Hernández, J.A., Pranzini, E., 2014. Coastal scenic assessment and tourism management in western Cuba. *Tour. Manag.* 42, 307–320.
- An Overview, H., Zhou, X., Wang, J., Zheng, F., Wang, H., Yang, H., 2023. An Overview of Coastline Extraction from Remote Sensing Data. *Remote Sensing* 2023, Vol. 15, Page 4865 15, 4865. <https://doi.org/10.3390/RS15194865>
- Antara, M., Sumarniasih, M.S., 2017. Role of Tourism in Economy of Bali and Indonesia. *Journal of Tourism and Hospitality Management* 5, 34–44. <https://doi.org/10.15640/jthm.v5n2a4>
- A Widiawan, D., Nurdjaman, S., 2018. Tidal Current Circulation in Western Bali Sea Using a 2-D Hydrodynamic Model, in: *J. Phys.: Conf. Ser.* 1090. p. 12075. <https://doi.org/10.1088/1742-6596/1090/1/012075>
- Badan Pusat Statistik - Statistics of Bali Province., 2022. Provinsi Bali Dalam Angka 2022. Denpasar.
- Bagdanavičiute, I., Kelpšaitė, L., Soomere, T., 2015. Multi-criteria evaluation approach to coastal vulnerability index development in micro-tidal low-lying areas. *Ocean Coast. Manag.* 104, 124–135.
- Bakker, F.L., 1997. Balinese hinduism and the Indonesian state; Recent developments. *Bijdragen tot de taal-, land- en volkenkunde / Journal of the Humanities and Social Sciences of Southeast Asia* 153, 15–41. <https://doi.org/10.1163/22134379-90003943>

- Balaji, R., Kumar, S.S., Misra, A., 2017. Understanding the effects of seawall construction using a combination of analytical modelling and remote sensing techniques: Case study of Fansa, Gujarat, India. *Journal of Ocean and Climate: Science, Technology and Impacts* 8, 153–160. <https://doi.org/10.1177/1759313117712180>
- Balica, S.F., Wright, N.G., van der Meulen, F., 2012. A flood vulnerability index for coastal cities and its use in assessing climate change impacts, *Natural Hazards*. <https://doi.org/10.1007/s11069-012-0234-1>
- Barnard, P.L., Erikson, L.H., Foxgrover, A.C., Hart, J.A.F., Limber, P., O’neill, A.C., Van Ormondt, M., Vitousek, S., Wood, N., Hayden, M.K., Jones, J.M., 2019. Dynamic flood modeling essential to assess the coastal impacts of climate change. *Sci Rep* 9, 1–13. <https://doi.org/10.1038/s41598-019-40742-z>
- Belknap, D.F., Kraft, J.C., 1985. Influence of Antecedent Geology on Stratigraphic Preservation Potential and Evolution of Delaware’s Barrier Systems. *Mar Geol* 63, 235–262.
- Bell, R.G., Lawrence, J.H., Allan, S., Blackett, P., Stephens, S., 2017. *Coastal Hazards and Climate Change: guidance for local government*. Ministry for the Environment, Wellington.
- Berlianty, D., Yanagi, T., 2015a. Tide and Tidal Current in the Bali Strait, Indonesia. *Marine Research in Indonesia* 36, 25–36. <https://doi.org/10.14203/mri.v36i2.39>
- Berlianty, D., Yanagi, T., 2015b. Tide and Tidal Current in the Bali Stratit, Indonesia. *Marine Research in Indonesia* 36, 25–36. <https://doi.org/10.14203/MRI.V36I2.39>
- Bird, E.C.F., 1996. Coastal Erosion and Rising Sea-Level, in: Milliman, J., Haq, B. (Eds.), *Sea-Level Rise and Coastal Subsidence*. Kluwer Academic Publisher, pp. 87–103.
- Birkman, J., 2006. Measuring Vulnerability to Promote Disaster-Resilient Societies: Conceptual Frameworks and Definitions, in: Birkmann, J. (Ed.), . *United Nations University Press, Tokyo*, pp. 9–54.
- BMKG, 2020. Analisis Gelombang Laut Ekstrem Terkait Banjir Rob di Pesisir Selatan Bali Tanggal 27 Mei 2020 [WWW Document]. Badan Meteorologi, Klimatologi, dan Geofisika.
- Boak, E.H., Turner, I.L., 2005. Shoreline definition and detection: A review. *J Coast Res*. <https://doi.org/10.2112/03-0071.1>
- Boruff, B.J., Emrich, C., Cutter, S.L., 2005. Erosion hazard vulnerability of US coastal counties. *J. Coast. Res.* 21.
- Boussetta, A., Niculescu, S., Bengoufa, S., Zagrarni, M.F., 2022. Spatio-temporal analysis of shoreline changes and erosion risk assessment along Jerba island (Tunisia) based on remote-sensing data and geospatial tools. *Reg Stud Mar Sci* 55, 102564. <https://doi.org/10.1016/J.RSMA.2022.102564>
- Brown, C.F., Brumby, S.P., Guzder-Williams, B., Birch, T., Brooks Hyde, S., Mazzariello, J., Czerwinski, W., Pasquarella, V.J., Haertel, R., Ilyushchenko, S., Schwehr, K., Weisse, M., Stolle, F., Hanson, C., Guinan, O., Moore, R., Tait, A.M., 2022. Dynamic World, Near real-time global 10 m land use land cover mapping. *Sci Data* 9, 1–17. <https://doi.org/10.1038/s41597-022-01307-4>
- Brown, L.R., 2001. *Rising Sea Level Forcing Evacuation of Island Country* [WWW Document]. Earth Policy Institute. URL http://www.earth-policy.org/plan_b_updates/2001/update2 (accessed 12.22.20).

- Cazenave, A., Cozannet, G. Le, 2014. Sea level rise and its coastal impacts. *Earths Future* 2, 15–34. <https://doi.org/10.1002/2013ef000188>
- Cazenave, A., Dieng, H.-B., Meyssignac, B., von Schuckmann, K., Decharme, B., Berthier, E., 2014a. The rate of sea-level rise. *Nat Clim Chang* 4, 358–361. <https://doi.org/10.1038/nclimate2159>
- Cazenave, A., Dieng, H.B., Meyssignac, B., Von Schuckmann, K., Decharme, B., Berthier, E., 2014b. The rate of sea-level rise. *Nat Clim Chang* 4, 358–361. <https://doi.org/10.1038/NCLIMATE2159>
- Chen, C., Liang, J., Xie, F., Hu, Z., Sun, W., Yang, G., Yu, J., Chen, L., Wang, Lihua, Wang, Liyan, Chen, H., He, X., Zhang, Z., 2022. Temporal and spatial variation of coastline using remote sensing images for Zhoushan archipelago, China. *International Journal of Applied Earth Observation and Geoinformation* 107, 102711. <https://doi.org/10.1016/J.JAG.2022.102711>
- Chen, S., Qiao, F., Jiang, W., Guo, J., Dai, D., 2019. Impact of surface waves on wind stress under low to moderate wind conditions. *J. Phys. Oceanogr.* 49, 2017–2028.
- Chen, Y., Dong, J., Xiangming Xiao, |, Ma, Z., Tan, K., Melville, D., Li, B., Lu, H., Liu, J., Liu, F., 2019. Effects of reclamation and natural changes on coastal wetlands bordering China's Yellow Sea from 1984 to 2015. *Land Degrad Dev* 1–12. <https://doi.org/10.1002/ldr.3322>
- Church, J.A., White, N.J., 2011. Sea-Level Rise from the Late 19th to the Early 21st Century. *Surv Geophys* 32, 585–602.
- Church, J.A., White, N.J., Aarup, T., Wilson, W.S., Woodworth, P.L., Domingues, C.M., Hunter, J.R., Lambeck, K., 2008. Understanding Global Sea Levels: Past, Present and Future. *Sustain Sci* 3, 9–22. <https://doi.org/10.1007/s11625-008-0042-4>
- Cohen, J., 1960. A Coefficient of Agreement for Nominal Scales. *Educ. Psychol. Meas.* 20, 37–46.
- Congalton, R.G., Oderwald, R.G., Mead, R.A., 1983. Assessing Landsat Classification Accuracy Using Discrete Multivariate Analysis Statistical Techniques. *Photogramm. Eng. Remote Sens.* 49, 1671–1678.
- Cooper, J.A.G., McKenna, J., 2008. Social justice in coastal erosion management: The temporal and spatial dimensions. *Geoforum* 39, 294–306. <https://doi.org/10.1016/j.geoforum.2007.06.007>
- Cooper, M.J.P., Beevers, M.D., Oppenheimer, M., 2008. The potential impacts of sea level rise on the coastal region of New Jersey, USA. *Clim. Change* 90, 475–492.
- Crossland, C.J., Baird, D., Ducrotoy, J.-P., Lindeboom, H., Buddemeier, R.W., Dennison, W.C., Maxwell, B.A., Smith, S. V., Swaney, D.P., 2005. The Coastal Zone — a Domain of Global Interactions. https://doi.org/10.1007/3-540-27851-6_1
- Darwish, K., Smith, S., 2021. A Comparison of Landsat-8 OLI, Sentinel-2 MSI and PlanetScope Satellite Imagery for Assessing Coastline Change in El-Alamein, Egypt. *Engineering Proceedings* 2021, Vol. 10, Page 23 10, 23. <https://doi.org/10.3390/ECSA-8-11258>
- Dasgupta, S., Laplante, B., Meisner, C., Wheeler, D., Yan, J., 2009. The impact of sea level rise on developing countries: A comparative analysis. *Clim Change* 93, 379–388. <https://doi.org/10.1007/s10584-008-9499-5>
- De Lima, L.T., Fernández-Fernández, S., Espinoza, J.M.D.A., Albuquerque, M.D.G., Bernardes, C., 2021. End Point Rate Tool for QGIS (EPR4Q): Validation Using DSAS and AMBUR. *ISPRS International Journal of Geo-Information* 2021, Vol. 10, Page 162 10, 162. <https://doi.org/10.3390/IJGI10030162>

- Dellepiane, S., De Laurentiis, R., Giordano, F., 2004. Coastline extraction from SAR images and a method for the evaluation of the coastline precision. <https://doi.org/10.1016/j.patrec.2004.05.022>
- Devoy, R.J.N., 2015. Sea-Level Rise: Causes, Impacts, and Scenarios for Change. *Coastal and Marine Hazards, Risks, and Disasters* 197–241. <https://doi.org/10.1016/B978-0-12-396483-0.00008-X>
- Dewi, I.G.S., 2019. Penolakan masyarakat terhadap reklamasi Teluk Benoa Provinsi Bali. *Diponegoro Private Law Review* 4, 390–400.
- Dewi, R.S., Bijker, W., 2020. Dynamics of shoreline changes in the coastal region of Sayung, Indonesia. *The Egyptian Journal of Remote Sensing and Space Science* 23, 181–193. <https://doi.org/10.1016/J.EJRS.2019.09.001>
- Diez, P.G., Perillo, G.M.E., Piccolo, M.C., 2007. Vulnerability to Sea-Level Rise on the Coast of the Buenos Aires Province. *J. Coast. Res.* 2007, 119–126.
- Dillenburg, S.R., Roy, P.S., Cowell, P.J., Tomazelli, L.J., 2000. Influence of Antecedent Topography on Coastal Evolution as Tested by the Shoreface Translation-Barrier Model (STM). Source: *Journal of Coastal Research* 16, 71–81.
- Dimiyati, M., Rafli, M., Damayanti, A., 2022. Differences of Coastline Changes in the Area Affected by Land Cover Changes and Coastal Geomorphological South Bali 1995 - 2021. *International Journal of Remote Sensing and Earth Sciences (IJReSES)* 19, 167–176. <https://doi.org/10.30536/IJRESES.2022.V19.A3781>
- Doherty, Y., Harley, M.D., Vos, K., Splinter, K.D., 2022. A Python toolkit to monitor sandy shoreline change using high-resolution PlanetScope cubesats. *Environmental Modelling & Software* 157, 105512. <https://doi.org/10.1016/J.ENVSOF.2022.105512>
- Domazetović, F., Šiljeg, A., Marić, I., Faričić, J., Vassilakis, E., Panda, L., 2021. Automated coastline extraction using the very high resolution worldview (WV) satellite imagery and developed coastline extraction tool (CET). *Applied Sciences (Switzerland)* 11, 9482. <https://doi.org/10.3390/APP11209482/S1>
- Domínguez, L., Anfuso, G., Gracia, F.J., 2005. Vulnerability assessment of a retreating coast in SW Spain. *Environ. Geol.* 47, 1037–1044.
- Doornkamp, J.C., 1998. Coastal flooding, global warming and environmental management, *Journal of Environmental Management*.
- Dwi Artama, K., Gede, W., Karang, A., Putra, N.G., 2019. Deteksi Perubahan Garis Pantai Menggunakan Citra Synthetic Aperture Radar (SAR) di Pesisir Tenggara Bali (Kabupaten Gianyar dan Klungkung). *Journal of Marine and Aquatic Sciences* 5, 278–288.
- Dwiputra, M.R., Osawa, T., Karang, I.W.G.A., 2020. Land Subsidence Analysis Observe By PS-InSAR Method in Southern Part of Bali, Indonesia (A Case Study of Denpasar and Badung Area). *Ecotrophic* 14, 214–223.
- Ellison, J.C., 1999. Impacts of Sediment Burial on Mangroves. *Mar Pollut Bull* 37, 420–426. [https://doi.org/10.1016/S0025-326X\(98\)00122-2](https://doi.org/10.1016/S0025-326X(98)00122-2)
- Elvansa, F., Hendrawan, I.G., Mandhara Brasika, I.B., 2022. Potensi Terjadinya Banjir Rob Akibat Penurunan Muka Tanah dan Kenaikan Muka Air Laut di Kabupaten Badung, Bali. *Journal of Marine Research and Technology* 5, 64. <https://doi.org/10.24843/JMRT.2022.V05.I02.P02>

- Enríquez, A., Marcos, M., Álvarez-Ellacuría, A., Orfila, A., Gomis, D., 2016. Changes in beach shoreline due to sea level rise and waves under climate change scenarios: application to the Balearic Islands (Western Mediterranean). *Natural Hazards and Earth System Sciences Discussions* 1–25.
- Esendağlı, Ç., Selim, S., Demir, N., 2022. Comparison of shoreline extraction indexes performance using Landsat 9 satellite images in the heterogeneous coastal area, in: *4th Intercontinental Geoinformation Days*. Tabriz, Iran, pp. 199–202.
- Feagin, R.A., Sherman, D.J., Grant, W.E., 2005. Coastal Erosion, Global Sea-Level Rise, and The Loss of Sand Dune Plant Habitats. *Front. Ecol. Environ.* 3, 359–364.
- Finkl, C.W., 2016. Coasts, in: Harff, J., Meschede, M., Petersen, S., Thiede, Jö. (Eds.), *Encyclopedia of Marine Geosciences*. Springer Netherlands, Dordrecht, pp. 103–113. https://doi.org/10.1007/978-94-007-6238-1_152
- Fitzpatrick-Lins, K., 1981. Comparison of sampling procedures and data analysis for a land- use and land-cover map. *Photogramm. Eng. Remote Sens.* 47, 343–351.
- Fraïola, K.M.S., Miura, T., Martinez, J., Lopes, K.H., Amidon, F., Torres-Pérez, J., Spalding, H.L., Williams, T., So, K., Sachs, E., Kosaki, R.K., 2023. Using commercial high-resolution satellite imagery to monitor a nuisance macroalga in the largest marine protected area in the USA. *Coral Reefs* 42, 253–259. <https://doi.org/10.1007/S00338-022-02336-6/FIGURES/6>
- Fuchs, R.J., 2010. *Cities at Risk: Asia's Coastal Cities in an Age of Climate Change Analysis from the East-West Center*.
- Furqan, A., Winandi, F.I., 2018. The Impact of Climate Change on Coastal Tourism Destination: Case of Kuta Beach, Bali, Indonesia. *ASEAN Journal on Hospitality and Tourism* 16, 84. <https://doi.org/10.5614/AJHT.2018.16.2.3>
- Gandhi, S.M., Sarkar, B.C., 2016. Reconnaissance and Prospecting, in: Gandhi, S., Sarkar, B. (Eds.), . Elsevier, pp. 53–79.
- Gao, W., Du, J., Gao, S., Xu, Y., Li, B., Wei, X., Zhang, Z., Liu, J., Li, P., 2023. Shoreline change due to global climate change and human activity at the Shandong Peninsula from 2007 to 2020. *Front Mar Sci* 9, 1123067. <https://doi.org/10.3389/FMARS.2022.1123067/BIBTEX>
- García-Sánchez, G., Mancho, A.M., Ramos, A.G., Coca, J., Pérez-Gómez, B., Álvarez-Fanjul, E., Sotillo, M.G., García-León, M., García-Garrido, V.J., Wiggins, S., 2021. Very High Resolution Tools for the Monitoring and Assessment of Environmental Hazards in Coastal Areas. *Front Mar Sci* 7, 605804. <https://doi.org/10.3389/FMARS.2020.605804/BIBTEX>
- Gens, R., 2010. Remote sensing of coastlines: detection, extraction and monitoring. *Int J Remote Sens* 31, 1819–1836. <https://doi.org/10.1080/01431160902926673>
- Ge, Y., Zhang, J.-Y., 2011. Analysis of the impact on ecosystem and environment of marine reclamation-A case study in Jiaozhou Bay. <https://doi.org/10.1016/j.egypro.2011.03.020>
- Ghionis, G., Lazogiannis, Konstantinos, Poulos, Serafeim, Drakopoulos, P., Lazogiannis, Kostas, Poulos, Serafim, 2014. Toward precise shoreline detection and extraction from remotely sensed images with the use of wet and dry sand spectral signatures. *Fresenius Environ Bull* 23.
- Gittman, R.K., Scyphers, S.B., Smith, C.S., Neylan, I.P., Grabowski, J.H., 2016. Ecological Consequences of Shoreline Hardening: A Meta-Analysis. *Bioscience* 66, 763–773. <https://doi.org/10.1093/BIOSCI/BIW091>

- Gordon, A.L., 2005. Oceanography of the Indonesian Seas and Their Throughflow. *Oceanography* 18. <https://doi.org/https://doi.org/10.5670/oceanog.2005.01>
- Gordon, A.L., Susanto, R.D., 1998. Makassar Strait Transport: Initial Estimate Based on Arlindo Results Ocean Salinity and the global hydrological cycle View project Time variable Eddy Diffusivities View project, Article in *Marine Technology Society Journal*.
- Gornitz, V., 1991. Global Coastal Hazards from Future Sea Level Rise. *Palaeogeogr. Palaeoclimatol. Palaeoecol.* 89, 379–398.
- Gornitz, V.M., White, T.W., Daniels, D.C., 1997. A Coastal Hazards Data Base for the U.S. West Coast, in: Environmental Science Division. Oak Ridge National Laboratory, Tennessee, USA, pp. 1–40.
- Gornitz, V., White, T.W., Cushman, R.M., 1991. Vulnerability of the U.S. to Future Sea-Level Rise. Oak Ridge National Laboratory, Tennessee, USA, pp. 1–15.
- Government of Bali Province, 2015. Laporan Status Lingkungan Hidup Daerah Provinsi Bali 2015. Government of Bali Province, Denpasar, pp. 39–46.
- Govind, P.J., Verchick, R.R.M., 2015. Natural Disaster and Climate Change, in: Gonzalez, C.G., Razaque, J., Alam, S., Atapattu, S. (Eds.), *International Environmental Law and the Global South*. Cambridge University Press, Cambridge, pp. 491–507. <https://doi.org/DOI:10.1017/CBO9781107295414.024>
- Griffiths, D., House, C., Rangel-Buitrago, N., Thomas, T., 2019. An assessment of areal and transect-based historic shoreline changes in the context of coastal planning. *J Coast Conserv* 23, 315–330. <https://doi.org/10.1007/S11852-018-0661-6/FIGURES/11>
- Guha, S., 2016. Capability of NDVI Technique in Detecting Mangrove Vegetation. *International Journal of Advanced Biological Research* 6, 253–258.
- Gusmawati, N.F., Zhi, C., Souldard, B., Lemonnier, H., Selmaoui-Folcher, N., 2016. Aquaculture Pond Precise Mapping in Perancak Estuary, Bali, Indonesia. <https://doi.org/10.2112/SI75-128.1> 75, 637–641. <https://doi.org/10.2112/SI75-128.1>
- Gutierrez, B.T., Williams, S.J., Thieler, E.R., 2009. Ocean Coast, in: Titus, J.G., Anderson, K.E., Cahoon, D.R., Gesch, D.B., Gill, S.K., Gutierrez, B.T., Thieler, E.R., Williams, S.J. (Eds.), *Coastal Sensitivity to Sea-Level Rise: A Focus on the Mid-Atlantic Region*. U.S. Environmental Protection Agency, Washington DC, pp. 43–56.
- Hammar-Klose, E.S., Thieler, E.R., 2001. Coastal vulnerability to sea-level rise: a preliminary database for the U.S. Atlantic, Pacific, and Gulf of Mexico Coasts, Data Series, Data Series 68. USGS: Woods Hole, MA, USA. <https://doi.org/10.3133/ds68>
- Handiani, D.N., Heriati, A., Gunawan, W.A., 2022. Comparison of coastal vulnerability assessment for Subang Regency in North Coast West Java-Indonesia. *Geomatics, Natural Hazards and Risk* 13, 1178–1206. <https://doi.org/10.1080/19475705.2022.2066573>
- Hanifa, A.D., Syamsudin, F., Zhang, C., Mutsuda, H., Chen, M., Zhu, X.H., Kaneko, A., Taniguchi, N., Li, G., Zhu, Z.N., Gohda, N., 2020. Tomographic measurement of tidal current and associated 3-h oscillation in Bali Strait. *Estuar Coast Shelf Sci* 236, 106655. <https://doi.org/10.1016/J.ECSS.2020.106655>
- Han, W., Zhang, L., Meehl, G.A., Kido, S., Tozuka, T., Li, Y., McPhaden, M.J., Hu, A., Cazenave, A., Rosenbloom, N., Strand, G., West, B.J., Xing, W., 2022. Sea level extremes and compounding

- marine heatwaves in coastal Indonesia. *Nat Commun* 13. <https://doi.org/10.1038/s41467-022-34003-3>
- Hastuti, A.W., Nagai, M., Suniada, K.I., 2022a. Coastal Vulnerability Assessment of Bali Province, Indonesia Using Remote Sensing and GIS Approaches. *Remote Sensing* 2022, Vol. 14, Page 4409 14, 4409. <https://doi.org/10.3390/RS14174409>
- Hastuti, A.W., Nagai, M., Suniada, K.I., 2022b. Coastal Vulnerability Assessment of Bali Province, Indonesia Using Remote Sensing and GIS Approaches. *Remote Sens (Basel)* 14. <https://doi.org/10.3390/rs14174409>
- Heikal, E.M., Koraim, A.S., Rafea, A.A., Elbagory, I.A., 2023. The effect of groins characteristic on sandy beach stability. *The Egyptian Journal of Aquatic Research*. <https://doi.org/10.1016/J.EJAR.2023.04.005>
- Hinkel, J., Klein, R.J.T., 2009. Integrating knowledge to assess coastal vulnerability to sea-level rise: The development of the DIVA tool. *Global Environmental Change* 19, 384–395. <https://doi.org/10.1016/j.gloenvcha.2009.03.002>
- Hoang, V.C., Tanaka, H., Mitobe, Y., 2017. A Method for Correcting Tidal Effect on Shoreline Position Extracted from an Image with Unknown Capture Time. *Geosciences* 2017, Vol. 7, Page 62 7, 62. <https://doi.org/10.3390/GEOSCIENCES7030062>
- Hossain, M.S., Hashim, M., Bujang, J.S., Zakaria, M.H., Muslim, A.M., 2018. Assessment of the impact of coastal reclamation activities on seagrass meadows in Sungai Pulai estuary, Malaysia, using Landsat data (1994–2017). <https://doi.org/10.1080/01431161.2018.1547931> 40, 3571–3605. <https://doi.org/10.1080/01431161.2018.1547931>
- Hufschmidt, G., 2011. A comparative analysis of several vulnerability concepts. *Natural Hazards* 58, 621–643. <https://doi.org/10.1007/s11069-011-9823-7>
- Huisman, O., de By, R.A., 2009. Principles of geographic information systems: an introductory textbook. The International Institute for Geo-Information Science and Earth Observation (ITC), Enschede .
- Husnayaen, Rimba, A.B., Osawa, T., Parwata, I.N.S., As-syakur, A.R., Kasim, F., Astarini, I.A., 2018. Physical assessment of coastal vulnerability under enhanced land subsidence in Semarang, Indonesia, using multi-sensor satellite data. *Advances in Space Research* 61, 2159–2179.
- Husrin, S., Pratama, R., Putra, A., Sofyan, H., Hasanah, N.N., Yuanita, N., Meilano, I., 2016. The Mechanisms of Coastal Erosion in Northeast Bali. *Jurnal Segara* 12, 109–120. <https://doi.org/10.15578/segara.v12i2.149>
- IPCC, 2019. Sea level rise and implications for low-lying islands, coasts and communities.
- IPCC, 2018. Global Warming of 1.5°C, Global Warming of 1.5°C. Cambridge University Press. <https://doi.org/10.1017/9781009157940>
- IPCC, 2001. Climate Change 2001: The Scientific Basis, Contribution of Working Group I to the Third Assessment Report of the Intergovernmental Panel on Climate Change. Cambridge University Press, Cambridge. [https://doi.org/10.1016/S1058-2746\(02\)86826-4](https://doi.org/10.1016/S1058-2746(02)86826-4)
- Islam, M.A., Hossain, M.S., Murshed, S., 2015. Assessment of Coastal Vulnerability Due to Sea Level Change at Bhola Island, Bangladesh: Using Geospatial Techniques. *J. Indian Soc. Remote Sens.* 43, 625–637.

- Istiqomah, M.F., Sutrisno, S., Wijaya, A., 2018. Analisis Perubahan Garis Pantai Kabupaten Jembrana dengan Menggunakan Citra Satelit Landsat 8. *Al-Fiziya: Journal of Materials Science, Geophysics, Instrumentation and Theoretical Physics* 1. <https://doi.org/10.15408/fiziya.v1i1.8989>
- Jana, A.B., Hegde, A.V., 2016. GIS Based Approach for Vulnerability Assessment of the Karnataka Coast, India. *Advances in Civil Engineering* 2016, 1–10.
- Janga, B., Asamani, G.P., Sun, Z., Cristea, N., 2023. A Review of Practical AI for Remote Sensing in Earth Sciences. *Remote Sensing* 2023, Vol. 15, Page 4112 15, 4112. <https://doi.org/10.3390/RS15164112>
- Jean-Michel, L., Eric, G., Romain, B.B., Gilles, G., Angélique, M., Marie, D., Clément, B., Mathieu, H., Olivier, L.G., Charly, R., Tony, C., Charles-Emmanuel, T., Florent, G., Giovanni, R., Mounir, B., Yann, D., Pierre-Yves, L.T., 2021. The Copernicus Global 1/12° Oceanic and Sea Ice GLORYS12 Reanalysis. *Front Earth Sci (Lausanne)* 9, 698876. <https://doi.org/10.3389/FEART.2021.698876/BIBTEX>
- Jennings, S., 2004. Coastal tourism and shoreline management. *Ann Tour Res* 31, 899–922. <https://doi.org/10.1016/j.annals.2004.02.005>
- Jiménez, J.A., Osorio, A., Marino-Tapia, I., Davidson, M., Medina, R., Kroon, A., Archetti, R., Ciavola, P., Aarnikhof, S.G.J., 2007. Beach recreation planning using video-derived coastal state indicators. *Coast. Eng.* 54, 507–521.
- Jutz, S., Milagro-Pérez, M.P., 2018. Copernicus Program. *Comprehensive Remote Sensing* 1–9, 150–191. <https://doi.org/10.1016/B978-0-12-409548-9.10317-3>
- Kasim, F., Siregar, Vi.P., 2012. Coastal Vulnerability Assessment Using Integrated-Method of CVI-MCA: A Case Study on the Coastline of Indramayu. *Forum Geogr.* 26, 65–74.
- Kelly, P.M., Adger, W.N., 2000. THEORY AND PRACTICE IN ASSESSING VULNERABILITY TO CLIMATE CHANGE AND FACILITATING ADAPTATION.
- Kleypas, J.A., 1996. Coral reef development under naturally turbid conditions: Fringing reefs near Broad Sound, Australia. *Coral Reefs* 15, 153–167. <https://doi.org/10.1007/BF01145886/METRICS>
- Koroglu, A., Ranasinghe, R., Jiménez, J.A., Dastgheib, A., 2019. Comparison of Coastal Vulnerability Index applications for Barcelona Province. *Ocean Coast. Manag.* 178, 104799.
- Kuleli, T., Şenkal, O., Erdem, M., 2009. National assessment of sea level rise using topographic and census data for Turkish coastal zone. *Environ Monit Assess* 156, 425–434. <https://doi.org/10.1007/s10661-008-0495-z>
- Kumar, A.A., Kunte, P., 2012. Coastal vulnerability assessment for Chennai, east coast of India using geospatial techniques. *Nat. Hazards J. Int. Soc. Prev. Mitig. Nat. Hazards.* 64, 853–872.
- Kumar, T.S., Mahendra, R.S., Nayak, S., Radhakrishnan, K., Sahu, K.C., 2010. Coastal vulnerability assessment for Orissa State, East Coast of India. *J. Coast. Res.* 26, 523–534.
- Kunte, P.D., Jauhari, N., Mehrotra, U., Kotha, M., Hursthouse, A.S., Gagnon, A.S., 2014. Multi-hazards coastal vulnerability assessment of Goa, India, using geospatial techniques. *Ocean Coast. Manag.* 95, 264–281.

- Kuntoro, W.S., Ningsih, N.S., Rachmayani, R., 2020. Seasonal wave characteristics in Southern Bali Waters in 2014, in: IOP Conf. Ser.: Earth Environ. Sci 618. p. 12002. <https://doi.org/10.1088/1755-1315/618/1/012002>
- Lambin, E.F., 2001. Remote Sensing and Geographic Information Systems Analysis. International Encyclopedia of the Social & Behavioral Sciences 13150–13155. <https://doi.org/10.1016/B0-08-043076-7/04200-5>
- Laonamsai, J., Julphunthong, P., Saprathet, T., Kimmany, B., Ganchanasuragit, T., Chomcheawchan, P., Tomun, N., 2023. Utilizing NDWI, MNDWI, SAVI, WRI, and AWEI for Estimating Erosion and Deposition in Ping River in Thailand. *Hydrology* 2023, Vol. 10, Page 70 10, 70. <https://doi.org/10.3390/HYDROLOGY10030070>
- Larcombe, P., Costen, A., Woolfe, K.J., 2001. The hydrodynamic and sedimentary setting of nearshore coral reefs, central Great Barrier Reef shelf, Australia: Paluma Shoals, a case study. *Sedimentology* 48, 811–835. <https://doi.org/10.1046/J.1365-3091.2001.00396.X>
- Lawal, D.U., Matori, A.N., Hashim, A.M., Chandio, I.A., Sabri, S., Balogun, A.L., Abba, H.A., 2011. Geographic information system and remote sensing applications in flood hazards management: A review. *Res. J. Appl. Sci. Eng. Technol.* 3, 933–947.
- Leonardi, N., Ganju, N.K., Fagherazzi, S., 2016. A linear relationship between wave power and erosion determines salt-marsh resilience to violent storms and hurricanes. *Proc. Natl. Acad. Sci.* 113, 64–68.
- Lien, M.K., 2019. Vulnerability Assessment of Climate Change on Sea Level Rise Impacts on Some Economic Sectors in Binh Dinh Province, Vietnam. *Am. J. Clim. Change* 08, 302–324.
- Lillesand, T.M., Kiefer, R.W., Chipman, J.W., 2004. Digital Image Processing, in: Flahive, R., Powell, D. (Eds.), *Remote Sensing and Image Interpretation*. John Wiley & Sons, Inc., Hoboken, NJ, USA, pp. 491–637.
- Lim, C., Kon Kim, T., Lee, S., Jeong Yeon, Y., Lyul Lee, J., 2021. Assessment of potential beach erosion risk and impact of coastal zone development: a case study on Bongpo-Cheonjin Beach. *Hazards Earth Syst. Sci* 21, 3827–3842. <https://doi.org/10.5194/nhess-21-3827-2021>
- Lira-Loarca, A., Baquerizo, A., Longo, S., 2019. Interaction of Swell and Sea Waves with Partially Reflective Structures for Possible Engineering Applications. *Journal of Marine Science and Engineering* 2019, Vol. 7, Page 31 7, 31. <https://doi.org/10.3390/JMSE7020031>
- Li, Z., Chen, H., Nie, Q., 2021. Comparison of coastline extraction methods and block classification method to extract coastlines based on remote sensing. <https://doi.org/10.21203/rs.3.rs-154223/v1>
- López Royo, M., Ranasinghe, R., Jiménez, J.A., 2016. A Rapid, Low-Cost Approach to Coastal Vulnerability Assessment at a National Level. *J Coast Res* 32, 932–945. <https://doi.org/10.2112/JCOASTRES-D-14-00217.1>
- Maharta, I.P.R.F., Hendrawan, I.G., Suteja, Y., 2019. Prediksi Laju Sedimentasi di Perairan Teluk Benoa Menggunakan Pemodelan Numerik. *Journal of Marine and Aquatic Sciences* 5, 44. <https://doi.org/10.24843/jmas.2019.v05.i01.p06>
- Mahasin, M.Z., Rochwulaningsih, Y., Sulistiyono, S.T., 2020. Coastal Ecosystem as Salt Production Centre in Indonesia, in: *E3S Web of Conferences*. EDP Sciences, p. 07042. <https://doi.org/10.1051/E3SCONF/202020207042>

- Malik, A., Abdalla, R., 2016. Geospatial modeling of the impact of sea level rise on coastal communities: application of Richmond, British Columbia, Canada. *Model Earth Syst Environ* 2. <https://doi.org/10.1007/s40808-016-0199-2>
- Malini, B.H., Rao, K.N., 2004. Coastal erosion and habitat loss along the Godavari delta front-A fallout of dam construction(?). *Curr Sci* 87, 1232–1236.
- Mansaray, A.S., Dzialowski, A.R., Martin, M.E., Wagner, K.L., Gholizadeh, H., Stoodley, S.H., 2021. Comparing PlanetScope to Landsat-8 and Sentinel-2 for Sensing Water Quality in Reservoirs in Agricultural Watersheds. <https://doi.org/10.3390/rs13091847>
- Marfai, M.A., King, L., 2008. Potential vulnerability implications of coastal inundation due to sea level rise for the coastal zone of Semarang city, Indonesia. *Environmental Geology* 54, 1235–1245. <https://doi.org/10.1007/s00254-007-0906-4>
- Maselli, F., 2004. Monitoring forest conditions in a protected Mediterranean coastal area by the analysis of multiyear NDVI data. *Remote Sens Environ* 89, 423–433. <https://doi.org/10.1016/j.rse.2003.10.020>
- Masucci, G.D., Reimer, J.D., 2019. Expanding walls and shrinking beaches: Loss of natural coastline in Okinawa Island, Japan. *PeerJ* 2019. <https://doi.org/10.7717/PEERJ.7520/SUPP-1>
- McFeeters, S.K., 1996. The use of the Normalized Difference Water Index (NDWI) in the delineation of open water features. *Int J Remote Sens* 17, 1425–1432. <https://doi.org/10.1080/01431169608948714>
- McGranahan, G., Balk, D., Anderson, B., 2007. The rising tide: Assessing the risks of climate change and human settlements in low elevation coastal zones. *Environ Urban* 19, 17–37. <https://doi.org/10.1177/0956247807076960>
- Melet, A., Teatini, P., Le Cozannet, G., Jamet, C., Conversi, A., Benveniste, J., Almar, R., 2020. Earth Observations for Monitoring Marine Coastal Hazards and Their Drivers. *Surveys in Geophysics* 2020 41:6 41, 1489–1534. <https://doi.org/10.1007/S10712-020-09594-5>
- Mentaschi, L., Voudoukas, M.I., Pekel, J.F., Voukouvalas, E., Feyen, L., 2018. Global long-term observations of coastal erosion and accretion. *Scientific Reports* 2018 8:1 8, 1–11. <https://doi.org/10.1038/s41598-018-30904-w>
- Mills, J.P., Buckley, S.J., Mitchell, H.L., Clarke, P.J., Edwards, S.J., 2005. Earth Surface Processes and Landforms *Earth Surf. Earth Surf. Process. Landforms* 30, 651–664. <https://doi.org/10.1002/esp.1165>
- Mishra, M., Acharyya, T., Chand, P., Santos, C.A.G., Kar, D., Das, P.P., Pattnaik, N., Silva, R.M. da, Nascimento, T.V.M. do, 2021. Analyzing shoreline dynamicity and the associated socioecological risk along the Southern Odisha Coast of India using remote sensing-based and statistical approaches. <https://doi.org/10.1080/10106049.2021.1882005> 37, 3991–4027. <https://doi.org/10.1080/10106049.2021.1882005>
- Mondejar, J.P., Tongco, A.F., 2019. Near infrared band of landsat 8 as water index: A case study around Cordova and Lapu-Lapu City, Cebu, Philippines. *Sustainable Environment Research* 1, 1–15. <https://doi.org/10.1186/S42834-019-0016-5/TABLES/3>
- Mujiburrahman, Rochwulaningsih, Y., Sulistiyono, S.T., Utama, M.P., 2020. Coastal Environmental Change and the Salt Farmer Marginalization in Kusamba, Bali, in: *E3S Web of Conferences* 202 ICENIS 2020. p. 10. <https://doi.org/10.1051/e3sconf/202020207046>

- Muñoz-Pérez, J.J., Medina, R., Tejedor, B., 2001. Evolution of longshore beach contour lines determined by the E.O.F. method. *Sci. Mar.* 65, 393–402.
- Murni, N.G.N.S., Ruki, M., Anatar, D.M.S., 2018. Beach Utilization as Tourist Attraction and Ritual in Badung Regency. *Atlantis Press*, pp. 538–542. <https://doi.org/10.2991/ICSS-18.2018.111>
- Murray, A.B., Ashton, A.D., 2013. Self-Organization of Large-Scale Coastline Shapes. *Philos. Transactions R. Soc. A* 371, 1–15.
- Narayana, A.C., 2016. Shoreline Changes, in: Kennish, M.J. (Ed.), *Encyclopedia of Estuaries*. Springer Netherlands, Dordrecht, pp. 590–602. https://doi.org/10.1007/978-94-017-8801-4_118
- Nardin, W., Vona, I., Fagherazzi, S., 2021. Sediment deposition affects mangrove forests in the Mekong delta, Vietnam. *Cont Shelf Res* 213, 104319. <https://doi.org/10.1016/J.CSR.2020.104319>
- Negm, A., Nassar, K., 2016. Determination of Wave Reflection Formulae for Vertical and Sloped Seawalls Via Experimental Modelling, in: *Procedia Engineering* 154. pp. 919–927. <https://doi.org/10.1016/j.proeng.2016.07.502>
- Nicholls, R.J., 2010. Impacts of and Responses to Sea-Level Rise, in: *Understanding Sea-Level Rise and Variability*. pp. 17–51. <https://doi.org/https://doi.org/10.1002/9781444323276.ch2>
- Nicholls, R.J., Cazenave, A., 2010. Sea-level rise and its impact on coastal zones. *Science* (1979) 328, 1517–1520.
- Nicholls, R.J., Wong, P.P., Burkett, V.R., Codignotto, J., Hay, J.E., McLean, R.F., Ragoonaden, S., Woodroffe, C.D., 2007. Coastal systems and low-lying areas. *Climate Change 2007: Impacts, Adaptation and Vulnerability*. 315–356.
- Nidhinarangkoon, P., Ritphring, S., Kino, K., Oki, T., 2023. Shoreline Changes from Erosion and Sea Level Rise with Coastal Management in Phuket, Thailand. *Journal of Marine Science and Engineering* 2023, Vol. 11, Page 969 11, 969. <https://doi.org/10.3390/JMSE11050969>
- O'Connor, M.C., Lymbery, G., Cooper, J.A.G., Gault, J., McKenna, J., 2009. Practice versus policy-led coastal defence management. *Mar Policy* 33, 923–929. <https://doi.org/10.1016/j.marpol.2009.03.007>
- Oktopura, A.A.D., Fauzi, A., Sugema, K., Mulyati, H., 2020. Aquaculture performance in Indonesia: economics and social perspectives, in: *IOP Conf. Ser.: Earth Environ. Sci.* 493. p. 12003. <https://doi.org/10.1088/1755-1315/493/1/012003>
- Onaka, S., Endo, S., Uda, T., 2013. Bali beach conservation project and issues related to beach maintenance after completion of project, in: *In Proceedings of the Seventh International Conference on Asian and Pacific Coasts*. pp. 198–203.
- Oppenheimer, M., Glavovic, B.C., Hinkel, J., van de Wal, R., Magnan, A.K., Abd-Elgawad, A., Cai, R., Cifuentes-Jara, M., DeConto, R.M., Ghosh, T., Hay, J., Isla, F., Marzeion, B., Meyssignac, B., Sebesvari, Z., 2019. Sea Level Rise and Implications for Low-Lying Islands, Coasts and Communities.
- Özyurt, G., Ergin, A., 2010. Improving coastal vulnerability assessments to sea-level rise: A new indicator-based methodology for decision makers. *J. Coast. Res.* 26, 265–273.
- Palmer, S.E., Perry, C.T., Smithers, S.G., Gulliver, P., 2010. Internal structure and accretionary history of a nearshore, turbid-zone coral reef: Paluma Shoals, central Great Barrier Reef, Australia. *Mar Geol* 276, 14–29. <https://doi.org/10.1016/J.MARGE.2010.07.002>

- Pelling, H.E., Uehara, K., Green, J.A.M., 2013. The impact of rapid coastline changes and sea level rise on the tides in the Bohai Sea, China. *J Geophys Res Oceans* 118, 3462–3472. <https://doi.org/10.1002/jgrc.20258>
- Pendleton, E.A., Theiler, E.R., Williams, S.J., 2005. Coastal Vulnerability Assessment of Gateway National Recreation Area (GATE) to Sea-Level Rise, Open-File Report 2004-1257; U.S. Geological Survey, Open-File Report 2004-1257. U.S. Geological Survey, USGS: Reston, Virginia, USA.
- Pendleton, E.A., Theiler, E.R., Williams, S.J., 2004. Coastal vulnerability assessment of Cape Hatteras National Seashore (CAHA) to sea-level rise, Open-File Report. U.S. Geological Survey 2004 - 1064, Open-File Report 2004-1064. USGS: Reston, Virginia, USA.
- Pendleton, E.A., Thieler, E.R., Williams, S.J., 2010. Importance of coastal change variables in determining vulnerability to sea- and lake-level change. *J. Coast. Res.* 26, 176–183.
- Peterson, C.H., Bishop, M.J., 2005. Assessing the environmental impacts of beach nourishment. *Bioscience* 55, 887–896.
- Pirazzoli, P.A., 1996. Sea level changes: the last 20000 years. Wiley, Chichester.
- Prabowo, U.N., 2016. Pemetaan Tingkat Resiko Gempa Bumi Berdasarkan Data Mikrotremor Di Kotamadya Denpasar, Bali. *Kurvatek* 1, 55–59.
- Purbo-Hadiwidjojo, M.M., Amin, T.C., Samodra, H., 1998. Peta Geologi Lembar Bali Nusatenggara.
- Putra, I.K.S.W., Yujana, C.A., Surayasa, N., 2017. Perencanaan Bangunan Pengaman Pantai (Revetment) dengan Bahan Geobag di Pantai Masceti, Kabupaten Gianyar. *Paduraksa* 6, 178–189.
- Putra, R.W., Firmansyah, M., Kamal, E., 2021. Study of management of Indonesian coastal and marine seas (Review: Benoa Bay reclamation). *Acta Aquatica: Aquatic Sciences Journal* 8, 175–180.
- Putri, K.A.P., Hasibuan, H.S., Tambunan, R.P., 2021. The Impact of Rising Sea Levels on Historical Sites Old City Semarang, in: *E3S Web of Conferences*. EDP Sciences. <https://doi.org/10.1051/e3sconf/202131704012>
- Putro, A.H.S., Lee, J.L., 2020. Analysis of Longshore Drift Patterns on the Littoral System of Nusa Dua Beach in Bali, Indonesia. *Journal of Marine Science and Engineering* 2020, Vol. 8, Page 749 8, 749. <https://doi.org/10.3390/JMSE8100749>
- Pye, K., Blott, S.J., 2006. Coastal processes and morphological change in the Dunwich-Sizewell Area, Suffolk, UK. *J Coast Res* 22, 453–473.
- QGIS Development Team, 2022. QGIS Geographic Information System.
- Rachmayani, R., Ningsih, N.S., Adiprabowo, S.R., Nurfitri, S., 2018. Ocean wave characteristic in the Sunda Strait using Wave Spectrum Model, in: *IOP Conference Series: Earth and Environmental Science* 139. Institute of Physics Publishing, p. 12025. <https://doi.org/10.1088/1755-1315/139/1/012025>
- Rahmawati, R.R., Putro, A.H.S., Lee, J.L., 2021. Analysis of Long-Term Shoreline Observations in the Vicinity of Coastal Structures: A Case Study of South Bali Beaches. *Water* 2021, Vol. 13, Page 3527 13, 3527. <https://doi.org/10.3390/W13243527>
- Rajendra, A., 2020a. Climate change impacts on the coastal tourist resorts of Bali, in: *The 4th International Conference on Climate Change 2019*, IOP Conf. Series: Earth and Environmental Science 423. IOP Publishing.

- Rajendra, A., 2020b. Climate change impacts on the coastal tourist resorts of Bali, in: IOP Conference Series: Earth and Environmental Science. <https://doi.org/10.1088/1755-1315/423/1/012044>
- Ranasinghe, R., Callaghan, D., Stive, M.J.F., 2012. Estimating coastal recession due to sea level rise: Beyond the Bruun rule. *Clim Change* 110, 561–574. <https://doi.org/10.1007/s10584-011-0107-8>
- Rao, K.N., Subraelu, P., Rao, T.V., Malini, B.H., Ratheesh, R., Bhattacharya, S., Rajawat, A.S., Ajai, 2009. Sea-level rise and coastal vulnerability: An assessment of Andhra Pradesh coast, India through remote sensing and GIS. *J. Coast. Conserv.* 12, 195–207.
- Ray, R.D., Dwi Susanto, R., 2019. A fortnightly atmospheric “tide” at Bali caused by oceanic tidal mixing in Lombok Strait. *Geosci Lett* 6, 1–9. <https://doi.org/10.1186/s40562-019-0135-1>
- Ribas, F., Portos-Amill, L., Falqués, A., Arriaga, J., Marcos, M., Ruessink, G., 2023. Impact of mean sea-level rise on the long-term evolution of a mega-nourishment. *Clim Change* 176, 1–26. <https://doi.org/10.1007/S10584-023-03503-6/FIGURES/13>
- Rizal, A.M., Ningsih, N.S., Sofian, I., Hanifah, F., Hilmi, I., 2019. Preliminary study of wave energy resource assessment and its seasonal variation along the southern coasts of Java, Bali, and Nusa Tenggara waters. *Journal of Renewable and Sustainable Energy* 11. <https://doi.org/10.1063/1.5034161/1018952>
- Rizzo, A., Anfuso, G., 2020. Coastal dynamic and evolution: Case studies from different sites around the world. *Water* (Basel).
- Rogers, K., Woodroffe, C.D., 2016. Geomorphology as an indicator of the biophysical vulnerability of estuaries to coastal and flood hazards in a changing climate. *J. Coast. Conserv.* 20, 127–144.
- Romieu, E., Welle, T., Schneiderbauer, S., Pelling, M., Vinchon, C., 2010. Vulnerability assessment within climate change and natural hazard contexts: Revealing gaps and synergies through coastal applications. *Sustain Sci* 5, 159–170. <https://doi.org/10.1007/s11625-010-0112-2>
- Rosane, O., 2023. 10 costliest climate disasters of 2022 [WWW Document]. World Economic Forum. URL <https://www.weforum.org/agenda/2023/01/10-costliest-climate-disasters-of-2022> (accessed 10.19.23).
- Rosenfield, G.H., Fitzpatrick-Lins, K., 1986. A coefficient of agreement as a measure of thematic classification accuracy. *Photogramm. Eng. Remote Sens.* 52, 223–227.
- Ružić, I., Jovančević, S.D., Benac, Č., Krvavica, N., 2019. Assessment of the coastal vulnerability index in an area of complex geological conditions on the krk island, northeast adriatic sea. *Geosciences* (Basel) 9, 1–17.
- Sallenger Jr., A.H., Krabill, W., Brock, J., Swift, R., Manizade, S., Stockdon, H., 2002. Sea-cliff erosion as a function of beach changes and extreme wave runup during the 1997-1998 El Nino. *Mar. Geol.* 187, 279–297.
- Sanchez-Arcilla, A., Jimenez, J.A., Valdemoro, H.I., 1998. The Ebro delta: Morphodynamics and vulnerability. *J. Coast. Res.* 14, 754–772. <https://doi.org/10.2307/4298833>
- Sanders, D., Baron-Szabo, R.C., 2005. Scleractinian assemblages under sediment input: their characteristics and relation to the nutrient input concept. *Palaeogeogr Palaeoclimatol Palaeoecol* 216, 139–181. <https://doi.org/10.1016/J.PALAEO.2004.10.008>

- Sayers, S., Reef, R., 2022. Short-Term Sedimentation Dynamics of Temperate Mangroves in Western Port Bay, Victoria. *Front Mar Sci* 9, 832148. <https://doi.org/10.3389/FMARS.2022.832148/BIBTEX>
- Scanpoint Gematics Ltd., 2022. Role of GIS in Disaster Management [WWW Document]. Scanpoint Gematics Ltd. URL <https://www.sgligis.com/gis-in-disaster-management/> (accessed 10.20.23).
- Scheuer, S., Haase, D., Meyer, V., 2011. Exploring multicriteria flood vulnerability by integrating economic, social and ecological dimensions of flood risk and coping capacity: From a starting point view towards an end point view of vulnerability. *Natural Hazards* 58, 731–751. <https://doi.org/10.1007/s11069-010-9666-7>
- Selim, S., Esendağlı, Ç., Dönmez, B., 2022. Comparison of different indices used for shoreline extraction from Landsat 8 Operational Land Imager in the context of coastal planning, in: Altuntaş, A., Alp, Ş. (Eds.), *Recent Studies in Planning and Design*. IKSAD Publishing House, Ankara, pp. 3–24.
- Setiyowati, D., Ayub, A.F., Zulkifli, M., 2016. *Statistic of Marine and Coastal Resources*. Badan Pusat Statistik.
- Shaw, J., Taylor, R.B., Forbes, D.L., 1998. *Sensitivity of the coasts of Canada to sea-level rise*. Geological Survey of Canada, Ottawa, Canada.
- Shendryk, Y., Rist, Y., Ticehurst, C., Thorburn, P., 2019. Deep learning for multi-modal classification of cloud, shadow and land cover scenes in PlanetScope and Sentinel-2 imagery. *ISPRS Journal of Photogrammetry and Remote Sensing* 157, 124–136. <https://doi.org/10.1016/J.ISPRSJPRS.2019.08.018>
- Shipton, C., O'Connor, S., Kealy, S., 2021. The biogeographic threshold of Wallacea in human evolution. *Quaternary International* 574, 1–12. <https://doi.org/10.1016/J.QUAINT.2020.07.028>
- Short, A.D., 1984. Clifed Coast, in: Schwartz, M. (Ed.), *Beaches and Coastal Geology*. Springer US, New York, NY, pp. 223–224.
- Sim, J., Wright, C.C., 2005. The kappa statistic in reliability studies: Use, interpretation, and sample size requirements. *Phys. Ther.* 85, 257–268.
- Siswanto, S., 2010. Seasonal Pattern of Wind Induced Upwelling Over Java-Bali Sea Waters and Surrounding Area. *International Journal of Remote Sensing and Earth Sciences* 5, 46–56. <https://doi.org/10.30536/J.IJRESES.2008.V5.A1228>
- Smith, M.J., Cromley, R.G., 2012. Measuring Historical Coastal Change using GIS and the Change Polygon Approach. *Transactions in GIS* 16, 3–15. <https://doi.org/10.1111/J.1467-9671.2011.01292.X>
- Sui, L., Wang, J., Yang, X., Wang, Z., 2020. Spatial-Temporal Characteristics of Coastline Changes in Indonesia from 1990 to 2018. *Sustainability* 2020, Vol. 12, Page 3242 12, 3242. <https://doi.org/10.3390/SU12083242>
- Sutawa, G.K., 2012. Issues on Bali Tourism Development and Community Empowerment to Support Sustainable Tourism Development. *Procedia Econ. Financ.* 4, 413–422.
- Syvitski, J.P.M., Kettner, A.J., Overeem, I., Hutton, E.W.H., Hannon, M.T., Brakenridge, G.R., Day, J., Vörösmarty, C., Saito, Y., Giosan, L., Nicholls, R.J., 2009. Sinking deltas due to human activities. *Nat Geosci* 2, 681–686. <https://doi.org/10.1038/ngeo629>

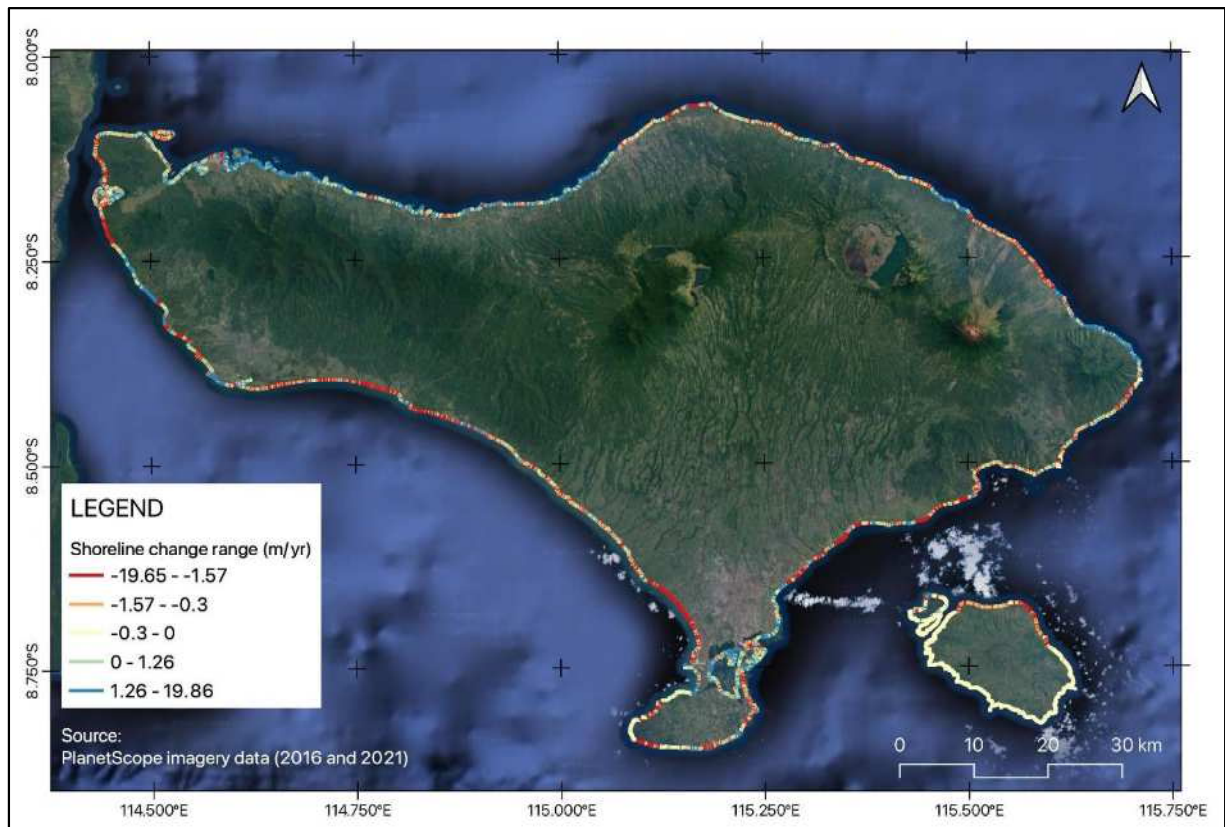
- Tanaka, N., Sato, S., 1976. Topographic change resulting from construction of a harbor on a beach: Kashima Port. *Coastal Engineering* 1977, 1824–1843.
- Tanto, T. Al, Putra, A., Kusumah, G., Farhan, A.R., S. Pranowo, W., Husrin, S., Ilham, 2017. Sedimentation rate in Benoa Bay coastal waters - Bali based on satellite imagery. *Jurnal Kelautan Nasional* 12, 101. <https://doi.org/10.15578/jkn.v12i3.4212>
- Thieler, E.R., 2000. National Assessment of Coastal Vulnerability to Future Sea-Level Rise, Fact Sheet 076-00. USGS, Woods Hole, MA, USA.
- Thieler, E.R., Hammar-Klose, E.S., 2000. National assessment of coastal vulnerability to sea-level rise; preliminary results for the U.S. Gulf of Mexico Coast, Open-File Report, Open-File Report 2000-179. USGS: Woods Hole, MA, USA. <https://doi.org/10.3133/ofr00179>
- Thieler, E.R., Hammar-Klose, E.S., 1999. National assessment of coastal vulnerability to sea-level rise; U.S. Atlantic Coast, Open-File Report, Open-File Report 99-593. USGS: Woods Hole, MA, USA. <https://doi.org/10.3133/ofr99593>
- Thomas, V., 2017. *Climate Change and Natural Disasters: Transforming Economies and Policies for a Sustainable Future*, *Climate Change and Natural Disasters: Transforming Economies and Policies for a Sustainable Future*. Taylor and Francis. <https://doi.org/10.4324/9781315081045>
- Tragaki, A., Gallousi, C., Karymbalis, E., 2018. Coastal Hazard Vulnerability Assessment Based on Geomorphic, Oceanographic and Demographic Parameters: The Case of the Peloponnese (Southern Greece). *Land (Basel)* 7, 1–16.
- Tran, T. V., Reef, R., Zhu, X., 2022. A Review of Spectral Indices for Mangrove Remote Sensing. *Remote Sensing* 2022, Vol. 14, Page 4868 14, 4868. <https://doi.org/10.3390/RS14194868>
- Triana, K., Wahyudi, A.J., 2020a. Sea level rise in Indonesia: The drivers and the combined impacts from land subsidence. *ASEAN Journal on Science and Technology for Development* 37, 115–121. <https://doi.org/10.29037/AJSTD.627>
- Triana, K., Wahyudi, A.J., 2020b. Sea level rise in Indonesia: The drivers and the combined impacts from land subsidence. *ASEAN Journal on Science and Technology for Development* 37, 115–121. <https://doi.org/10.29037/AJSTD.627>
- Triwahyuni, A., Asai, K., 2014. Numerical Simulation on Shoreline Change in Western Region of Badung Regency, Bali, Indonesia | *Journal of Environment*. *Journal of Environment* 1, 2356–3125.
- Tu, Y.H., Johansen, K., Aragon, B., El Hajj, M.M., McCabe, M.F., 2022. The radiometric accuracy of the 8-band multi-spectral surface reflectance from the planet SuperDove constellation. *International Journal of Applied Earth Observation and Geoinformation* 114, 103035. <https://doi.org/10.1016/J.JAG.2022.103035>
- Ubong, G., Edak, E., Odudu, E., 2017. Effects of wind speed and direction on ocean waves along Ibeno Atlantic Ocean. *Int. J. Adv. Sci. Res.* 2, 113–118.
- Uda, T., Onaka, S., Serizawa, M., 2015. Beach erosion downcoast of Pengambangan fishing port in western part of Bali Island, in: *Procedia Engineering*. Elsevier Ltd, pp. 494–501. <https://doi.org/10.1016/j.proeng.2015.08.318>
- Uda, T., Osuga, Y., Onaka, S., Serizawa, M., Furuike, K., 2004. Construction of Pengambangan Fishing Port on West Bai Island and Its Downcoast Erosion. *Proceedings of Civil Engineering in The Ocean* 20, 557–562. <https://doi.org/10.2208/prooe.20.557>

- UNISDR, 2009a. Terminology on Disaster Risk Reduction. Geneva.
- UNISDR, 2009b. Global Assessment Report on Disaster Risk Reduction - Risk and Poverty in a Changing Climate: Invest Today for a Safer Tomorrow. United Nation International Strategy for Disaster Reduction, Geneva, Switzerland.
- Unnikrishnan, A.S., Shankar, D., 2007. Are sea-level-rise trends along the coasts of the north Indian Ocean consistent with global estimates? *Glob. Planet. Change* 57, 301–307.
- Valdemoro, H.I., Jiménez, J.A., 2006. The influence of shoreline dynamics on the use and exploitation of Mediterranean tourist beaches. *Coast. Manag.* 34, 405–423.
- van Aalst, M.K., 2006. The impacts of climate change on the risk of natural disasters. *Disaster* 30, 5–18. <https://doi.org/10.1111/j.1467-9523.2006.00303.x>
- van de Graaff, J., 2021. Typical examples of structural erosion [WWW Document]. http://www.coastalwiki.org/wiki/Typical_examples_of_structural_erosion.
- Wang, G., Liu, Y., Wang, H., Wang, X., 2014. A comprehensive risk analysis of coastal zones in China. *Estuar. Coast. Shelf Sci.* 140, 22–31.
- Wang, X., Chen, W., Zhang, L., Jin, D., Lu, C., 2010. Estimating the ecosystem service losses from proposed land reclamation projects: A case study in Xiamen. *Ecol. Econ.* 69, 2549–2556.
- Wang, X., Yan, F., Su, F., 2021. Changes in coastline and coastal reclamation in the three most developed areas of China, 1980–2018. *Ocean Coast Manag* 204, 105542. <https://doi.org/10.1016/J.OCECOAMAN.2021.105542>
- Ward, P.J., Marfai, M.A., Yulianto, F., Hizbaron, D.R., Aerts, J.C.J.H., 2011. Coastal inundation and damage exposure estimation: A case study for Jakarta. *Natural Hazards* 56, 899–916. <https://doi.org/10.1007/s11069-010-9599-1>
- Wicaksono, A., Wicaksono, P., 2019. Geometric Accuracy Assessment for Shoreline Derived from NDWI, MNDWI, and AWEI Transformation on Various Coastal Physical Typology in Jepara Regency using Landsat 8 OLI Imagery in 2018. *Geoplanning: Journal of Geomatics and Planning* 6, 55–72. <https://doi.org/10.14710/GEOPLANNING.6.1.55-72>
- Widhianthini, W., 2022. Performance of Agricultural Sector in Bali. *KnE Life Sciences* 2022, 579–592–579–592. <https://doi.org/10.18502/KLS.V7I3.11163>
- Widiawan, D.A., Nurdjaman, S., 2018. Tidal Current Circulation in Western Bali Sea Using a 2-D Hydrodynamic Model, in: *IOP J. Phys Conf. Ser.* p. 12075. <https://doi.org/10.1088/1742-6596/1090/1/012075>
- Willroth, P., Diez, J.R., Arunotai, N., 2011. Modelling the economic vulnerability of households in the Phang-Nga Province (Thailand) to natural disasters. *Natural Hazards* 58, 753–769. <https://doi.org/10.1007/s11069-010-9635-1>
- Wisha, U.J., Al Tanto, T., Pranowo, W., Husrin, S., Kusumah, G., Maryono, A., 2019. Numerical Simulation of Ocean Wave Using High-Order Spectral Modeling Techniques: Its Influence on Transport Sediment in Benoa Bay, Bali, Indonesia. *Omni-Akuatika* 15. <https://doi.org/10.20884/1.oa.2019.15.2.554>
- WorldRiskReport 2022, 2022. Focus: Digitalization.

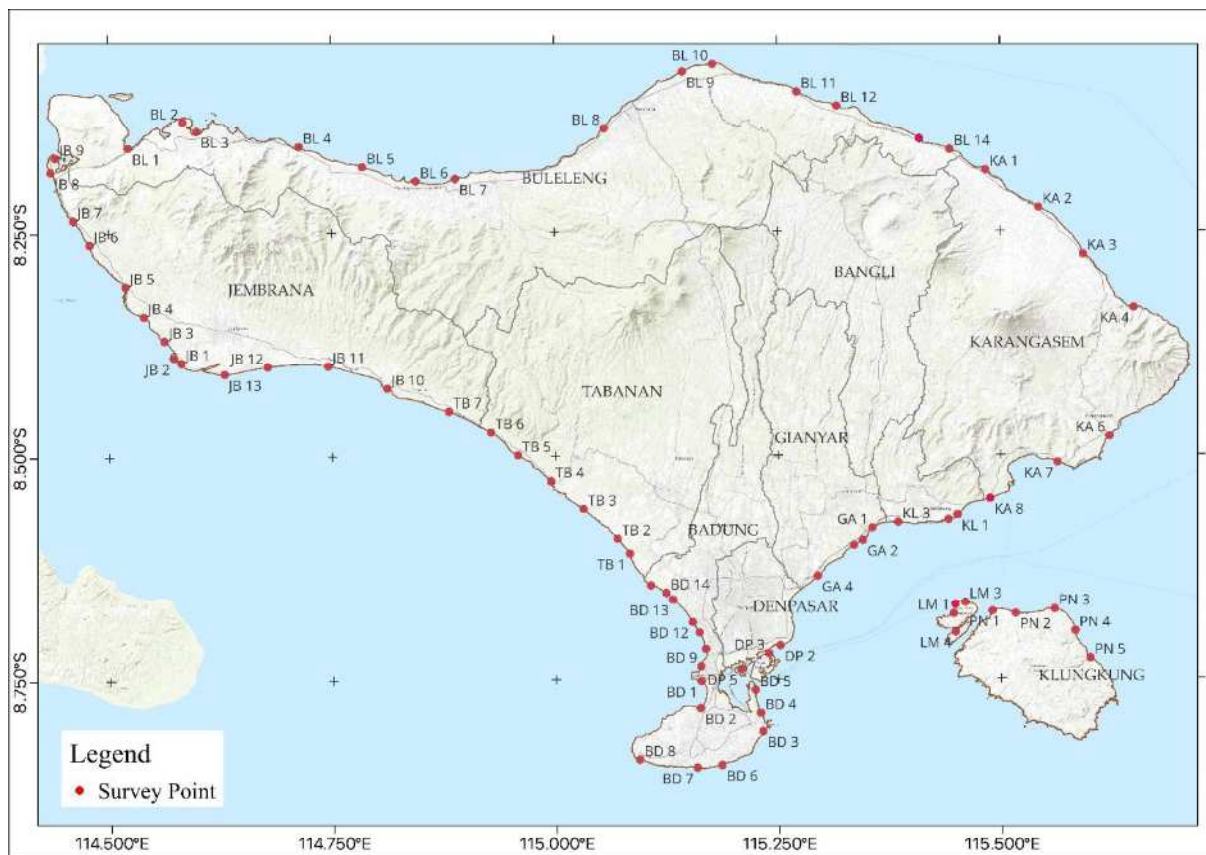
- Wu, L., Rutgersson, A., Sahlee, E., Larsen, X.G., 2016. Swell impact on wind stress and atmospheric mixing in a regional coupled atmosphere-wave model. *J Geophys Res Oceans* 121, 1–16. <https://doi.org/10.1002/2015JC011576>
- Wyrski, K., 1961. Tides and Tidal Currents, in: *Physical Oceanography of The Southeast Asian Waters*. The University of California, La Jolla, California, USA, pp. 155–163. <https://doi.org/10.2337/diacare.28.3.716>
- Xu, H., 2007. Modification of normalised difference water index (NDWI) to enhance open water features in remotely sensed imagery. *Int J Remote Sens* 27, 3025–3033. <https://doi.org/10.1080/01431160600589179>
- Xu, Shaochun, Xu, Shuai, Zhou, Y., Yue, S., Zhang, X., Gu, R., Zhang, Y., Qiao, Y., Liu, M., 2021. Long-Term Changes in the Unique and Largest Seagrass Meadows in the Bohai Sea (China) Using Satellite (1974–2019) and Sonar Data: Implication for Conservation and Restoration. *Remote Sensing* 2021, Vol. 13, Page 856 13, 856. <https://doi.org/10.3390/RS13050856>
- Yang, J., Gong, P., Fu, R., Zhang, M., Chen, J., Liang, S., Xu, B., Shi, J., Dickinson, R., 2013. The role of satellite remote sensing in climate change studies. *Nat Clim Chang* 3, 875–883. <https://doi.org/10.1038/nclimate1908>
- Yastika, P.E., Shimizu, N., Nyoman Pujianiki, N., Rai, G., Temaja, M., Nyoman, I., Antara, G., Osawa, T., 2020. Detection of silent subsidence over extensive area by SBAS DInSAR: a case study of Southern Bali, Indonesia, in: *E3S Web of Conferences*. pp. 1–9. <https://doi.org/10.1051/e3sconf/20201>
- Zambrano-Medina, Y.G., Plata-Rocha, W., Monjardin-Armenta, S.A., Franco-Ochoa, C., 2023. Assessment and Forecast of Shoreline Change Using Geo-Spatial Techniques in the Gulf of California. *Land* 2023, Vol. 12, Page 782 12, 782. <https://doi.org/10.3390/LAND12040782>
- Zhang, K., Douglas, B.C., Leatherman, S.P., 2004. Global warming and coastal erosion. *Clim. Change* 64, 41–58.
- Zhao, Q., Pan, J., Devlin, A.T., Tang, M., Yao, C., Zamparelli, V., Falabella, F., Pepe, A., 2022. On the Exploitation of Remote Sensing Technologies for the Monitoring of Coastal and River Delta Regions. *Remote Sensing* 2022, Vol. 14, Page 2384 14, 2384. <https://doi.org/10.3390/RS14102384>
- Zhu, X., Linham, M.M., Nicholls, R.J., 2010. Technologies for Climate Change Adaptation - Coastal Erosion and Flooding., *TNA Guidebook Series*. ed, Citation. Danmarks Tekniske Universitet, Risø Nationallaboratoriet for Baeredygtig Energi. .
- Zhu, Z.T., Cai, F., Chen, S.L., Gu, D.Q., Feng, A.P., Cao, C., Qi, H.S., Lei, G., 2018. Coastal vulnerability to erosion using a multi-criteria index: A case study of the Xiamen coast. *Sustainability* 11, 1–20.
- Zikra, M., Suntoyo, Lukijanto, 2015. Climate Change Impacts on Indonesian Coastal Areas. *Procedia Earth and Planetary Science* 14, 57–63. <https://doi.org/10.1016/j.proeps.2015.07.085>

APPENDIXES


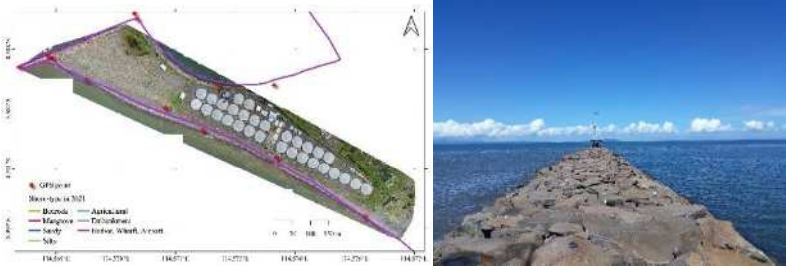


Distribution of shoreline change rate (m/yr)














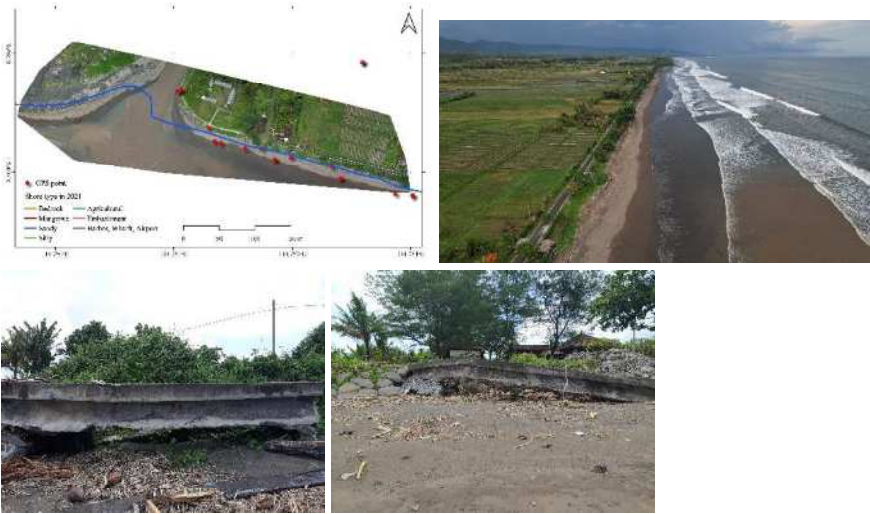
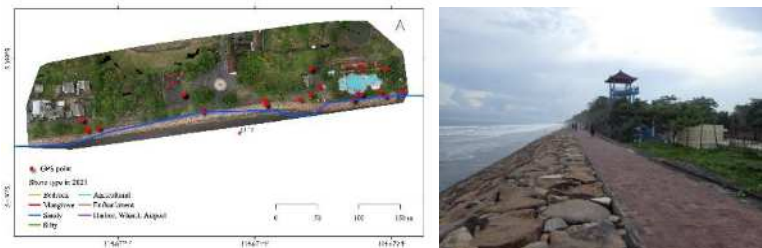
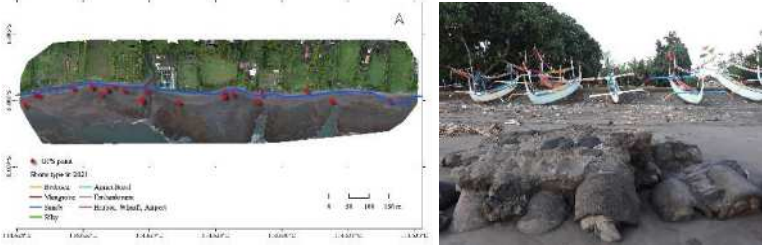
Sampling Location Points for Model Validations




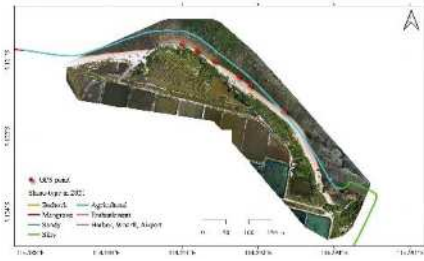













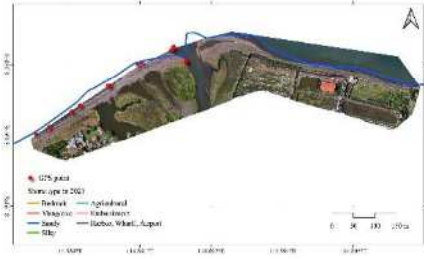




Data/Information of Sampling Locations












ID	Location	Data/Information
JB1	<p>Sirkuit All in One</p> <p>Village: Pengambengan Sub-district: Negara Regency: Jembrana</p>	 <p>Date: 10 March 2023</p> <p>Natural sandy shoreline. Sedimentation occurs.</p>
JB2	<p>Pengambengan Port</p> <p>Pengambengan; Negara; Jembrana</p>	 <p>Date: 10 March 2023</p> <p>Artificial shoreline. The photo was taken in the south breakwater of Pengambengan Port. The sediment deposition (accretion process) is utilized as a millennial shrimp pond for aquaculture activities.</p>
JB3	<p>Cupel Beach I</p> <p>Cupel; Negara; Jembrana</p>	 <p>Date: 10 March 2023</p> <p>Natural sandy shoreline with revetments to protect the shores.</p>
JB4	<p>Pebuhan Beach</p> <p>Banyu Biru; Negara; Jembrana</p>	 <p>Date: 10 March 2023</p> <p>Natural sandy shoreline. Erosion causes severe damage to buildings (settlement)—no meaningful preventive/control/protection action against erosion. The residents tried to protect their homes using simple sandbags.</p>

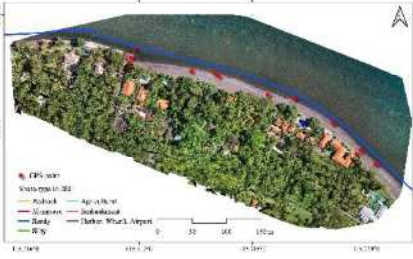








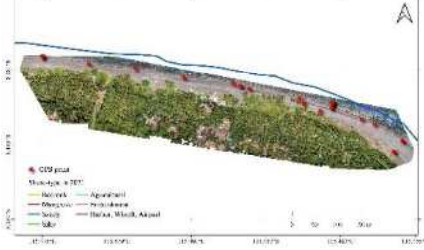

<p>JB5</p>	<p>Candikusumah Beach</p> <p>Candikusuma; Melaya; Jembrana</p>		 <p>Date: 10 March 2023</p> <p>Natural sandy shoreline. Erosion occurs and causes damage to buildings (settlements)—already installed with revetment to protect the shores.</p>
<p>JB6</p>	<p>Karang Impian Beach Swing</p> <p>Melaya; Melaya; Jembrana</p>	  	<p>Date: 10 March 2023</p> <p>Natural sandy shoreline. Shorelines constantly change due to natural processes such as erosion, sediment deposition, and fluctuating water levels, which influence the dynamics of riverbanks.</p>
<p>JB7</p>	<p>PT Ocean Blue Mutiara</p> <p>Melaya; Melaya; Jembrana</p>		 <p>Date: 10 March 2023</p> <p>Natural sandy shoreline with a vegetation barrier. The location near the riverbank can influence the shoreline change—no settlement.</p>
<p>JB8</p>	<p>Pelepasliaran Curik Bali (Cekik)</p> <p>Gilimanuk; Melaya; Jembrana</p>		 <p>Date: 10 March 2023</p> <p>Natural sandy shoreline with a vegetation and settlement barrier.</p>
<p>JB9</p>	<p>Museum Purba Gilimanuk</p> <p>Gilimanuk; Melaya; Jembrana</p>		<p>Date: 10 March 2023</p> <p>A calm bay with a mangrove barrier.</p>




<p>JB10</p>	<p>Pulukan Beach</p> <p>Pulukan; Pekutatan; Jembrana</p>	 <p>Date: 17 March 2023</p> <p>Natural sandy shoreline. It is vegetated with <i>Ipomea pes-caprae</i> as the beach barrier.</p>
<p>JB11</p>	<p>Yehembang Beach / INAP III</p> <p>Yehembang; Mendoyo Jembrana</p>	 <p>Date: 17 March 2023</p> <p>Natural sandy shoreline. Some of the coastal infrastructures have been damaged.</p>
<p>JB12</p>	<p>Dlod Berawah Beach</p> <p>Delodberawah; Mendoyo; Jembrana</p>	 <p>Date: 17 March 2023</p> <p>Natural shoreline (sandy beach). Revetments have already been installed along the coast to prevent erosion.</p>
<p>JB13</p>	<p>Perancak Beach</p> <p>Perancak; Jembrana; Jembrana</p>	 <p>Date: 10 March 2023</p> <p>Natural shoreline (sandy beach). Erosion occurs on some beaches—no prevention actions.</p>



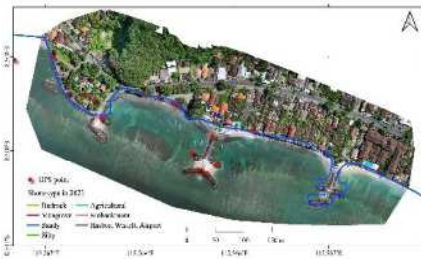





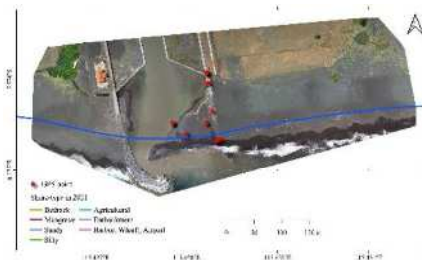
<p>BL1</p>	<p>Karang Sewu Beach</p> <p>Sumberklampok; Gerokgak; Buleleng</p>	  	<p>Date: 11 March 2023</p> <p>Natural shoreline (mangrove) with silty substrate.</p>
<p>BL2</p>	<p>Tambak Pejarakan</p> <p>Pejarakan; Gerokgak; Buleleng</p>		 <p>Date: 11 March 2023</p> <p>The natural sandy shoreline is occupied with shrimp farming.</p>
<p>BL3</p>	<p>Penerusan Bay</p> <p>Sumberkima; Gerokgak; Buleleng</p>	 	<p>Date: 11 March 2023</p> <p>Natural shoreline (mangrove) with sand substrate.</p>
<p>BL4</p>	<p>Gondol Bay</p> <p>Penyabangan; Gerokgak; Buleleng</p>	  	<p>Date: 11 March 2023</p> <p>Natural sandy shoreline. Vegetated with <i>Ipomea pes-caprae</i> and <i>Spinifex</i> (sand binder) as the beach barrier</p>



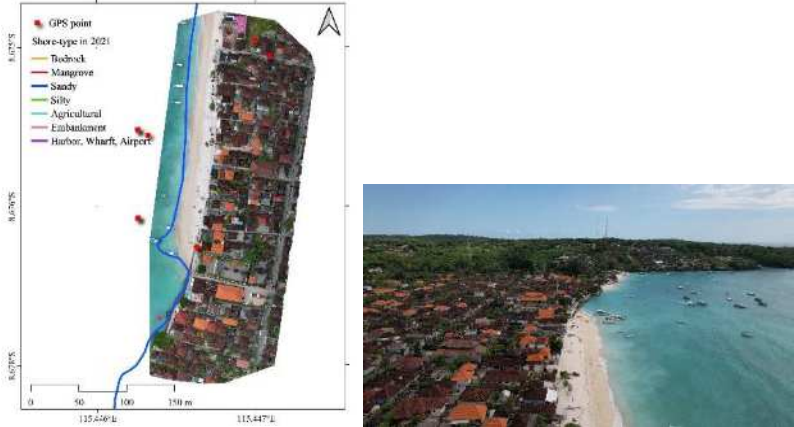
<p>BL5</p>	<p>Pura Segara Desa Gerokgak</p> <p>Gerokgak; Gerokgak; Buleleng</p>		 <p>Date: 11 March 2023</p> <p>The coastline directly borders the sea. There are no large expanses of sand.</p>
<p>BL6</p>	<p>Pura Segara Desa Tinga Tinga</p> <p>Celukanbawang; Gerokgak; Buleleng</p>	  	<p>Date: 11 March 2023</p> <p>Natural shoreline (sandy beach). Revetments have already been installed along the coast to prevent erosion. There are visible traces of erosion from the damaged temple walls.</p>
<p>BL7</p>	<p>Kalisada Beach</p> <p>Kalisada; Seririt; Buleleng</p>	 	 <p>Date: 11 March 2023</p> <p>Natural sandy shoreline with gravel. Near the riverbank. Shorelines constantly change due to natural processes.</p>
<p>BL8</p>	<p>Pemaron Beach</p> <p>Pemaron; Buleleng; Buleleng</p>		





			<p>Date: 11 March 2023</p> <p>Natural sandy shoreline. Revetments have already been installed along the coast to prevent erosion.</p>
<p>BL9</p>	<p>Yeh Lembu Beach</p> <p>Bungkulan; Sawan; Buleleng</p>	 	  <p>Date: 11 March 2023</p> <p>Natural coarse sand beach with vegetation barriers. Erosion probably occurs.</p>
<p>BL10</p>	<p>Pura Segara Kubutambahan</p> <p>Kubutambahan; Kubutambahan; Buleleng</p>		 <p>Date: 11 March 2023</p> <p>Natural black sand beach.</p>
<p>BL11</p>	<p>Pura Ponjok Batu</p> <p>Pacung; Tejakula; Buleleng</p>	 	  <p>Date: 12 March 2023</p> <p>Natural rocky and pebble stone beach. Narrow beach area.</p>

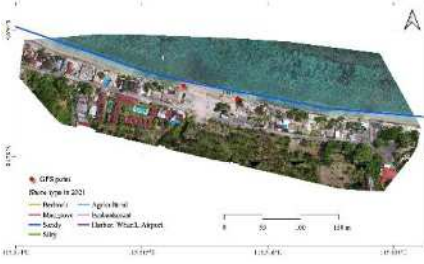









<p>BL12</p>	<p>Pura Dalem Beach</p> <p>Bondalem; Tejakula; Buleleng</p>	 	 <p>Date: 12 March 2023</p> <p>Natural pebbles and sandy beach. In some locations there are erosion occurs.</p>
<p>BL13</p>	<p>Tegal Desa Beach</p> <p>Sambireteng; Tejakula; Buleleng</p>	 	 <p>Date: 12 March 2023</p> <p>Natural pebbles and sandy beach, with narrow shores. The shore installed the seawalls to prevent erosion.</p>
<p>BL14</p>	<p>Black Sand Beach</p> <p>Tembok; Tejakula; Buleleng</p>	 	 <p>Date: 11 March 2023</p> <p>Natural pebbles and sandy beach. The shores installed seawall with stone-filled gabions to protect the shore from erosion. The erosion or coastal flooding probably occurs when high waves arise.</p>
<p>KA1</p>	<p>Silent Salt Beach</p> <p>Tianyar; Kubu; Karangasem</p>		

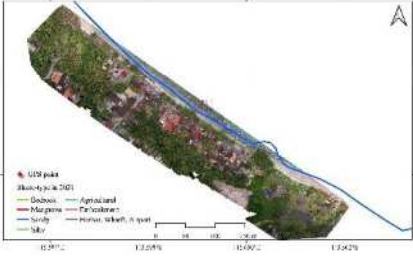







			<p>Date: 12 March 2023 Natural sandy shores.</p>
<p>KA2</p>	<p>Unit Kekerangan BPIUUK</p> <p>Sukadana; Kubu; Karangasem</p>		 <p>Date: 12 March 2023 Natural rocky shores. Narrow shores.</p>
<p>KA3</p>	<p>Tulamben Beach</p> <p>Sukadana; Kubu; Karangasem</p>	 	 <p>Date: 12 March 2023 A natural rocky beach (pebbles and gravel). Need actions to prevent erosion.</p>
<p>KA4</p>	<p>Jemeluk Beach</p> <p>Purwakerti; Abang; Karangasem</p>		 <p>Date: 12 March 2023 Natural sandy shores with pebbles. Narrow shores.</p>
<p>KA5</p>	<p>Lipah Beach</p> <p>Bunutan; Abang; Karangasem</p>		<p>Date: 12 March 2023 Natural sandy shores with pebbles. Narrow shores.</p>

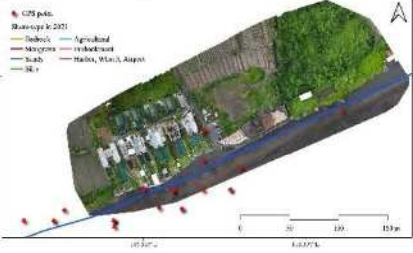










<p>KA6</p>	<p>Jasri Beach</p> <p>Subangan; Karangasem; Karangasem</p>			<p>Date: 13 March 2023</p> <p>Natural sandy shores with boulders for erosion prevention.</p>
<p>KA7</p>	<p>Candidasa Beach</p> <p>Bugbug; Karangasem; Karangasem</p>			<p>Date: 13 March 2023</p> <p>Natural sandy shores, installed with groins for erosion prevention.</p>
<p>KA8</p>	<p>Yeh Malet Beach</p> <p>Antiga Kelod; Manggis; Karangasem</p>		<p>Date: 13 March 2023</p> <p>Natural black sandy shores.</p>	
<p>KL1</p>	<p>Kusamba Beach</p> <p>Kusamba; Dawan; Klungkung</p>			<p>Date: 13 March 2023</p> <p>Natural black sandy shores. Some shores installed seawalls with stone-filled gabions and revetments to protect the shore from erosion.</p>
<p>KL2</p>	<p>Karagdadi Beach</p> <p>Gunaksa; Dawan; Klungkung</p>			

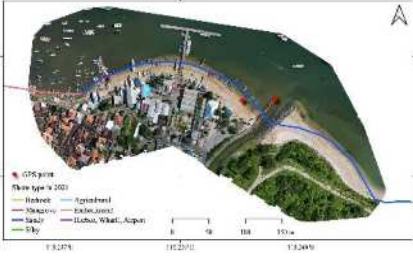









		 <p>Date: 13 March 2023</p> <p>Natural black sandy shores. Erosion causes severe damage to buildings and inundates the paddy field when high waves arise. Some shores installed seawalls with stone-filled gabions and revetments to protect the shore from erosion.</p>
<p>KL3</p>	<p>Lepang Beach</p> <p>Takmung; Banjarangkan; Klungkung</p>	 <p>Date: 12 March 2023</p> <p>Natural black sandy shores. Erosion occurs and inundates the paddy field when high waves arise. Some shores installed seawalls with stone-filled gabions and revetments to protect the shore from erosion.</p>
<p>LM1</p>	<p>D'Camel Fastboat Point</p> <p>Jungutbatu; Nusa Penida; Klungkung</p>	 <p>Date: 14 March 2023</p> <p>Natural sandy shores.</p>



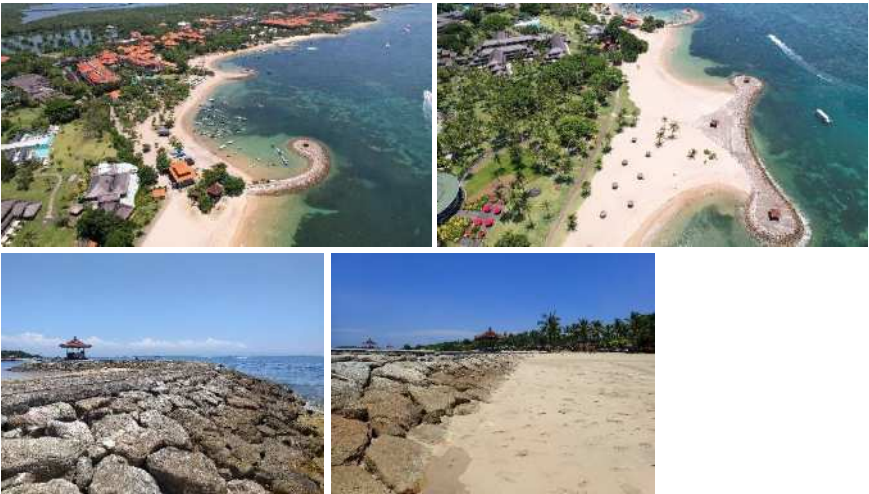
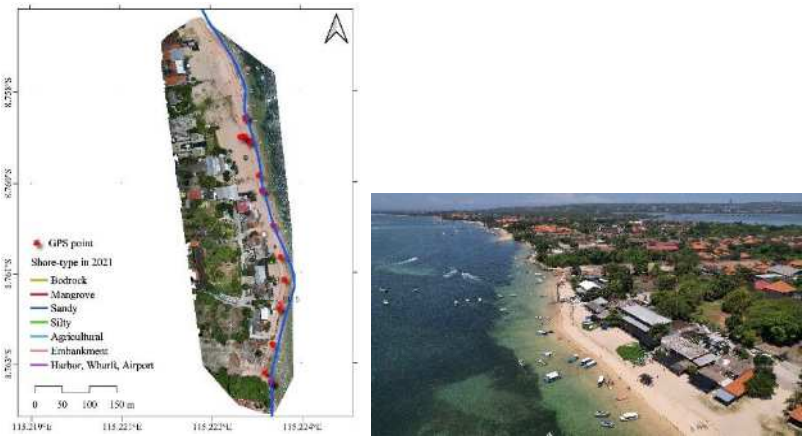
<p>LM2</p>	<p>Pasir Putih Beach</p> <p>Jungutbatu; Nusa Penida; Klungkung</p>	 <p>The map shows the coastline of Pasir Putih Beach with various features: GPS points (red dots), shore-type in 2021 (yellow line), Redrock (red line), Mangrove (green line), Sandy (blue line), Silty (light blue line), Agricultural (green area), Embankment (grey line), and Harbor, Wharf (purple line). The map includes a scale bar (0-150m) and coordinates. The photos show an aerial view of the beach, a sandy shore with a concrete structure, and a rocky shore with driftwood.</p> <p>Date: 14 March 2023</p> <p>Natural sandy shores. An erosion occurred at some points. Strong waves strike and damage the infrastructure.</p>
<p>LM3</p>	<p>Pura Sakenan Desa Adat Jungutbatu</p> <p>Jungutbatu; Nusa Penida; Klungkung</p>	 <p>The aerial view shows a mangrove forest along the coast with a sandy beach and a concrete structure. The water is shallow and clear.</p> <p>Date: 14 March 2023</p> <p>Natural shoreline (mangrove) with sandy substrate.</p>
<p>LM4</p>	<p>Song Tepo Beach</p> <p>Lembongan; Nusa Penida; Klungkung</p>	 <p>The aerial view shows a rocky coastline with a narrow beach and a concrete structure. The water is shallow and clear.</p> <p>Date: 14 March 2023</p> <p>Natural rocky shores. Narrow shores.</p>
<p>PN1</p>	<p>Ped Port/ Toyapakeh</p> <p>Toyapakeh; Nusa Penida; Klungkung</p>	 <p>The photos show a sandy beach with rubble and a concrete structure. The water is shallow and clear.</p> <p>Date: 14 March 2023</p> <p>Natural sandy shores with rubble.</p>


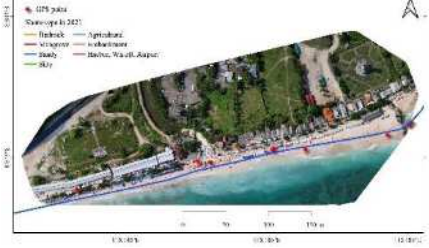






<p>PN2</p>	<p>Merta Beach</p> <p>Ped; Nusa Penida; Klungkung</p>	   <p>Date: 14 March 2023</p> <p>Natural sandy shores with rubble. The shores installed seawalls protect the shore from erosion and waves.</p>
<p>PN3</p>	<p>Batumunggul Beach</p> <p>Batumunggul; Nusa Penida; Klungkung</p>	   <p>Date: 14 March 2023</p> <p>Natural sandy shores. Erosion occurs. The shores installed seawalls protect the shore from erosion and waves.</p>
<p>PN4</p>	<p>Bakung Beach</p> <p>Batumunggul; Nusa Penida; Klungkung</p>	    <p>Date: 14 March 2023</p> <p>Natural sandy shores with rubble. The wave strikes and damages the infrastructure.</p>












<p>PN5</p>	<p>Suana Beach</p> <p>Suana; Nusa Penida; Klungkung</p>	  <p>Date: 14 March 2023</p> <p>Natural sandy shores. Erosion occurs. The shores installed seawalls with stone-filled gabions and revetments to protect the shore from erosion.</p>
<p>GA1</p>	<p>Lebih Beach</p> <p>Lebih; Gianyar; Gianyar</p>	    <p>Date: 13 March 2023</p> <p>Natural black sandy shores. Erosion and coastal flooding occur when high waves arise. The shores installed seawalls with stone-filled gabions and revetments to protect the shore from erosion.</p>
<p>GA2</p>	<p>Masceti Beach</p> <p>Medahan; Blahbatuh; Gianyar</p>	  <p>Date: 13 March 2023</p> <p>Natural black sandy shores. Erosion occurs in this area. The shores installed seawalls with stone-filled gabions and revetments to protect the shore from erosion.</p>

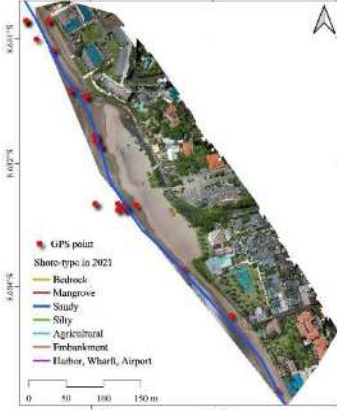


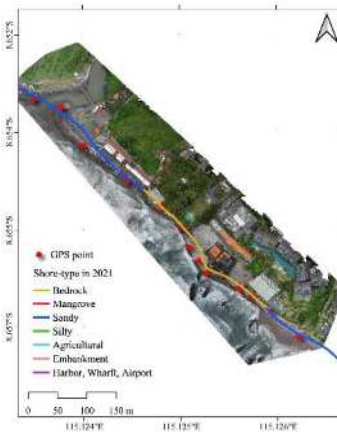



<p>GA3</p>	<p>Keramas Beach</p> <p>Keramas; Blahbatuh; Gianyar</p>	   <p>Date: 13 March 2023</p> <p>Natural black sandy shores. Low-lying coastal area.</p>
<p>GA4</p>	<p>Pabean Beach</p> <p>Ketewel; Sukawati; Gianyar</p>	    <p>Date: 13 March 2023</p> <p>Natural black sandy shores. The shores installed seawalls to protect the shore from erosion and waves.</p>
<p>DP2</p>	<p>Mertasari Beach</p> <p>Sanur Kauh; Denpasar Selatan; Denpasar</p>	    <p>Date: 15 March 2023</p> <p>Natural sandy shores. The shores installed groins and sandbags to protect the shore from erosion and waves.</p>





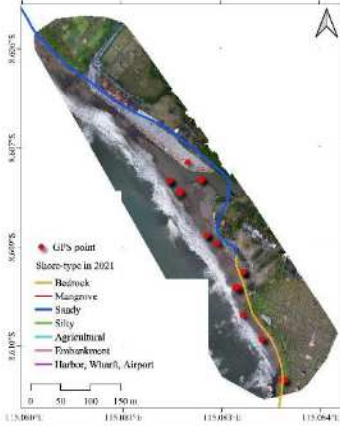





<p>DP3</p>	<p>Serangan Pier</p> <p>Serangan; Denpasar Selatan; Denpasar</p>	 	 <p>Date: 15 March 2023</p> <p>Natural sandy shores and artificial shores. Erosion occurs.</p>
<p>DP4</p>	<p>Blue Sea Jet Cruise</p> <p>Pedungan; Denpasar Selatan; Denpasar</p>		 <p>Date: 15 March 2023</p> <p>The natural shoreline from mangrove and silty substrate. Including artificial shorelines from the expansion of the harbor.</p>
<p>DP5</p>	<p>Pelabuhan Bandar Nelayan</p> <p>Pedungan; Denpasar Selatan; Denpasar</p>		 <p>Date: 15 March 2023</p> <p>The natural shoreline from mangrove and silty substrate. Including artificial shorelines from the expansion of the harbor.</p>
<p>BD1</p>	<p>Kelan Beach</p> <p>Tuban; Kuta; Badung</p>	 	 <p>Date: 16 March 2023</p> <p>Natural sandy shores. An erosion occurred at some points. The wave strikes and damages the infrastructure.</p>

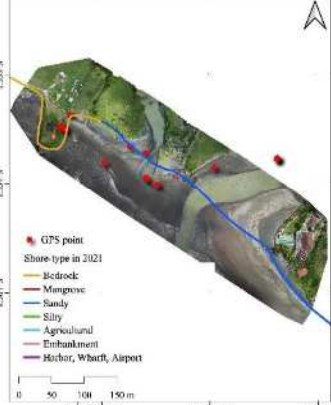

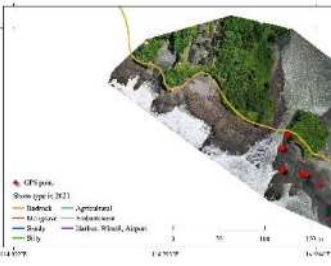





<p>BD2</p>	<p>Muaya Beach</p> <p>Jimbaran; Kuta Selatan; Badung</p>	 <p>Date: 16 March 2023</p> <p>Natural sandy shores.</p>
<p>BD3</p>	<p>Mengiat Beach</p> <p>Benoa; Kuta Selatan; Badung</p>	 <p>Date: 15 March 2023</p> <p>Natural sandy shores.</p>
<p>BD4</p>	<p>Samuh Beach</p> <p>Benoa; Kuta Selatan; Badung</p>	 <p>Date: 15 March 2023</p> <p>Natural sandy shores, installed with groins, beach nourishment, and offshore breakwater to prevent the shores from erosion.</p>
<p>BD5</p>	<p>Pacific Bahari Beach</p> <p>Tanjung Benoa; Kuta Selatan; Badung</p>	

		 <p data-bbox="496 450 1366 551">Date: 15 March 2023 Natural sandy shores with rubble. An erosion occurred at some points. The wave strikes and damages the infrastructure.</p>
<p data-bbox="193 562 248 589">BD6</p>	<p data-bbox="280 562 467 589">Pandawa Beach</p> <p data-bbox="280 640 429 745">Kutuh; Kuta Selatan; Badung</p>	   <p data-bbox="855 864 1366 1088">Date: 15 March 2023 Natural rocky (cliff) shores. Narrow shores. An erosion occurred at some point. There is the possibility of cliff erosion from waves when crashing against the coastline, eroding until a notch is formed. The wave strikes and damages the infrastructure.</p>
<p data-bbox="193 1111 248 1137">BD7</p>	<p data-bbox="280 1111 448 1137">Melasti Beach</p> <p data-bbox="280 1189 429 1294">Ungasan; Kuta Selatan; Badung</p>	   <p data-bbox="855 1413 1366 1581">Date: 15 March 2023 Natural rocky (cliff) shores. Narrow shores. There is the possibility of cliff erosion from waves when crashing against the coastline, eroding until a notch is formed.</p>
<p data-bbox="193 1659 248 1686">BD8</p>	<p data-bbox="280 1659 440 1715">Nyang Nyang Beach</p> <p data-bbox="280 1767 429 1872">Pecatu; Kuta Selatan; Badung</p>	 <p data-bbox="951 1659 1366 1760">Date: 15 March 2023 Natural rocky (cliff) shores. Narrow shores.</p>

<p>BD9</p>	<p>Jerman Beach</p> <p>Kuta; Kuta; Badung</p>	   <p>Date: 16 March 2023</p> <p>Natural sandy shores. It is installed with an offshore breakwater and seawalls with stone-filled gabions and revetments to protect the shore from erosion.</p>
<p>BD10</p>	<p>Kuta Beach</p> <p>Kuta; Kuta; Badung</p>	      <p>Date: 16 March 2023</p> <p>Natural sandy shores. Coastal erosion occurs. It is installed with seawalls with stone-filled gabions, revetments, and sandbags to protect the shore from erosion. Coastal flooding commonly occurs when high waves.</p>
<p>BD11</p>	<p>Double Six Beach</p> <p>Legian; Kuta; Badung</p>	  <p>Date: 16 March 2023</p> <p>Natural sandy shores.</p>

<p>BD12</p>	<p>Petitenget Beach</p> <p>Seminyak; Kuta; Badung</p>		 <p>Date: 16 March 2023 Natural sandy shores.</p>
<p>BD13</p>	<p>Canggu Beach</p> <p>Canggu; Kuta Utara; Badung</p>	 <p>Date: 16 March 2023 Natural sandy shores. Installed with seawalls with stone-filled gabions and revetments to protect the shore from erosion.</p>	
<p>BD14</p>	<p>Pererenan Beach</p> <p>Pererenan; Mengwi; Badung</p>	    <p>Date: 16 March 2023 Natural sandy shores. Installed with seawalls with stone-filled gabions and revetments to protect the shore from erosion.</p>	

<p>BD15</p>	<p>Cemagi Beach</p> <p>Cemagi; Mengwi; Badung</p>	   	<p>Date: 16 March 2023</p> <p>Natural rocky shores. Installed with seawalls with stone-filled gabions and revetments to protect the shore from erosion and high waves.</p>
<p>TB1</p>	<p>Kedungu Beach</p> <p>Belalang; Kediri; Tabanan</p>	    	<p>Date: 16 March 2023</p> <p>Natural rocky (cliff) and sandy shores. Installed with seawalls with stone-filled gabions and revetments to protect the shore from erosion and high waves</p>
<p>TB2</p>	<p>Yeh Gangga Beach</p> <p>Sudimara; Seririt; Tabanan</p>		<p>Date: 16 March 2023</p> <p>Natural sandy shores.</p>

<p>TB3</p>	<p>Abian Kapas Beach</p> <p>Beraban; Salemadeg Timur; Tabanan</p>		 <p>Date: 17 March 2023</p> <p>Natural sandy shores. The wave strikes and damages the infrastructure.</p>
<p>TB4</p>	<p>Soka Beach</p> <p>Antap; Salemadeg; Tabanan</p>	 	 <p>Date: 17 March 2023</p> <p>Natural rocky and sandy shores.</p>
<p>TB5</p>	<p>Mejan Beach</p> <p>Lalanginggah; Salemadeg Barat; Tabanan</p>	 	 <p>Date: 17 March 2023</p> <p>Natural rocky and sandy shores. An erosion occurs. The wave strikes and damages the infrastructure.</p>

<p>TB6</p>	<p>Selabih Beach</p> <p>Selabih; Salemadeg Barat; Tabanan</p>	    <p>Date: 17 March 2023</p> <p>Natural rocky and sandy shores. An erosion occurs. The wave strikes and damages the infrastructure.</p>
<p>TB7</p>	<p>Pura Khayangan Suci Cengng Kembar</p> <p>Pangyangan; Pekutatan; Jembrana</p>	  <p>Date: 17 March 2023</p> <p>Natural sandy shores.</p>